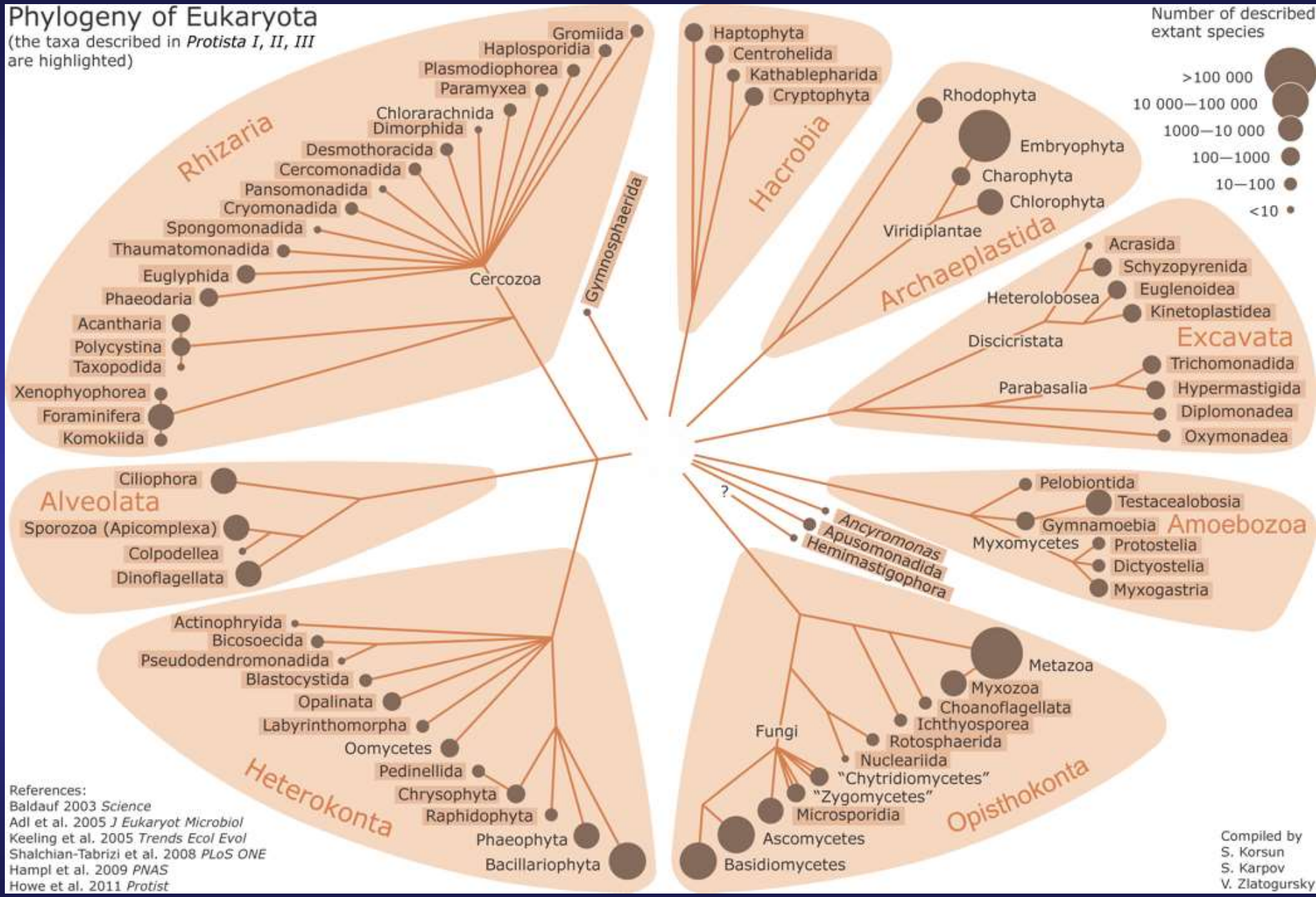

References:
Baldauf 2003 *Science*
Adl et al. 2005 *J Eukaryot Microbiol*
Keeling et al. 2005 *Trends Ecol Evol*
Shalchian-Tabrizi et al. 2008 *PLoS ONE*
Hampl et al. 2009 *PNAS*
Howe et al. 2011 *Protist*

Compiled by
S. Korsun
S. Karpov
V. Zlatogursky

Foraminifers as epibionts, predators, commensals, and parasites

Fissurina marginata как эктопаразит на фораминиферах *Discorbis spp.* (Le Calvez, 1947, др.). Никогда не культивировалась без хозяина.

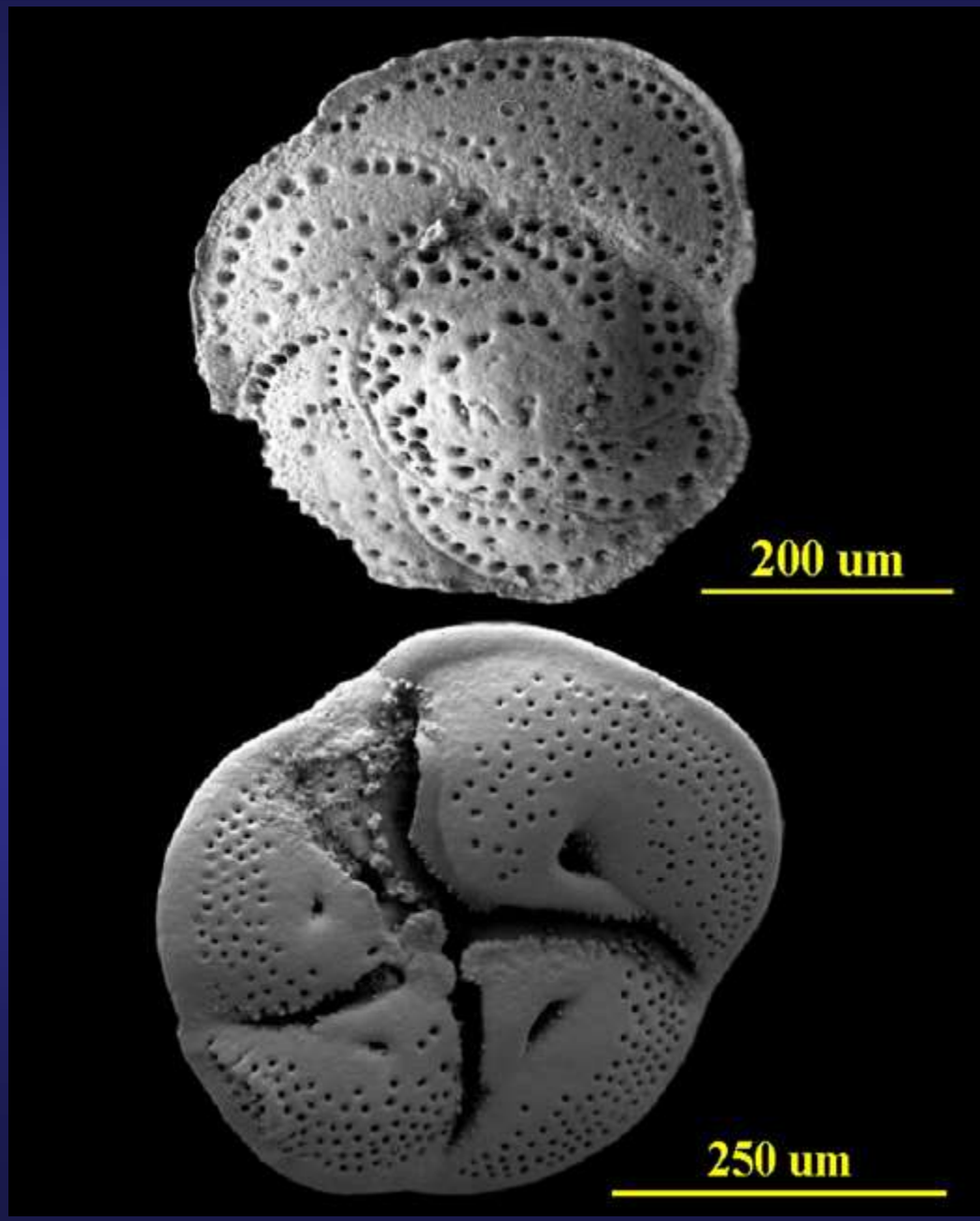

Rosalina carnivora была описана как комменсал, который высверливает ямы на поверхности раковины *Acesta (Lima) angolensis*. Автор не называла фораминиферу истинным паразитом (Todd, 1965)

Floresina amphiphaga preying upon *Amphistegina*.

Planorbulinopsis parasita является паразитом других фораминифер (***Alveolinella quoyi***) (Banner, 1971).

Hanzawaia strattoni в норме живет на *Notocorbula operculata*, но не считается паразитом, скорее комменсалом (Bock, Moore, 1968).

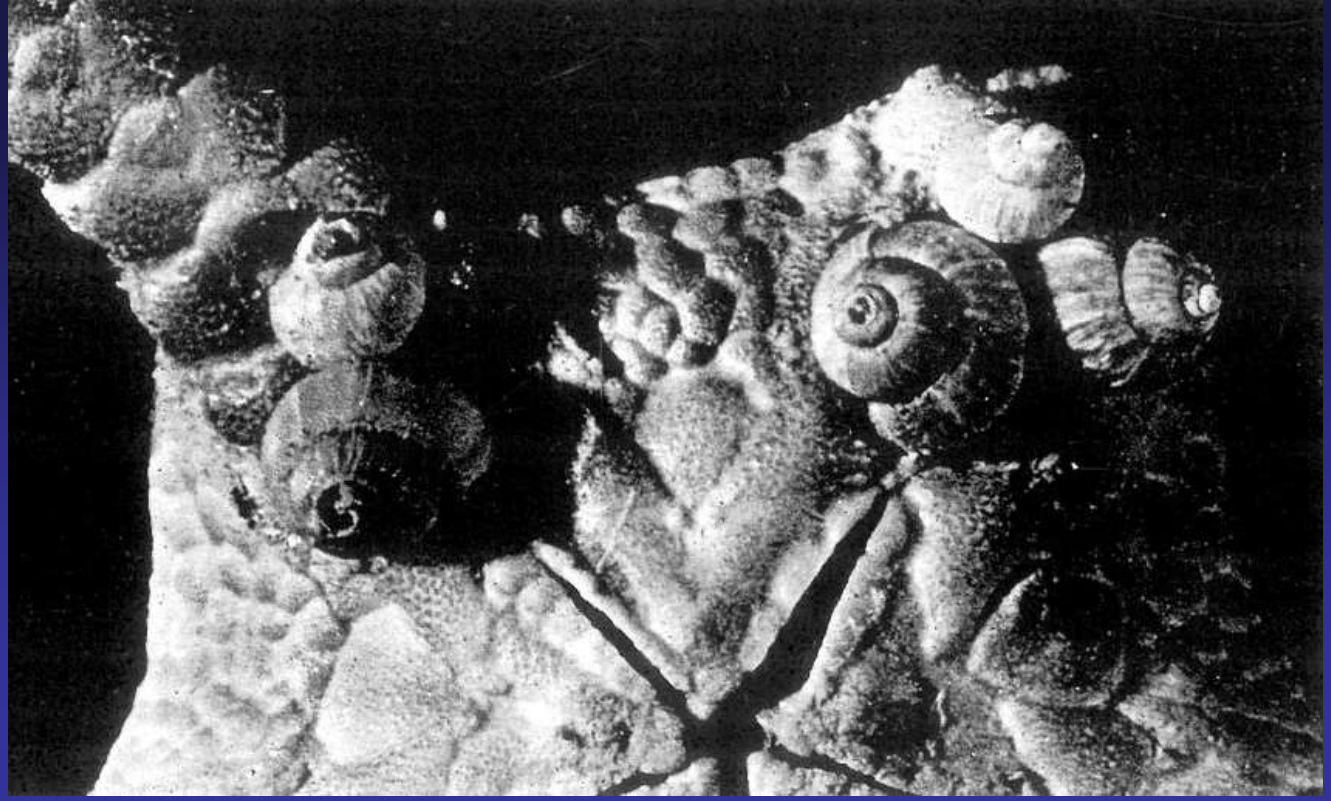

Гиперпаразитические фораминиферы поражают раковину гастроподы *Ophiolamia armigeri*, которая является паразитом змеехвостки *Ophiomusium armigerum*

Ophiolamia armigeri parasitic on *Ophiomusium armigerum*. The two males are considerably smaller than the females. The apex of the left male is distorted by a parasitic foraminiferid. Diameter of the ophiuroid 11.2 mm (Waren, Carney, 1981) .

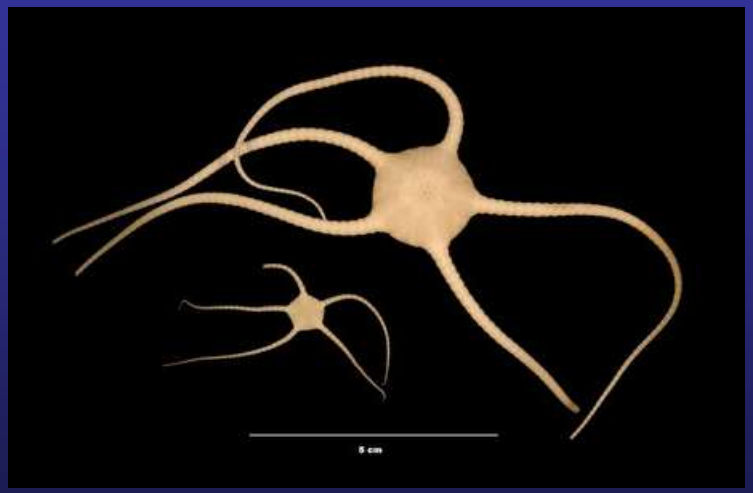

Stilapex montrouzieri (Eulimidae) attached to a large brittle star (*Macrophiothirx sp*), Moorea, French Polynesia

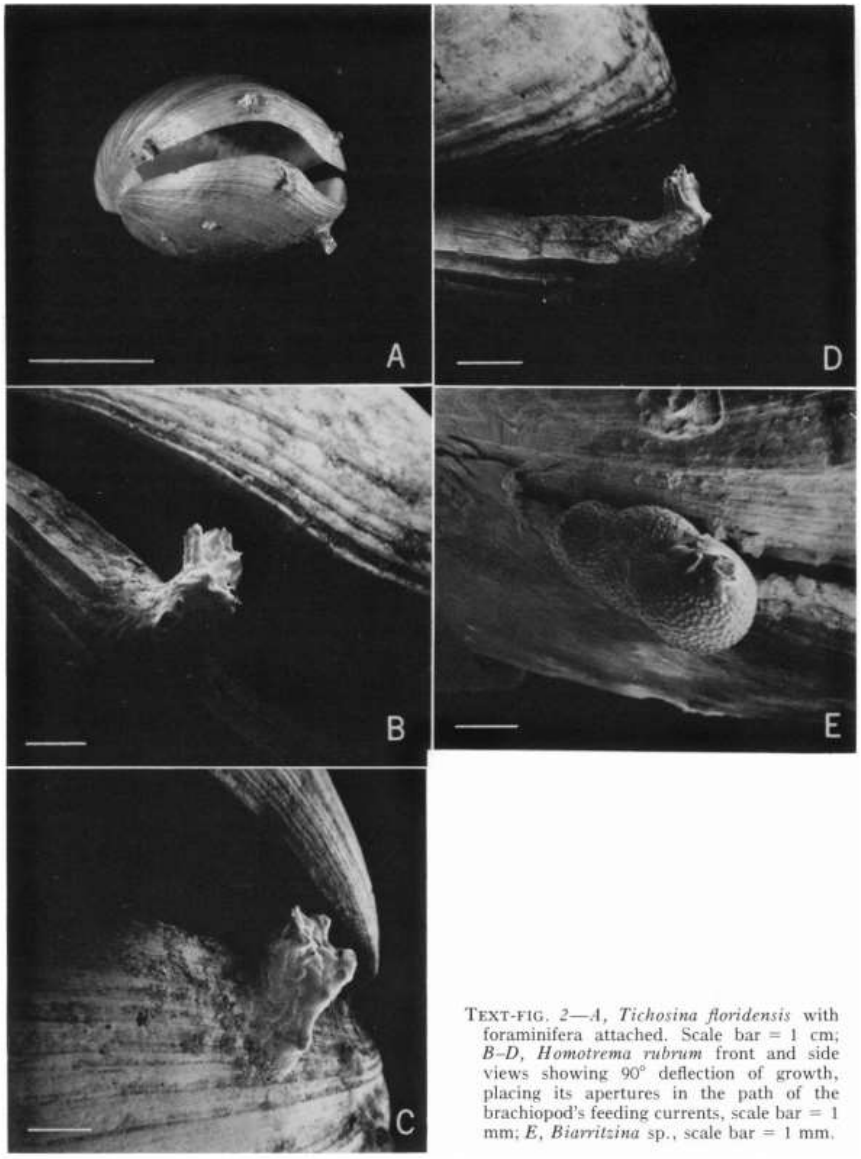

TEXT-FIG. 2—*A*, *Tichosina floridensis* with foraminifera attached. Scale bar = 1 cm; *B–D*, *Homotrema rubrum* front and side views showing 90° deflection of growth, placing its apertures in the path of the brachiopod's feeding currents, scale bar = 1 mm; *E*, *Biarritzina* sp., scale bar = 1 mm.

Foraminifers as epibionts on brachiopods

Семь видов фораминифер живет на брахиоподе *Tichosina floridensis*. Токи воды, создаваемые этой зверюшкой, используются для питания самой фораминиферой

A, *Tichosina fioridensis* with foraminifera attached. Scale bar--1 cm; B-D, *Homotrema rubrum* front and side views showing 90 deflection of growth, placing its apertures in the path of the brachiopod's feeding currents, scale bar =1 mm; E, *Biarritzina sp., scale bar = 1 mm.*

Foraminifers as epibionts on brachiopods

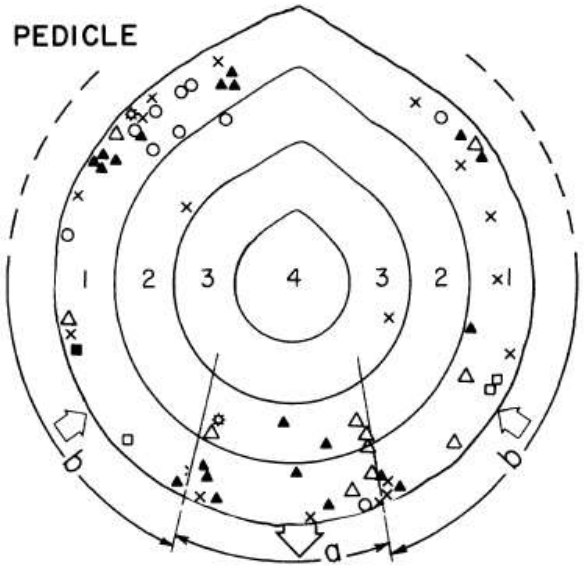

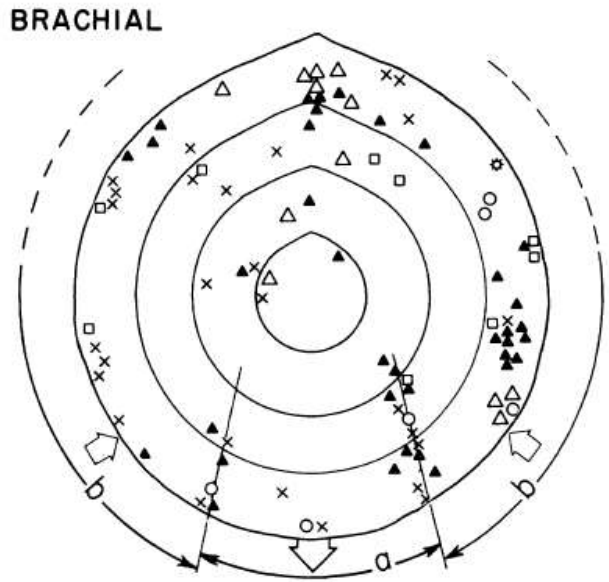

- *Biarritzina* sp.
- *Carpenteria balaniformis*
- *Cibicides refulgens*
- *Homotrema rubrum*
- *Rosalina floridensis*
- *Sporadotrema cylindricum*
- *Carpenteria monticularis*

Seven species of foraminifera aggregate near the commissure of the brachiopod *Tichosina floridensis* Cooper. Aggregation near the commissure and pronounced ecotypic response of the foraminifera to the feeding currents of the brachiopod suggest that these epizoic foraminifera derive benefits from brachiopod currents. The brachiopods do not appear to be affected by the epizoa, implying a commensal rather than a parasitic relationship. The density of individuals along the commissure was not significantly different between the incurrent and excurrent regions, suggesting similar resource availabilities. On this relatively deep water (100-200 m) brachiopod, epizoic foraminifera benefit both from a hard substrate and increased trophic resource availability (Zumwalt, DeLaca, 1980).

Distribution of seven species of foraminifera on the valves of T. fioridensis. Solid lines delineate the ontogenetic trace of the deflection marking the exhalent commissure. a= exhalent and b = inhalent commissure

Hyrrokkin sarcophaga as a parasite

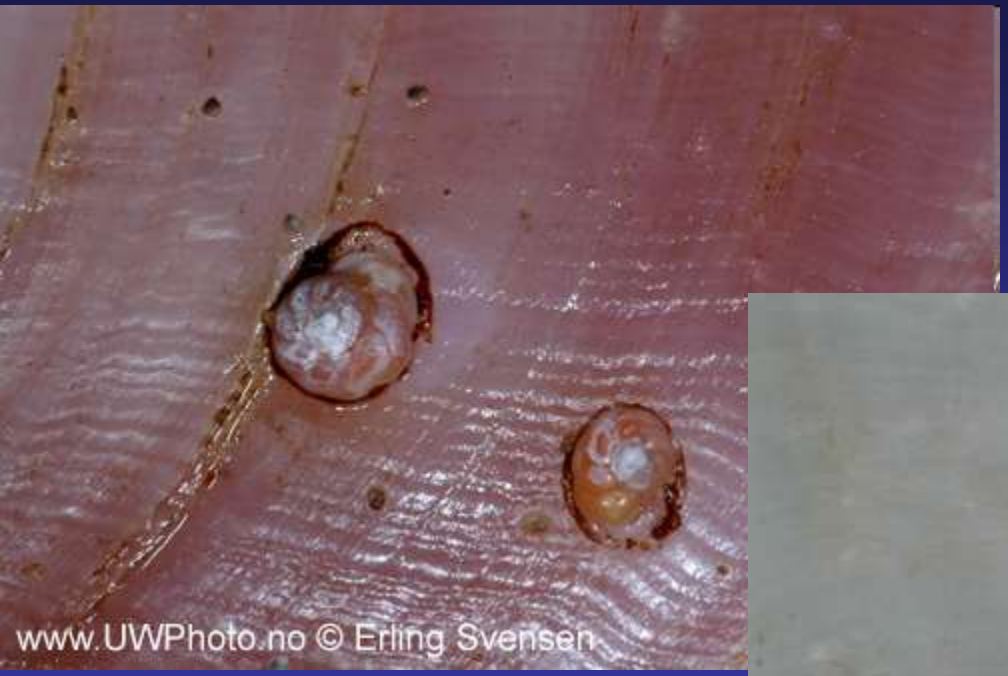

Hyrrokkin sarcophaga была известная под разными именами, позже все были сведены в один вид, паразиты моллюсков и губок (Cedhagen, 1994).

Hyrrokkin sarcophaga as a parasite

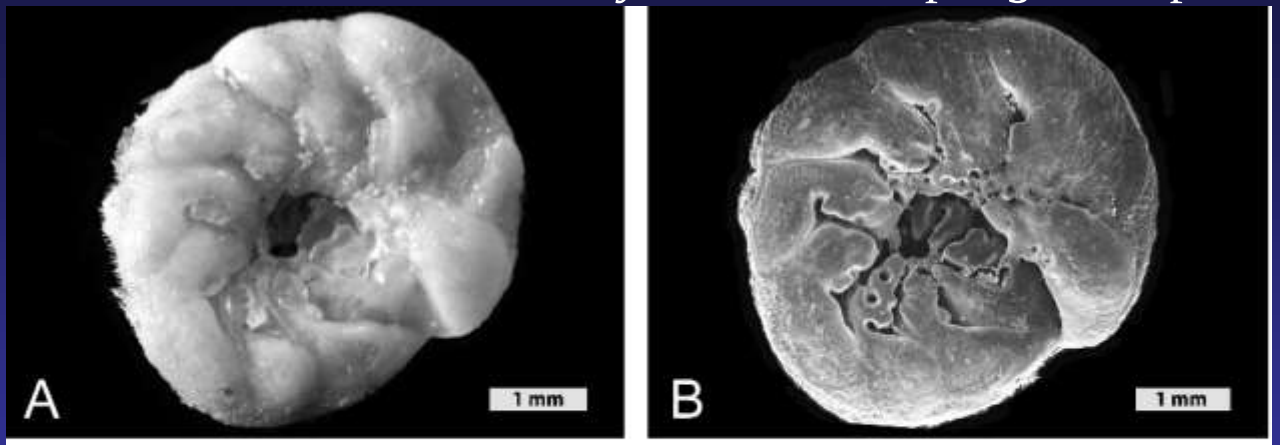

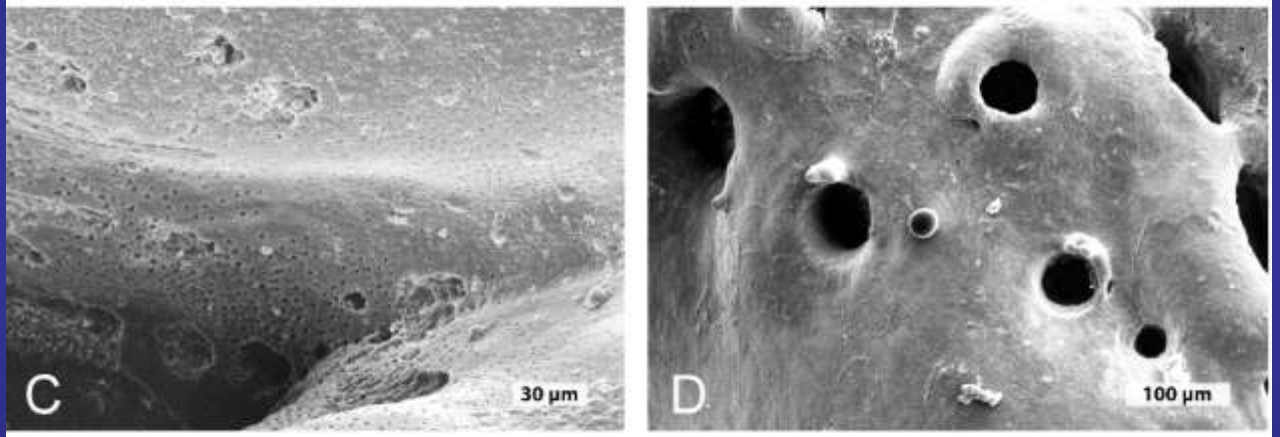

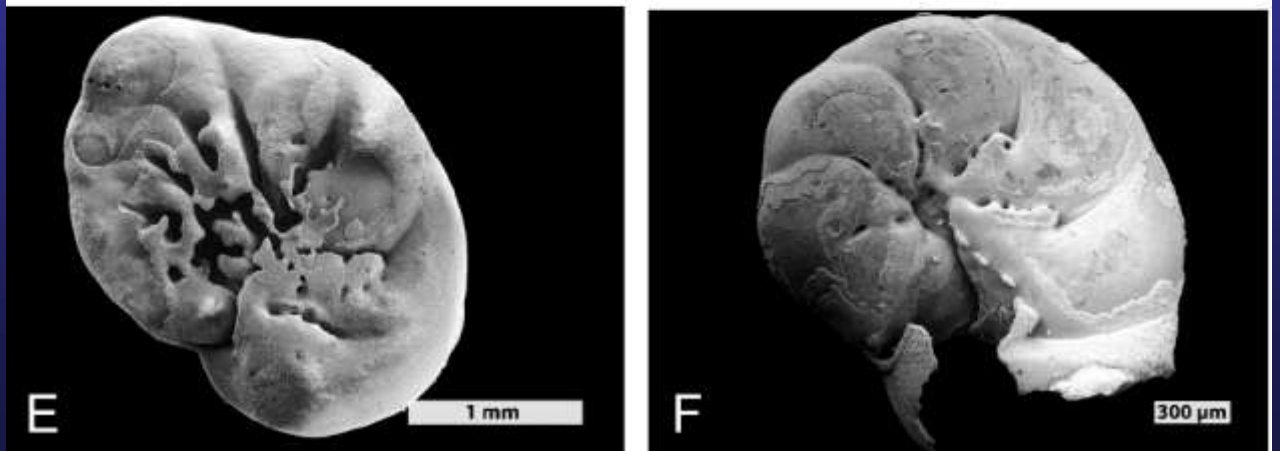

Fig. 8. Microspheric specimen of *Hyrrokkin sarcophaga* specimen (Hs) attached to *Lophelia pertusa*. (Sample No. 21). Scale bar = 500 µm.

Variations of *Hyrrokkin sarcophaga* test morphology (A: microscopic image, B-H: SEM). **A** Umbilical side of *H. sarcophaga* on *Lophelia pertusa* (Pos228-200-3). **B** SEM image of A accents the distribution of apertures. **C** Close-up of B showing numerous pores. **D** Close-up of the larger test apertures, where the protoplasm exits to form the 'whip'-shaped canals in the substrate. **E** Test from *L. pertusa*, irregular substrate morphologies influence the shape of the foraminifer (Pos228-200-3). **F** Test from geodiid host (POS228-201).

(Beuck et al., 2008)

Hyrrokkin carnivora and *H. sarcophaga* as parasites

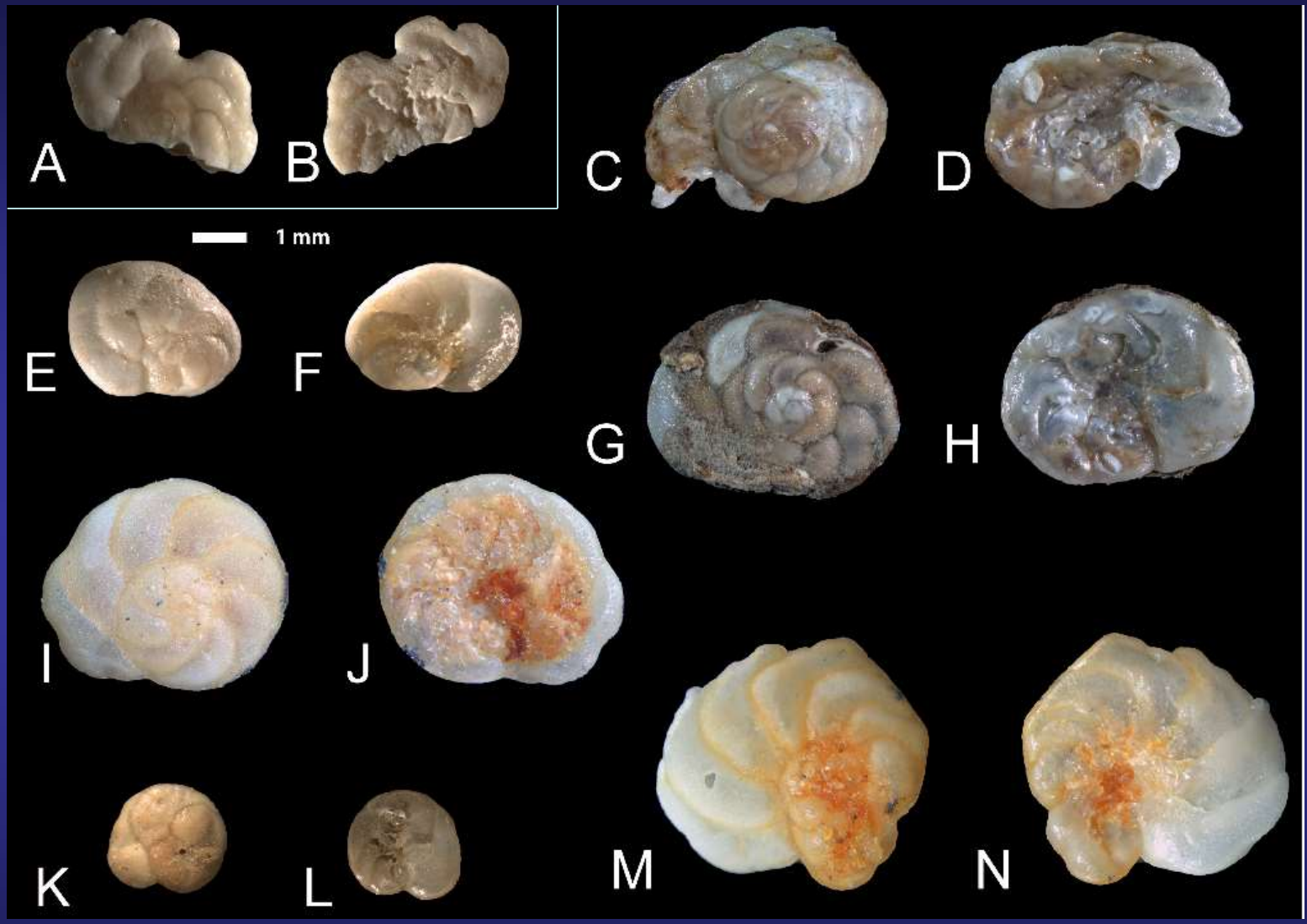

Recent *Hyrrokkin* spp. from various hosts show a high morphological variability, depending on their substrate topography (A-B: *Hyrrokkin carnivora*, Mauritania; C-N: *Hyrrokkin sarcophaga*, mid-Norway; upper side and umbilical side pictured adjacent; the same scale bar applies to all specimens). A-B *H. carnivora* (specimen from Fig. 4I), host *Acesta excavata*. C-D Host *Lophelia pertusa* (Pos228-228). E-F Host *Caryophyllia sarsiae* (M61-3-603-1). G-H like C-D, note the brown organic residuals skirting the test. I-J Host *A. excavata* (VH95-168). K-L Host geodiid sponge (POS228-201). M-N like I-J

Hyrrokkin sarcophaga as a parasite on sponges

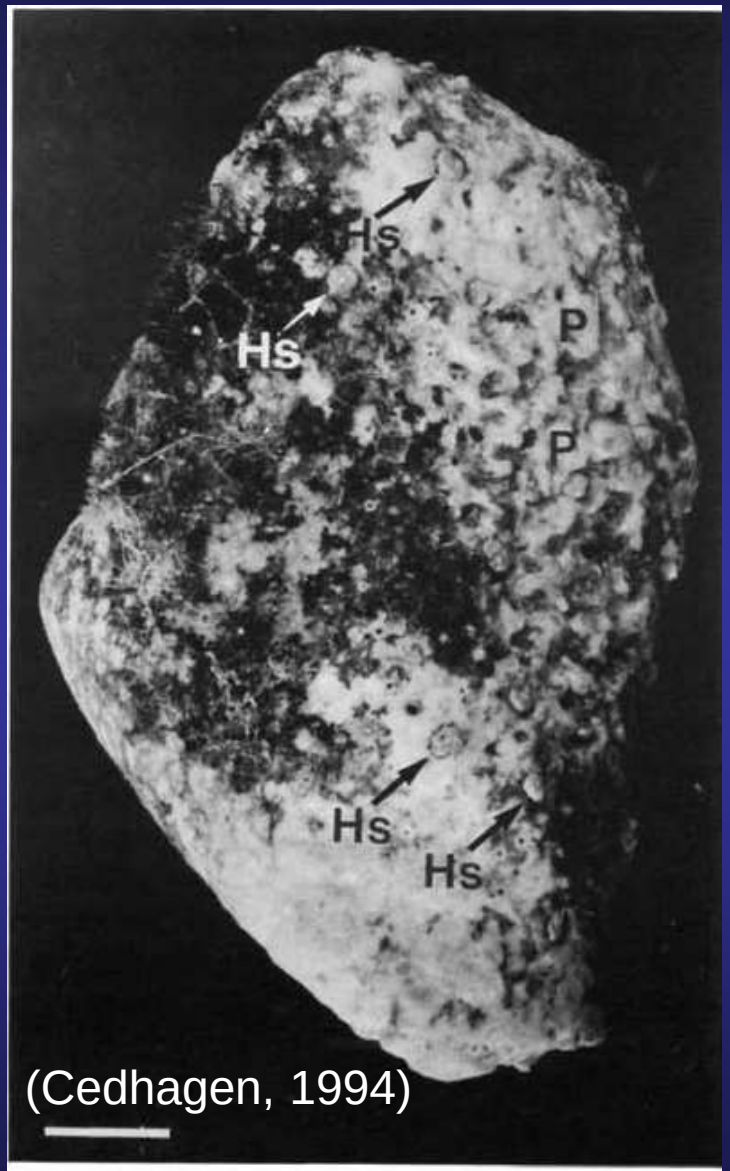

(Cedhagen, 1994)

Fig. 10. *Hyrrokkin sarcophaga* (Hs) sitting on a fragment of a large *Isops phlegraei* specimen. p = pits (see Sample No. 4).

Isops phlegraei

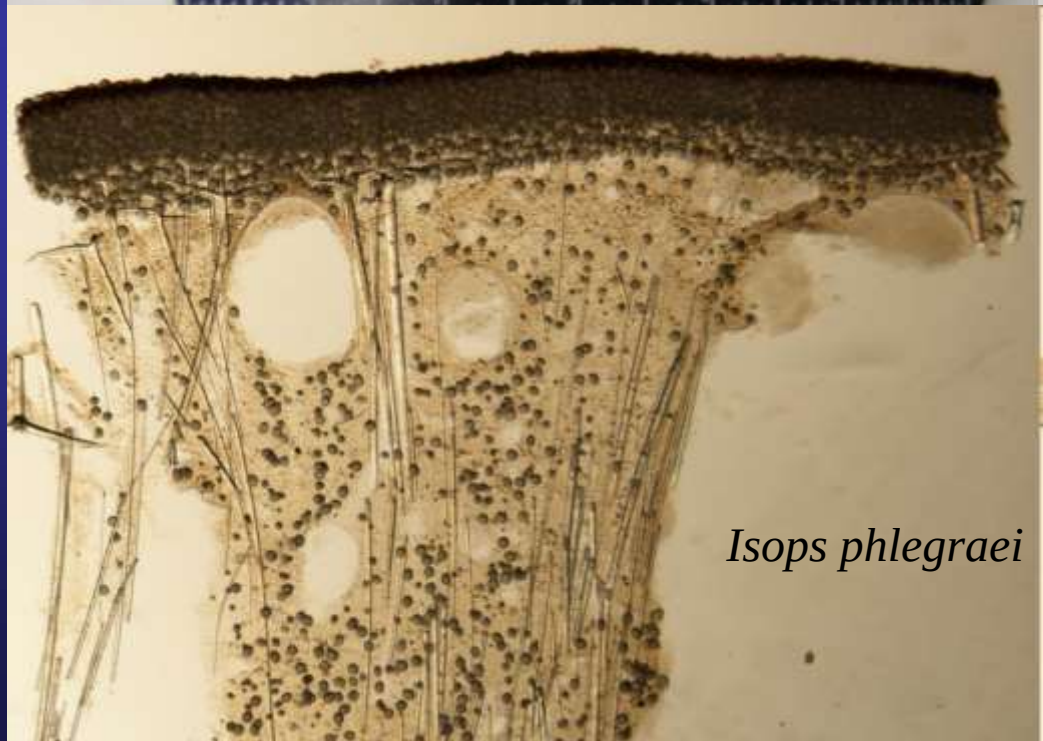

Isops phlegraei

Stelletta normani

Lophelia pertusa

На коралле *Lophelia pertusa* встречаются представители нескольких видов беспозвоночных: двустворчатные моллюски *Acesta excavata*, *Delectopecten vitreus*, морские желуди *Verruca stroemia* и фораминифера *Hyrrokkin sarcophaga*

Hyrrokkin sarcophaga as a parasite on corrals

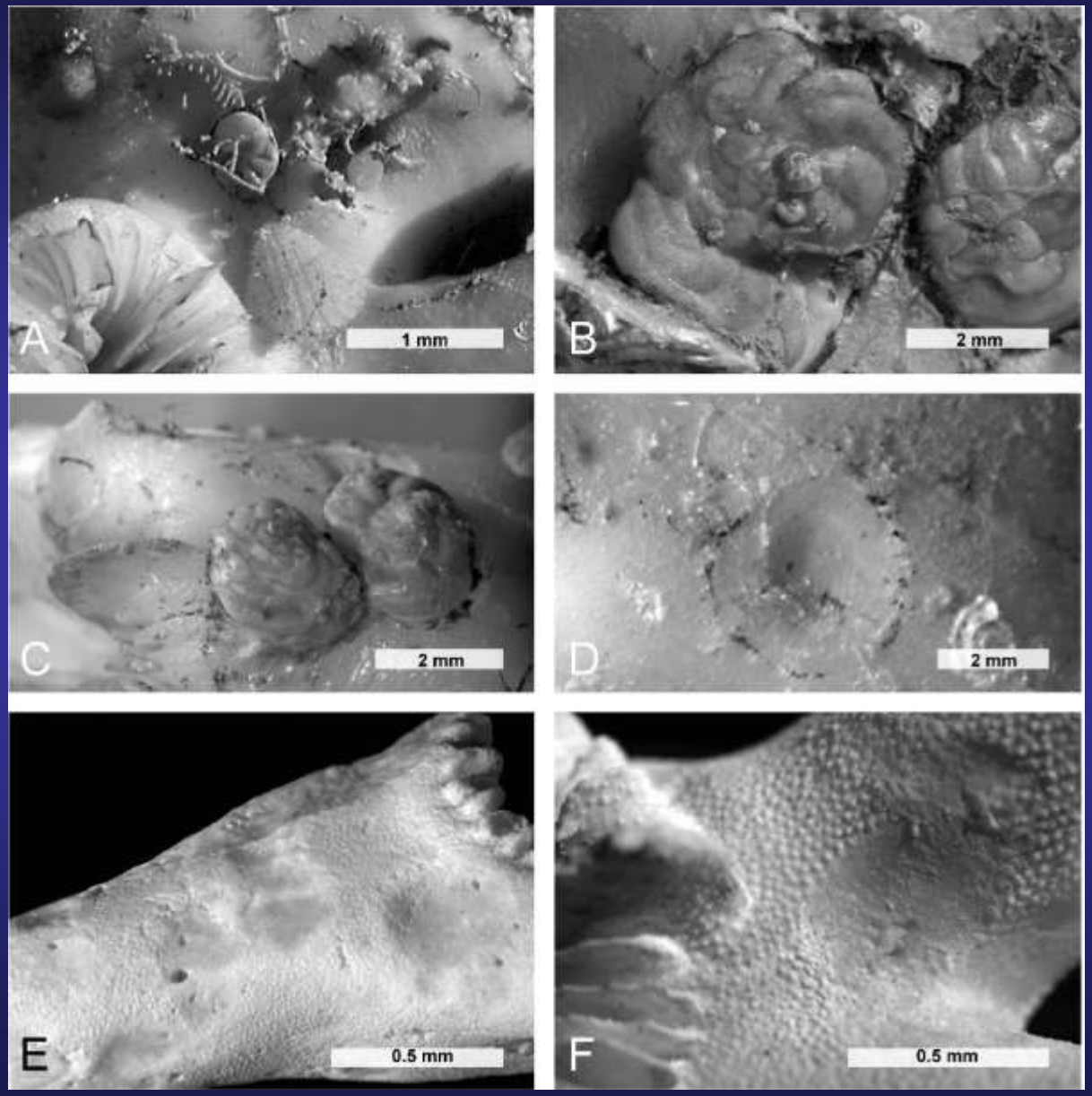

Microscopic images of Recent (A-D) and fossil (E-F) *Lophelia pertusa* samples. **A.** *Hyrrokkin sarcophaga* colonising dead framework in association with the brachiopod *Terebratulina retusa*, epizoic bryozoans and serpulids (Pos228-200-3). **B.** Two *Hyrrokkin sarcophaga* tests colonised by bryozoans and other foraminifers; note the partial embedding of the left individual (top) by the coral (JH5-99-4); image with courtesy of K. Kaszemeik. **C.** *Hyrrokkin* individuals preferentially colonise upper calyx portions (Pos228-200-3). **D.** *Hyrrokkin* groove on recently dead skeleton (LI94-163). **E.** Fossil, Last Glacial *L. pertusa* with numerous potential *Hyrrokkin* traces (CS96-64). **F.** Same coral as in E with potential *Hyrrokkin* groove in vicinity to the polyp; note the well preserved coral surface

(Beuck et al., 2008)

Sea Corn
Primnoa resedaeformis

Hyrrokkin sarcophaga as a parasite on corrals

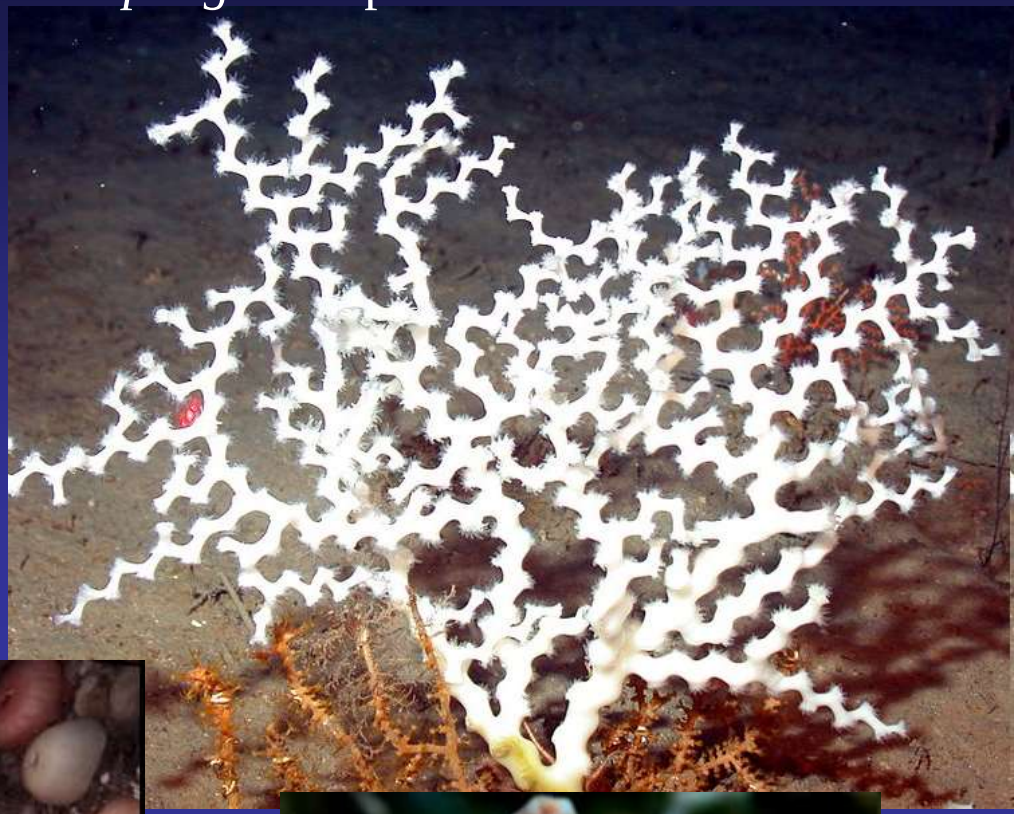

Zigzag coral
Madrepora oculata

Hyrrokkin sarcophaga as a parasite on corrals

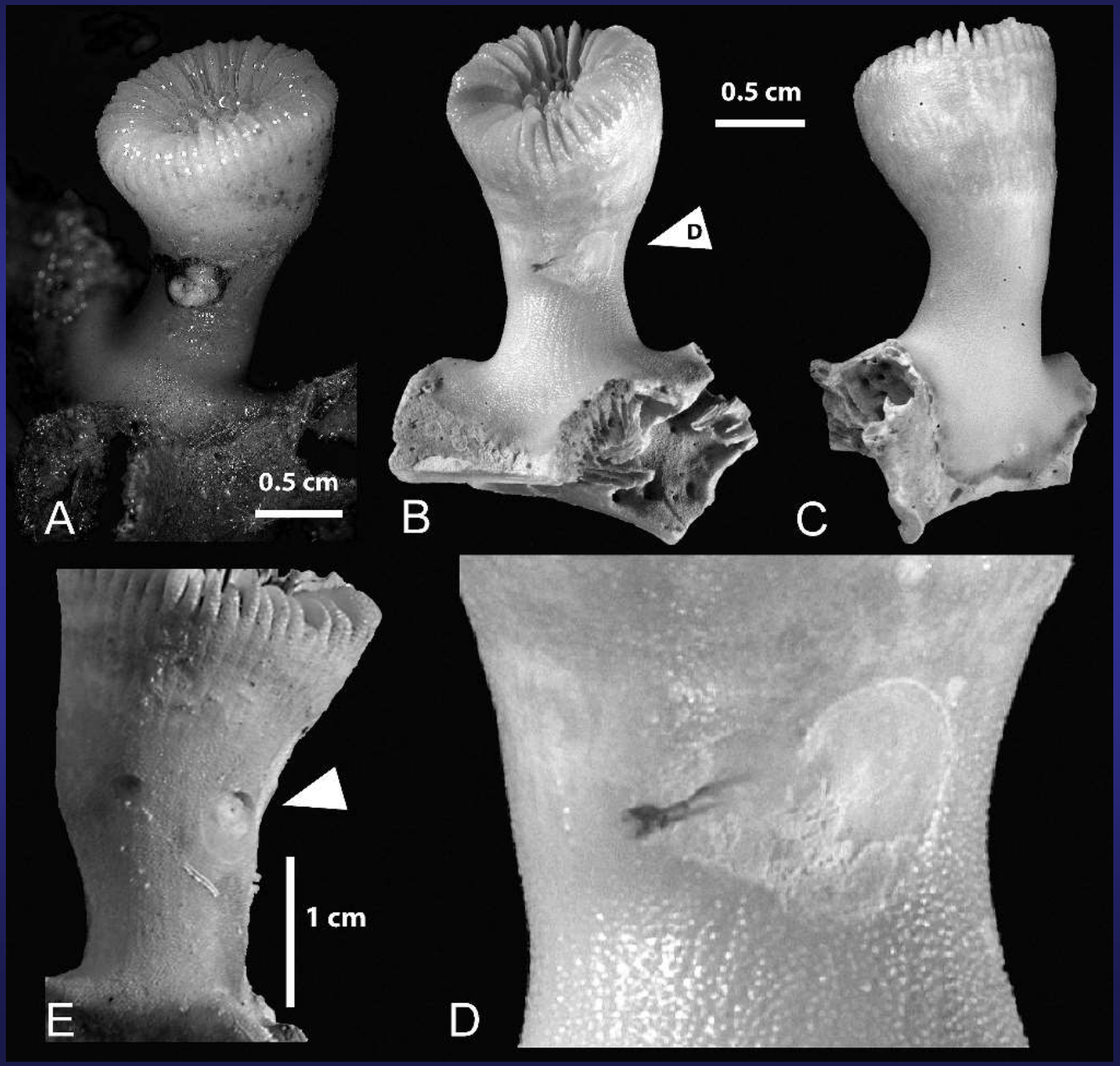

Overview images of *Caryophyllia sarsiae* samples from the Porcupine Seabight; samples M61-3-603-1 (A-D) and M61-3-603-2. (E). **A.** Live *Caryophyllia sarsiae* on dead *Lophelia pertusa* framework with live *Hyrrokkin sarcophaga* at the polyp's basal edge; note the brownish organic residue skirting the foraminiferan test. **B.** Sample cleaned from organic remains and the *Hyrrokkin* test, now exposing *Kardopomorphos polydioryx* igen. n., isp. n. **C.** The 'backside' of the corallite is free from foraminiferal traces. **D.** Close-up of the shallow pit showing that the protoplasm seems to form a shallow depression (left) apically to the latest chamber. **E.** Sample M61-3-603-2. Abandoned attachment scar of *Hyrrokkin sarcophaga* on a dead *Caryophyllia sarsiae*, exposing a central canal (white arrow)

(Beuck et al., 2008)

Hyrrokkin sarcophaga as a parasite on bivalves

Hyrrokkin sarcophaga as a parasite on bivalves

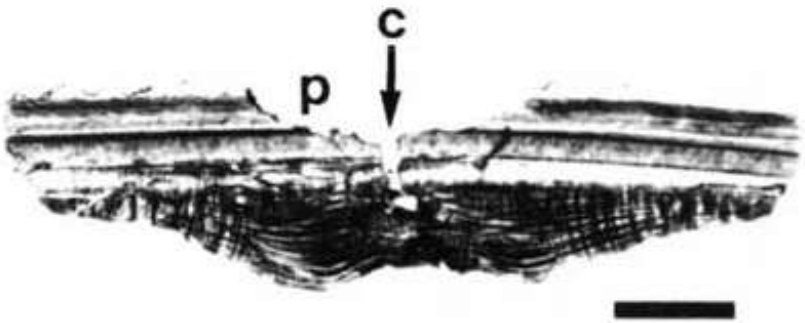

Fig. 6. Thin section of a pit (p) and a canal (c) made by *Hyrrokkin sarcophaga* sp. n. in the shell of *Lima (Acesta) excavata*. (Sample No. 32, SMNH No. 4587). Scale bar = 1 mm.

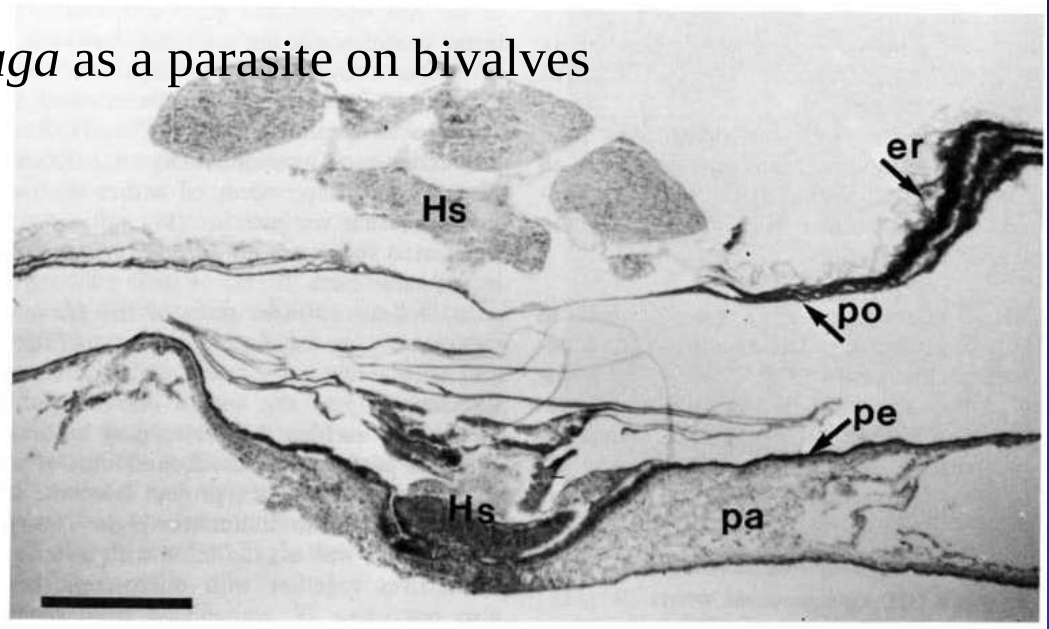

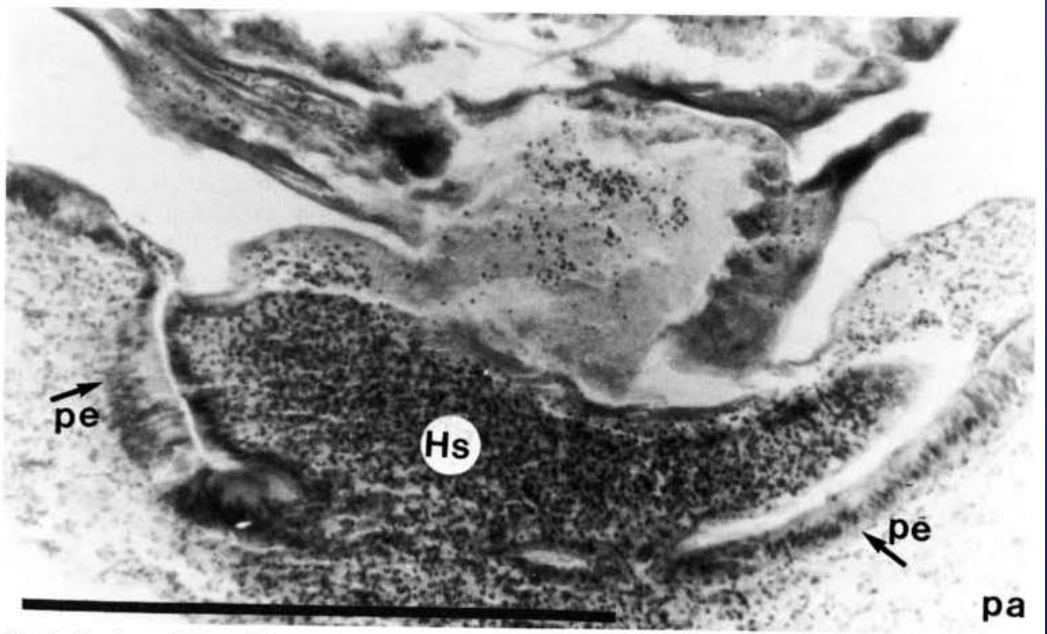

Fig. 9. Section of *Hyrrokkin sarcophaga* specimen (Hs) sitting on *Lima (Acesta) excavata*. The pseudopodia attack the tissues of the bivalve. pa = pallium, pe = pallial epithelium, po = periostracum, er = excreted residues (Sample No. 32). Scale bar = 1 mm.

(Cedhagen, 1994)

Hyrrokkin sarcophaga as a parasite on bivalves

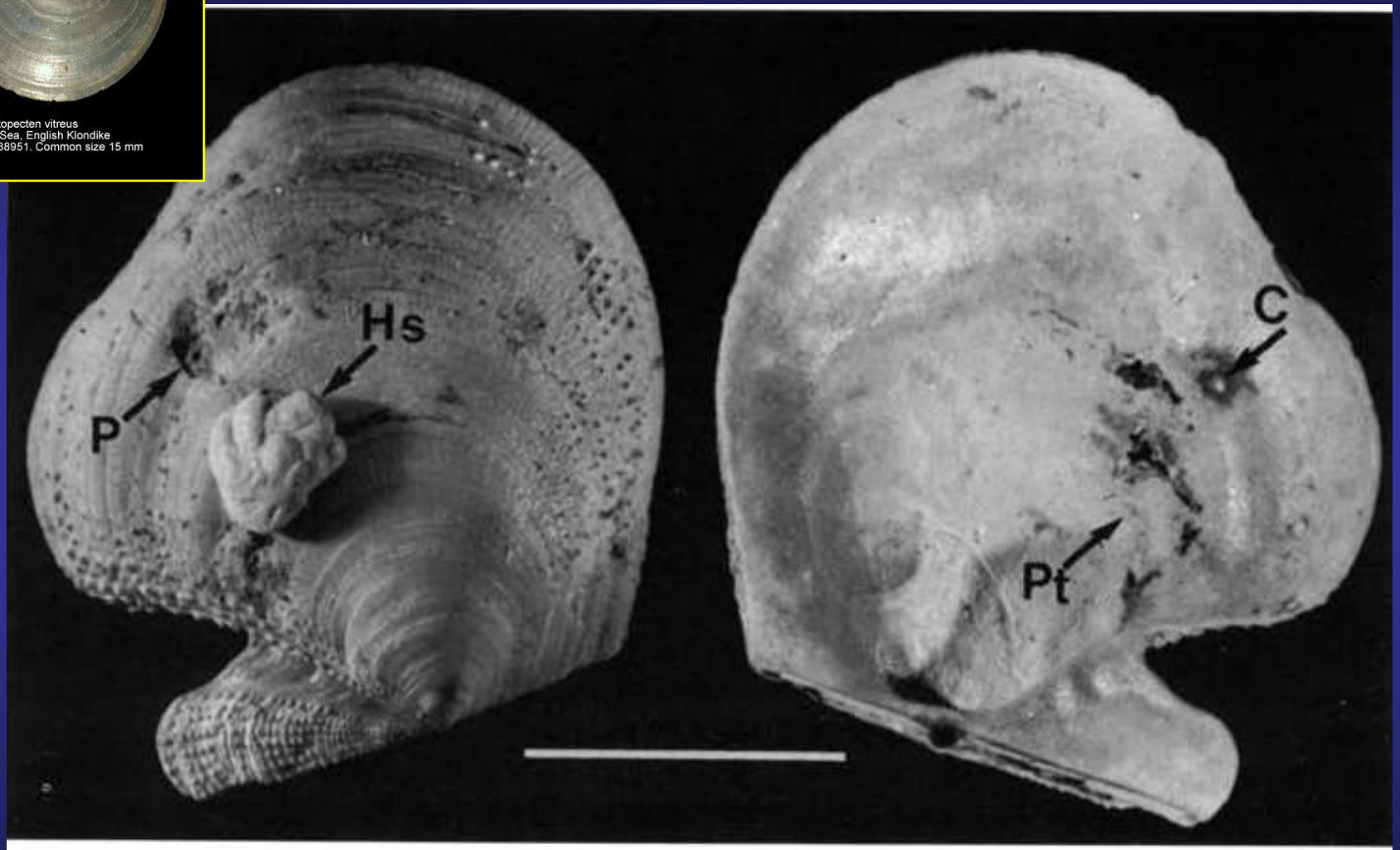

Fig. 11. A living *Hyrrokkin sarcophaga* specimen (Hs) sitting on a dead *Delectopecten vitreus* specimen. c = callus, p = pit, pt = penetration without a callus, (see Sample No. 45). Scale bar = 1 mm.

(Cedhagen, 1994)

Hyrrokkin sarcophaga as a predator

Они питаются полихетами *Placostegus tridentatus*, *Serpula vermicularis*, *Apomatus similis*, *Spirorbis sp*., колониями мшанок *Disporella hispida*, *Idmidronea atlantica* (different sources).

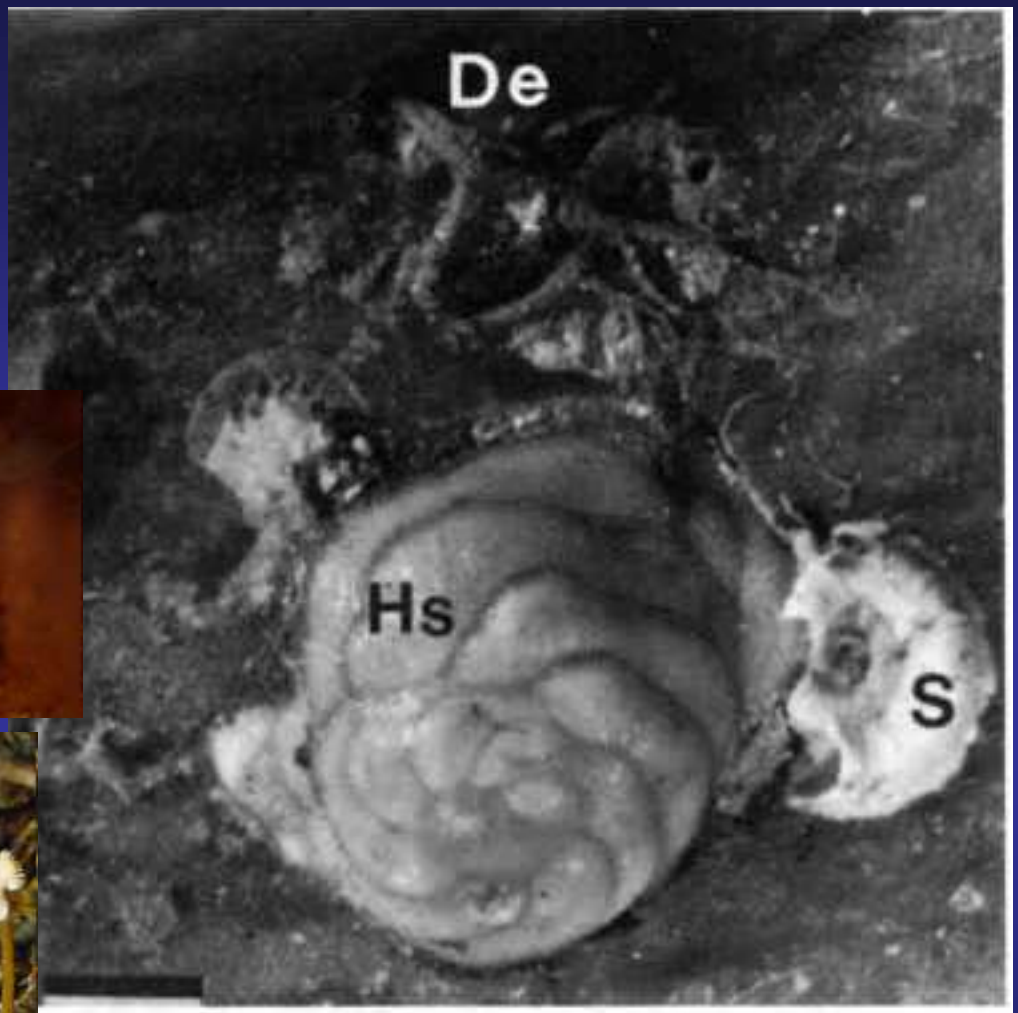

Fig. 13. *Hyrrokkin sarcophaga* parasitizing a *Lima (Acesta) excavata* specimen and simultaneously preying on a *Spirorbis* sp. specimen but not affecting a *Dendrophrya erecta* specimen nearby. (Sample No. 27). Scale bar = 1 mm.

(Cedhagen, 1994)

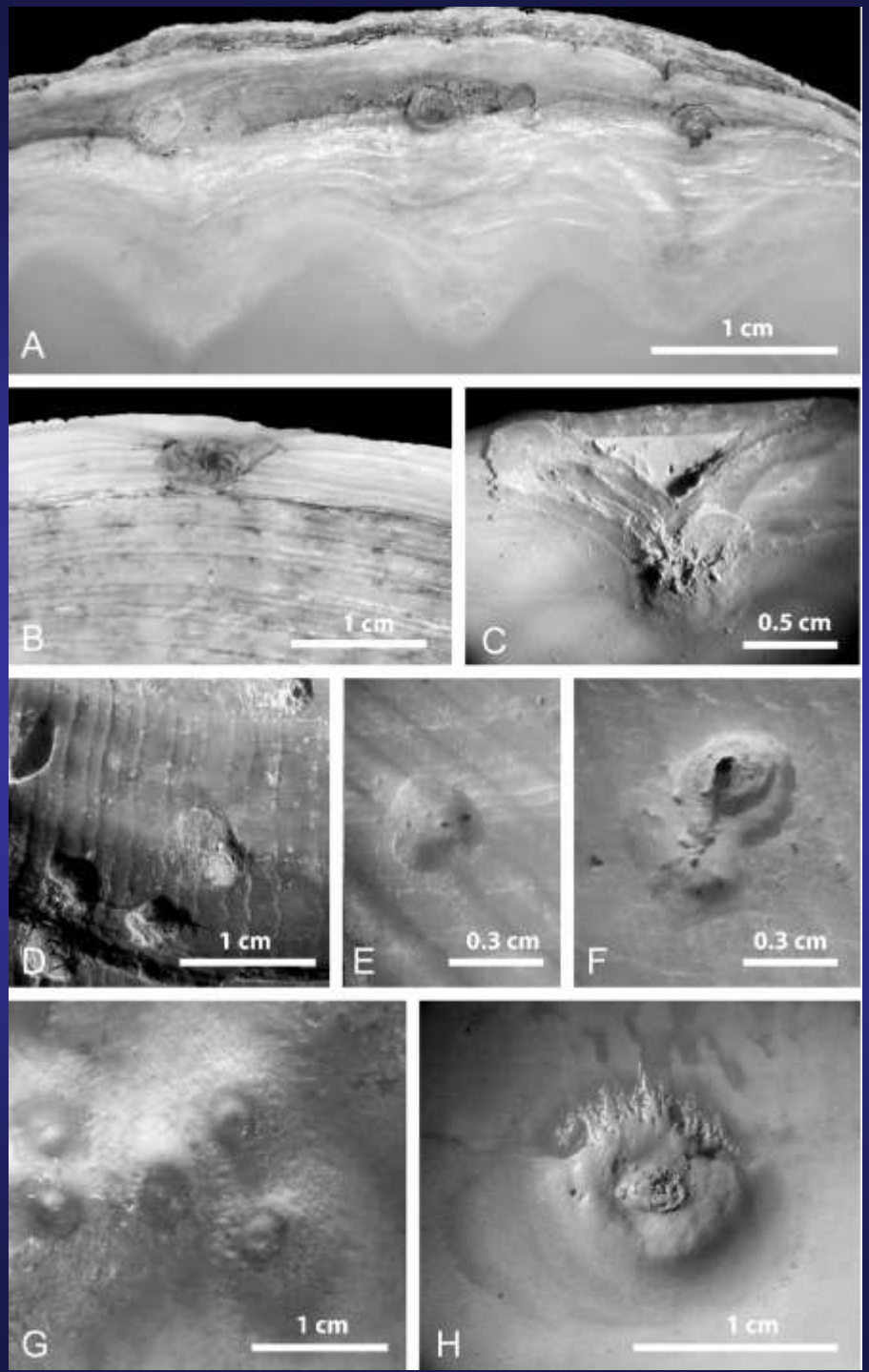

Hyrrokkin spp. as parasites

Hyrrokkin spp. and its traces on *Acesta* spp. and the bivalve's callus formation. **A.** Three attachments on the inner side of *A. patagonica* (Beagle Channel) with two in situ tests; note the retracted mantle precipitates and the partial embedding of the test to the right. This is the only sample with *Hyrrokkin* being attached to the internal side of *Acesta*. **B.** *H. carnivora* close to the margin of *A. excavata* (Mauritania). **C.** Irregular callus resulting from a retracted mantle, due to *H. sarcophaga* close to the margin of *A. excavata* (ALK232-BG-1066). **D.** *H. sarcophaga* scars on a Late Pleistocene *A. excavata* (COR2-8). **E-F.** Varying scar morphology depending on the penetrated mineralogical layers in *A. excavata* (E: calcite, F: calcite and crossed-lamellar aragonite underneath, COR2-39. **G.** Inside of D with callus pinnacles. **H.** Recent callus in *A. excavata* at the pallial line, note the sealed central canal (ALK232-1066-BG)

(Beuck et al., 2008)

Hyrrokkin spp. as parasites

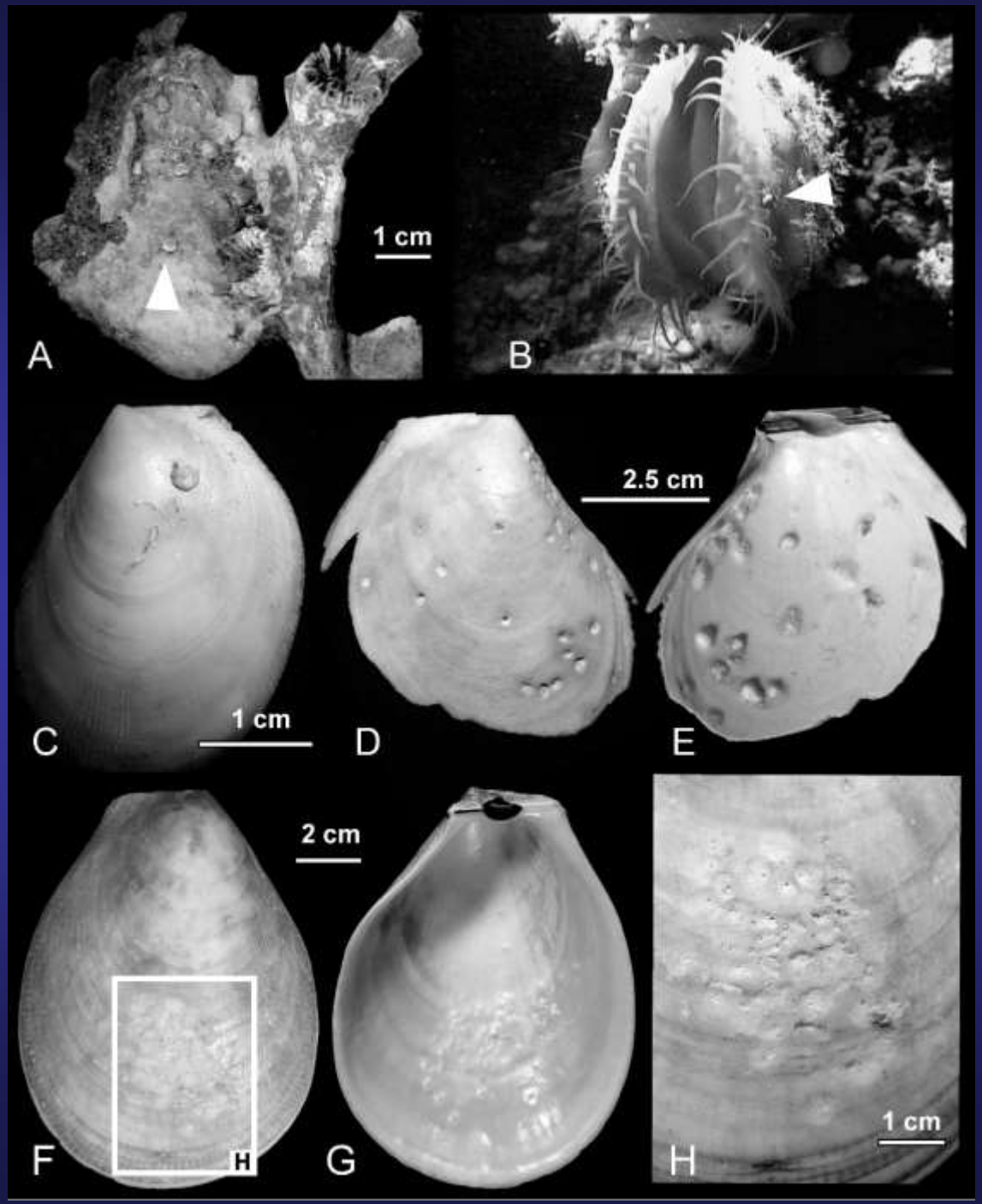

Overview images of *Hyrrokkin* substrates. **A.** Numerous individuals of *Hyrrokkin sarcophaga* (see white arrow) infesting a geodiid sponge, which has overgrown a dead *Lophelia pertusa* branch (LI94-163). **B.** Submersible image of a filtering *Acesta excavata* with a large *H. sarcophaga* specimen attached close to the valve margin (Sula Ridge, Norway). **C.** Juvenile *A. excavata* with a large *H. sarcophaga* specimen (Pos228-215). **D.** Outer surface of a Last Glacial Mediterranean *A. excavata* shell (COR2-39); note the high amount of grooves. **E.** Inner side of D showing the protuberances as reaction of the bivalve against infestation (aragonitic callus formation). **F.** Recent *A. excavata* (Mauritania) with a multitude of attachment scars produced by *Hyrrokkin carnivora*. **G.** Inner side of F, equivalent callus formation as observed for Norwegian *A. excavata* infested by *H. sarcophaga*. **H.** Close-up of F showing high attachment scar densities and part of a *H. carnivora* test.

(Beuck et al., 2008)

A Foraminiferal Parasite on the Sea Urchin *Echinocorys*: Ichnological Evidence from the Late Cretaceous (Lower Maastrichtian,Northern Germany)

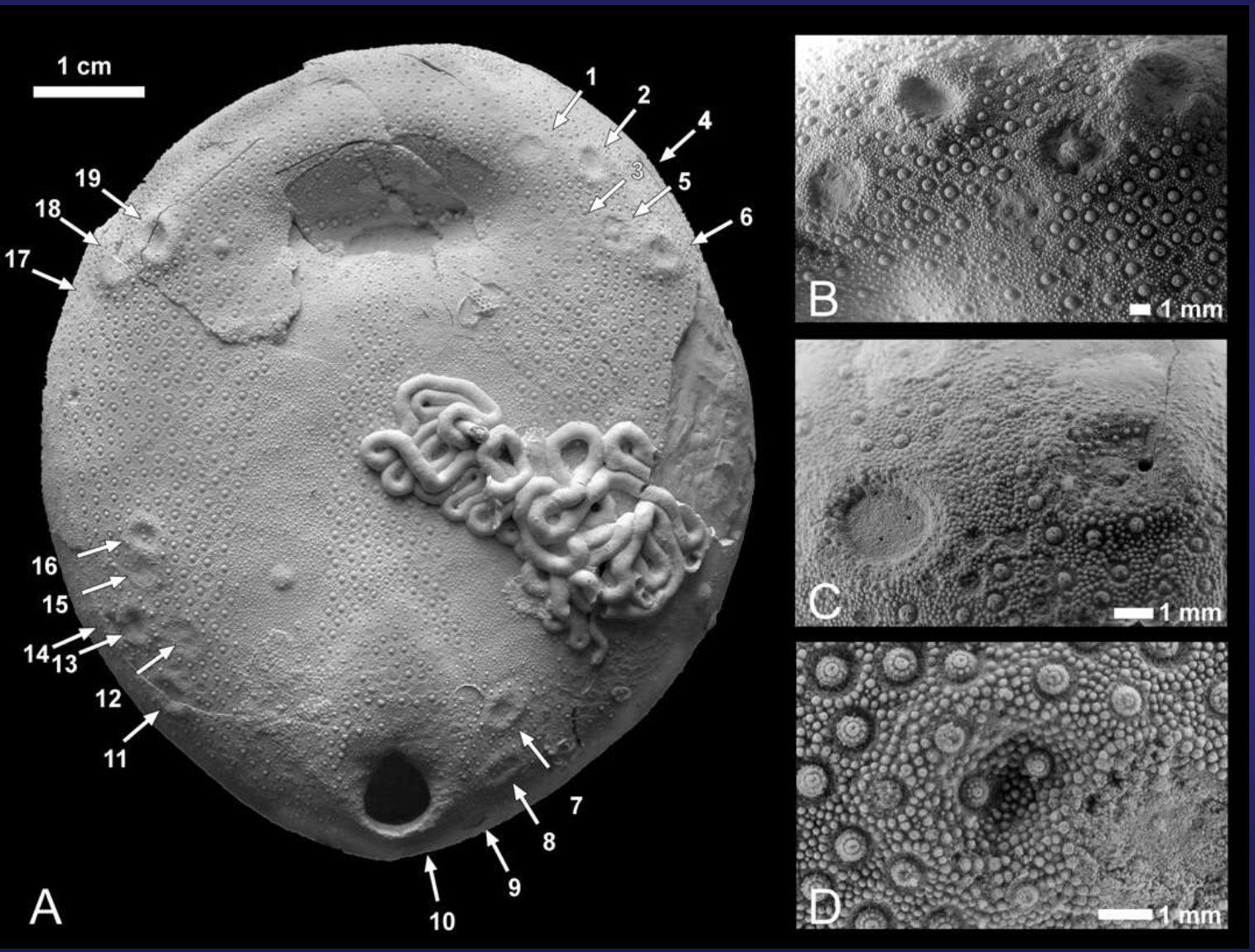

A. Oral side of *Echinocorys perconicus* (MB.E. 5424) exhibiting 19 circular attachment scars (traces numbered clockwise). **B.** Detail of trace 1 to 6 illustrating the morphological range of the trace with absent (3) to pronounced rim (2), and the absence or presence (5) of a central boss. **C.** Two traces, the left one of which (9) with no, the right one (10) with slight regeneration texture. **D.** Trace with pronounced regeneration pattern (6).

(Neumann_Wisshak, 2006)

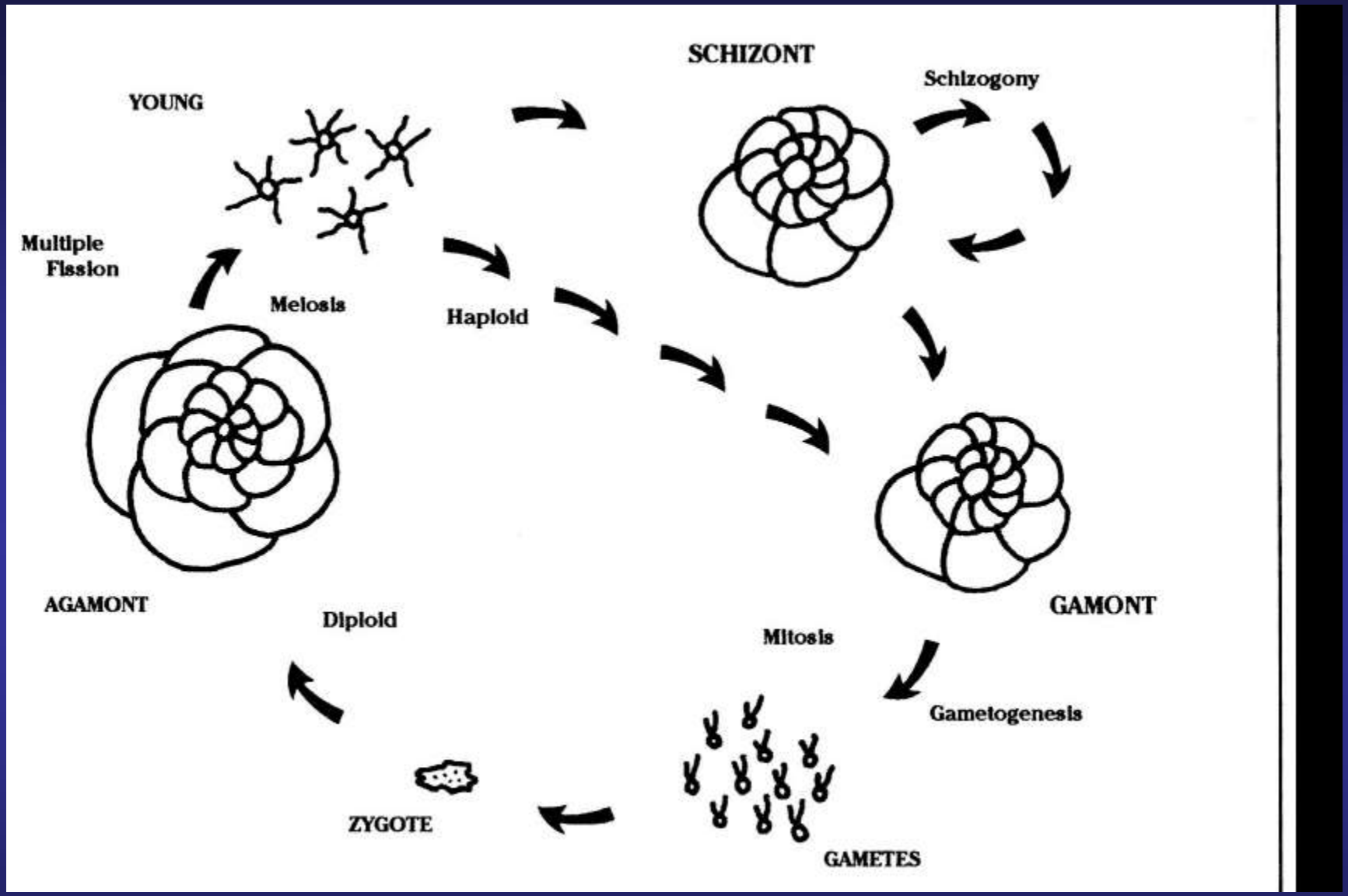

Outline of the formainieral life cycle which classically includes a regular alternation between a haploid, uninucleate, megalospheric gamont, and a diploid, multinuclaeate, microsphereic agamont. Meiosis occurs in the agamont as part of multiple fission, and gametes are produced by mitosis. In some species, the life cycle also includes a schizont which is produced from the agamont and reproduces asexually. It can interject numerous successive asexual cycles. Meiosis typically occurs in the aganont. However, the type of nuclear divisions in the schizont have not been documented for any species (Goldstein, 1999).

Other foraminifers as commensals or parasites

Cibicides spp., Acervulina inhaerens, Paromalina coronata, - часто обнаруживаются на раковине моллюсков, но никогда не вызывают коррозию створок.

Cibicides refulgens, *Rosalina globularis* осядают на раковину двустворки *Adamussium colbecki*, при этом предпочитают садиться на верхнюю створку. Они просверливают раковину двустворки и питаются мягкими тканями хозяина (Mullineaux, DeLaca, 1984; Alexander, DeLaca, 1987).

Cibicides spp., *Acervulina inhaerens*, *Paromalina coronata* as commensals on bivalves

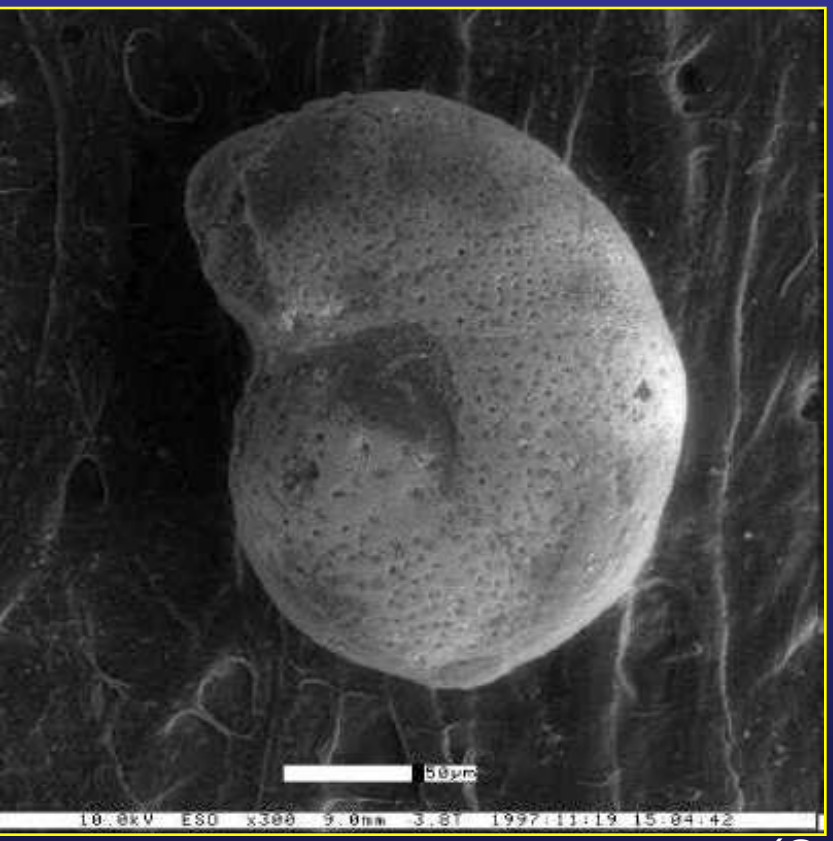

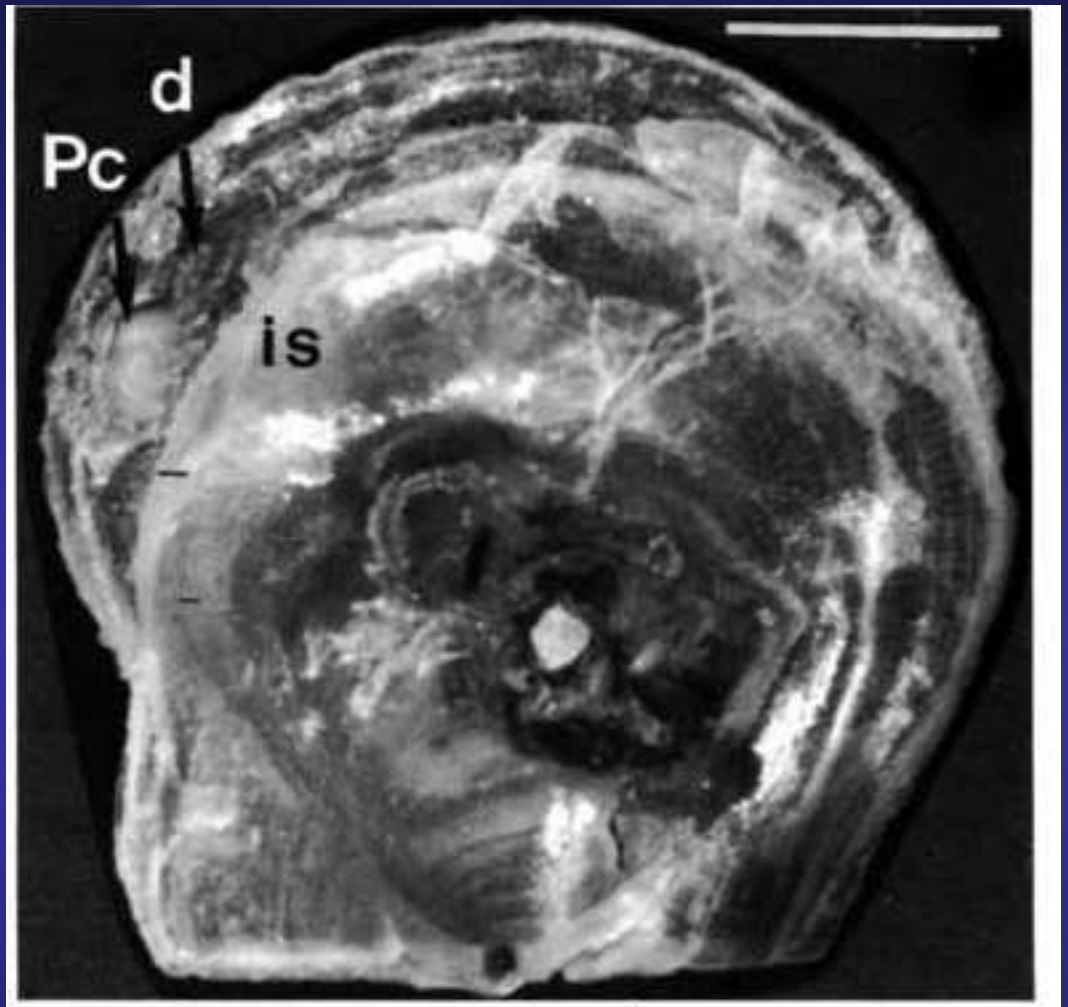

Fig. 12. *Delectopecten vitreus* with a *Paromalina coronata* specimen (Pc) on the inner edge of its shell, causing the bivalve to build an additional, internal shell (ic), d = detritus collected by the foraminiferan (Sample No. 58). Scale bar = 1 mm.

(Cedhagen, 1994)

Cibicides refulgens as a parasite

Adamussium colbecki
(Alexander, DeLaca, 1987)

Oblique view of the dorsal valve of *A. colbecki* with attached *C. refulgens* and associated agglutinated tubes reaching into the overlying water. Vertical tubes may extend to 5 mm and exhibit three orders of branching. Scale bar= 5mm.

Feeding adaptations of the goraminiferan *Cibicides refulgens* living epizoically and parasitically on the antarctic scallop *Adamussium colbecki*

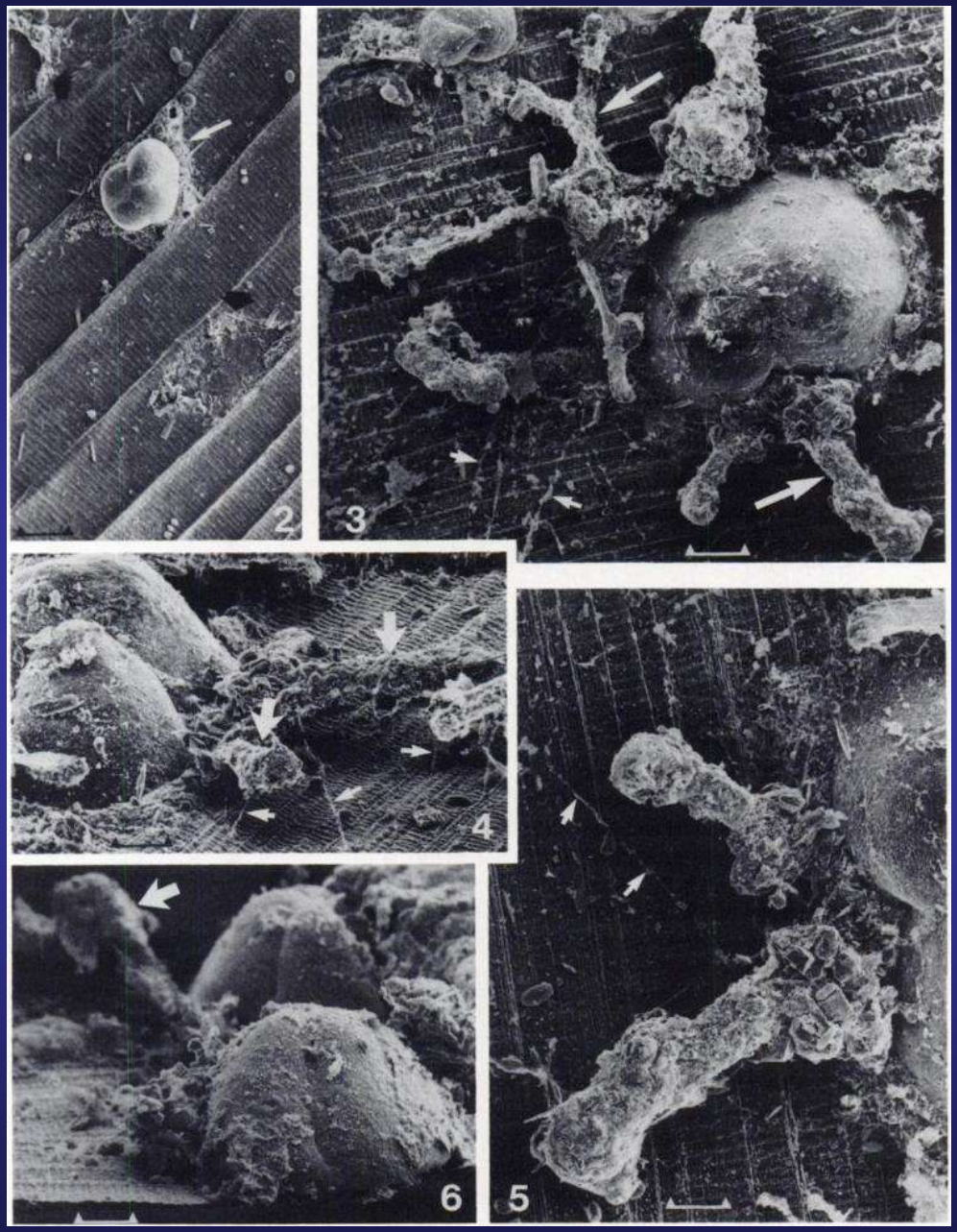

2. Juvenile *Cibicides refulgens* attached to surface of *A. colbecki* dorsal valve. A rudimentary peripheral agglutinated tube has been built (white arrow). Vertical tubes are not present. Two juveniles have been removed to show the shallow surface etching of the shell (black arrows). Scale bar= 163 mkm. 3. Plan view of an attached adult with a well developed agglutinated tube system (large arrows) and net of pseudopodia on the scallop shell surface (small arrows). Scale bar =200 mkm. 4. Oblique view of specimen in Figure 3. Pseudopodia (small arrows) can be seen traversing the space between the agglutinated tubes (large arrows) and the substrate. Scale bar = 143 mkm. 5. Detail of Figure 3 showing composition of agglutinated tubes and the presence of a fine pseudopod (arrows) radiating away from the foraminifer, across the shell surface. Scale bar = 102 mkm. 6. Oblique view of two attached adult *Cibicides refulgens*. An agglutinated tube can be seen clearly raised away from the scallop shell surface (arrow). Scale bar = 154 mkm.

(Alexander, DeLaca, 1987)

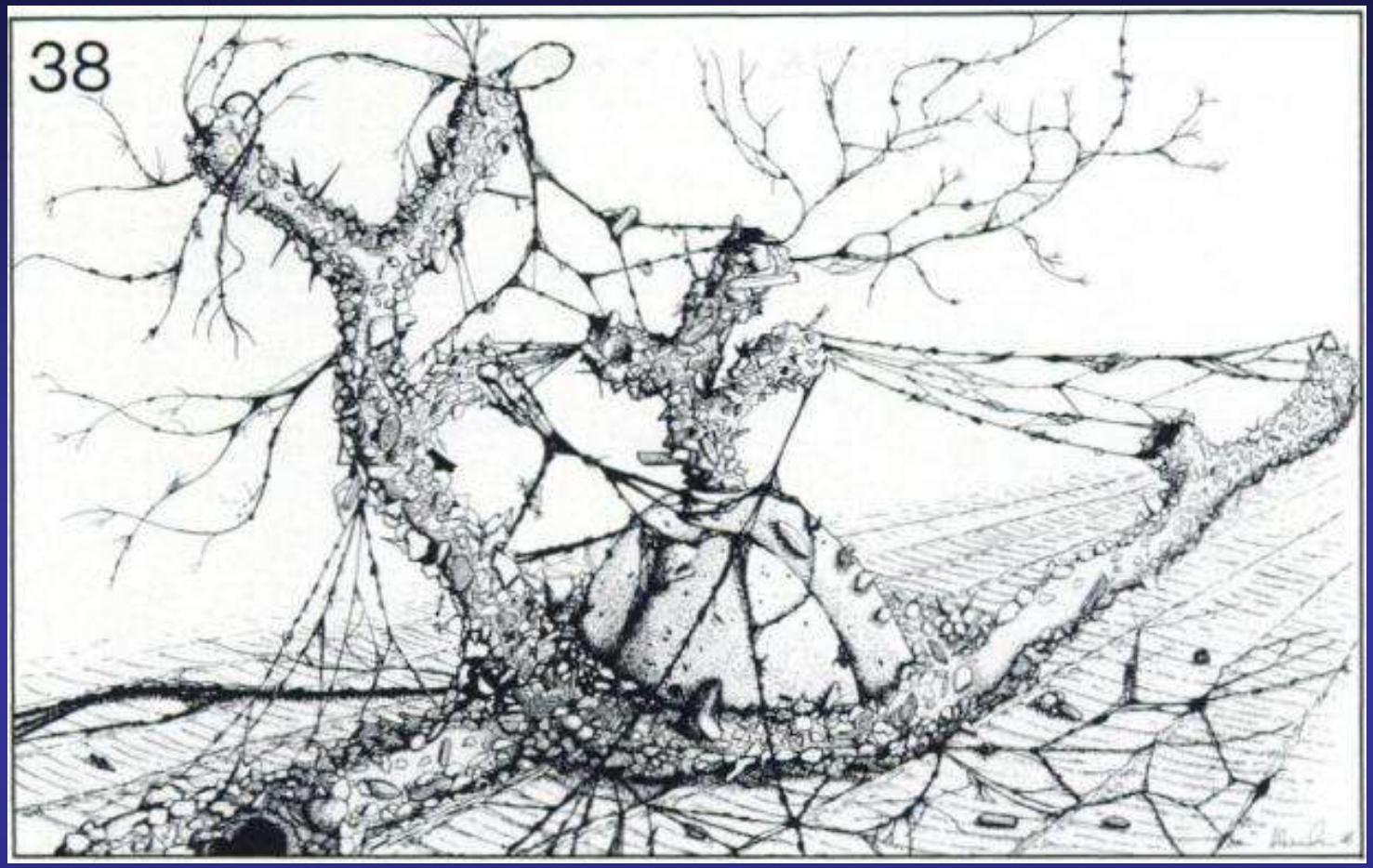

Cibicides refulgens attached to the shell of *Adamussium colbecki*. with pseudopodia deployed from agglutinated structures. (Not to scale.)

(Alexander, DeLaca, 1987)

Feeding Adaptations of the Foraminiferan *Cibicides Refulgens* Living Epizoically and Parasitically on the Antarctic Scallop *Adamussium colbeckii*

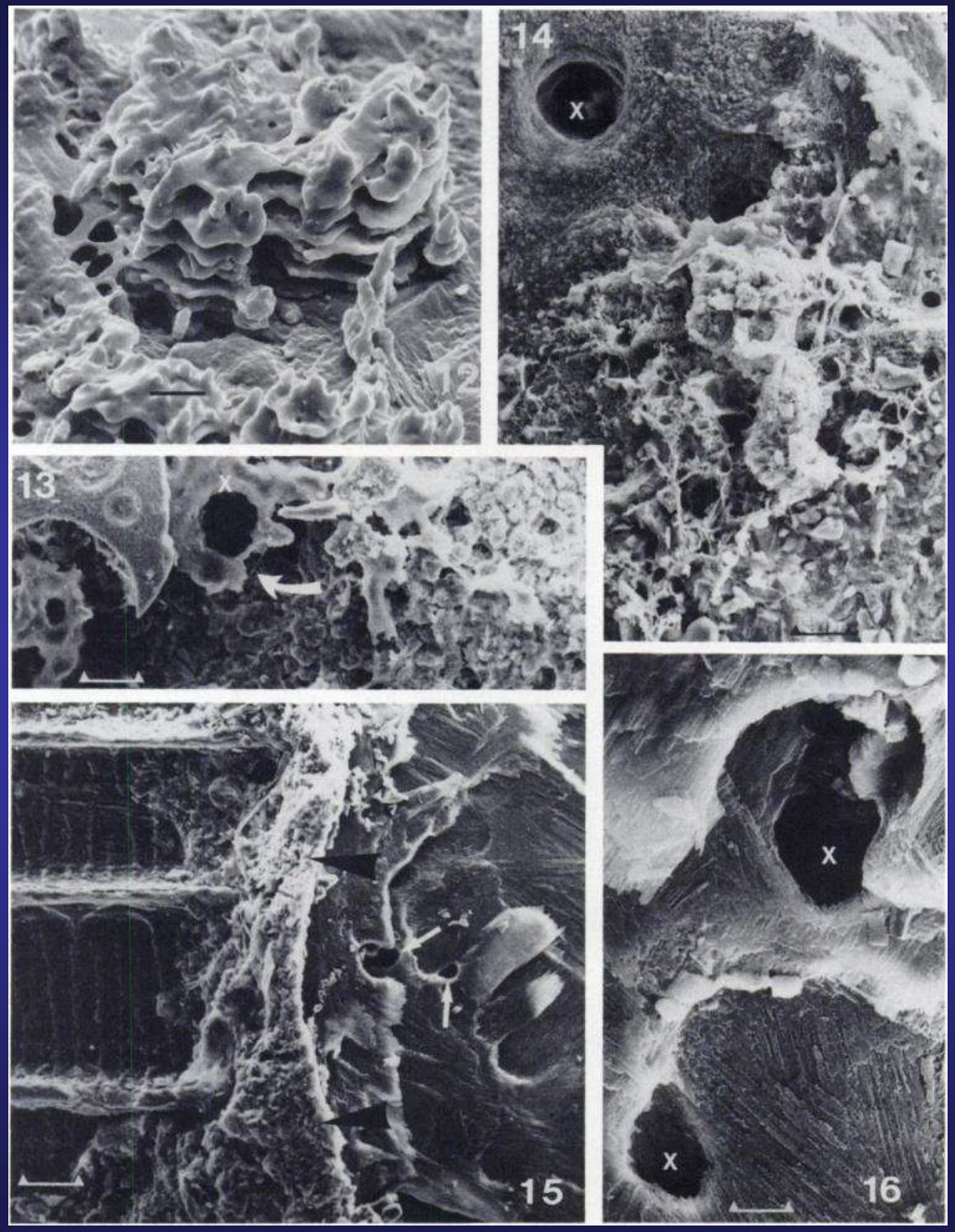

12. A resin cast of the central portion of a substrate pit formed by an adult *Cibicides refulgens*; the raised central area represents channels within the scallop shell which were originally occupied by foraminiferal cytoplasm. Scale bar =20 mkm. 13. Irregular etching of calcite at the pit edge. A bored hole in upper calcite layer (X) has been undercut by subsequent dissolution of lower layers (arrow). Scale bar = 31 mkm. 14. Peripheral area of a deep substrate pit showing transition from scallop shell surface (bottom right) to extensively etched pit base (top left) and a circular vertical boring (X). Scale bar = 18 mkm. 15. Transition from normal scallop shell surface (left) to a deep pit (right) eroded by a large adult *Cibicides refulgens*. Removal of the foraminifer has torn away the uppermost calcite layer, exposing unetched laminae beneath and canals penetrating deeper into the shell material (arrows). Part of the agglutinated peripheral tube remains secured to the shell surface (large arrowheads).Scale bar =36 mkm. 16. Detail of Figure 15 demonstrating the distinct canal borings (X) in shell material beneath the attached foraminifer. Scale bar = 6.7 mkm.

(Alexander, DeLaca, 1987)

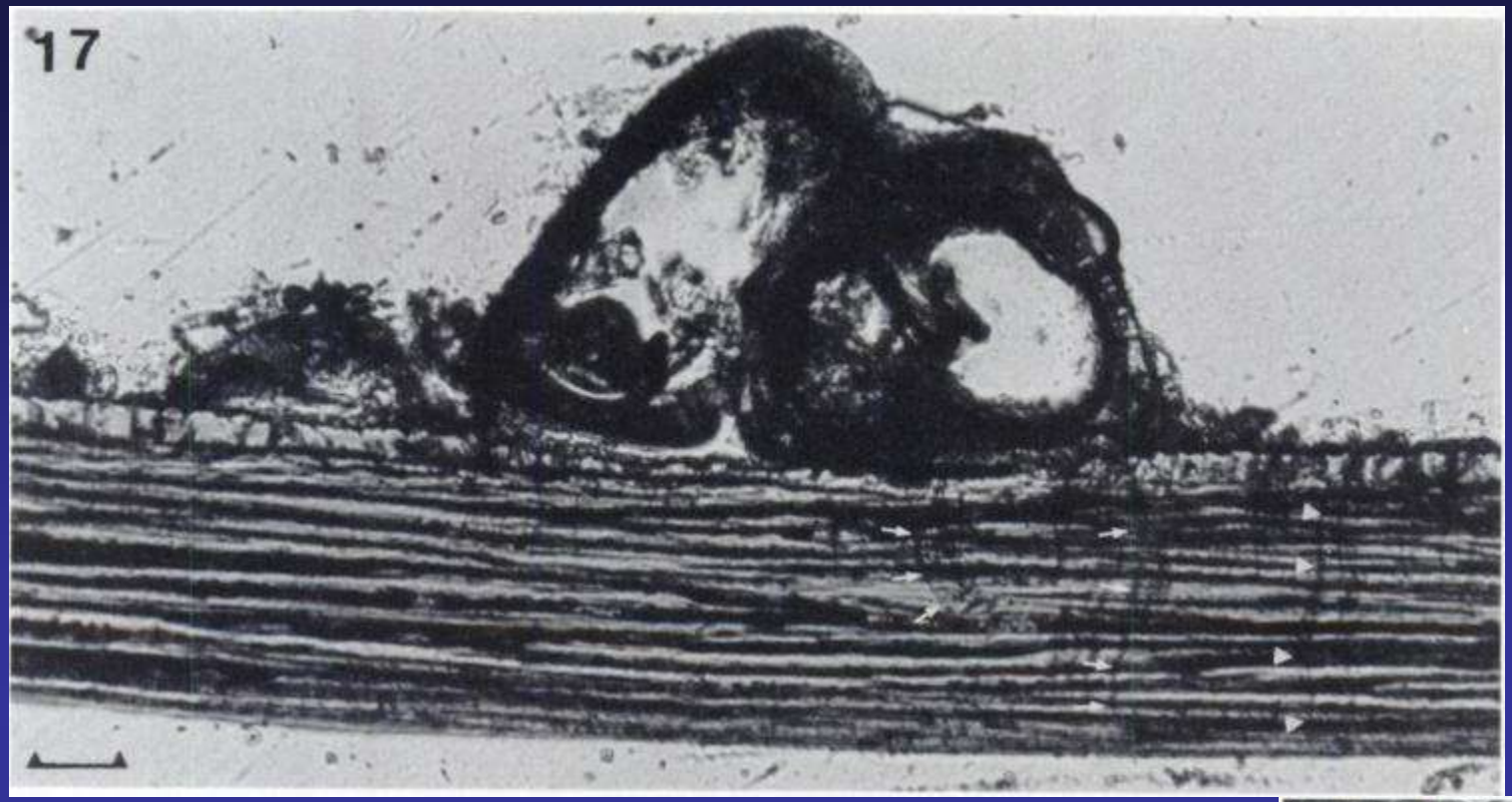

17. Thick cross section through a resin-embedded adult *Cibicides refulgens* attached to *Adamussium colbecki*. Groups of canals are discernible originating from the base of the pit and passing through most of the shell thickness (arrows). Scale bar = 200 mkm.
18. Detail of Figure17 showing the canals to be continuous through to the inner-most laminae of the scallop shell (arrows). Scale bar = 480 mkm.

(Alexander, DeLaca, 1987)

Foraminiferans as parasites of chitons

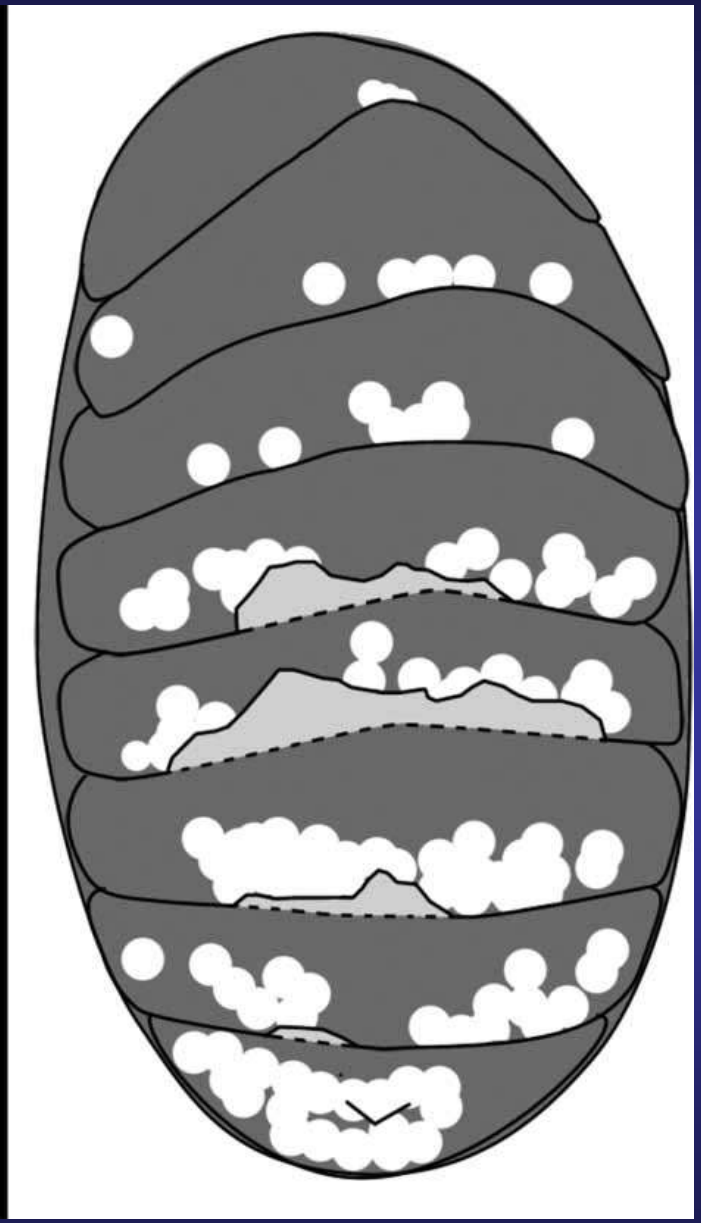

Photograph and line drawing of *Leptochiton arcticus* specimen heavily infested with epibiotic foraminifers, with anterior at top. White spots on line drawing indicate foraminifers or bioeroded scars caused by foraminifers; light grey areas indicate posterior margins of intermediate valves that have been completely broken away by the bioerosion of epibionts. Scale bar10 mm.

Hyrrokkin sarcophaga,
Cibicides refulgens,
Cibicides lobatulus,
Cibicides wuellerstorji

(Sigwart, 2009)

Leptochiton arcticus

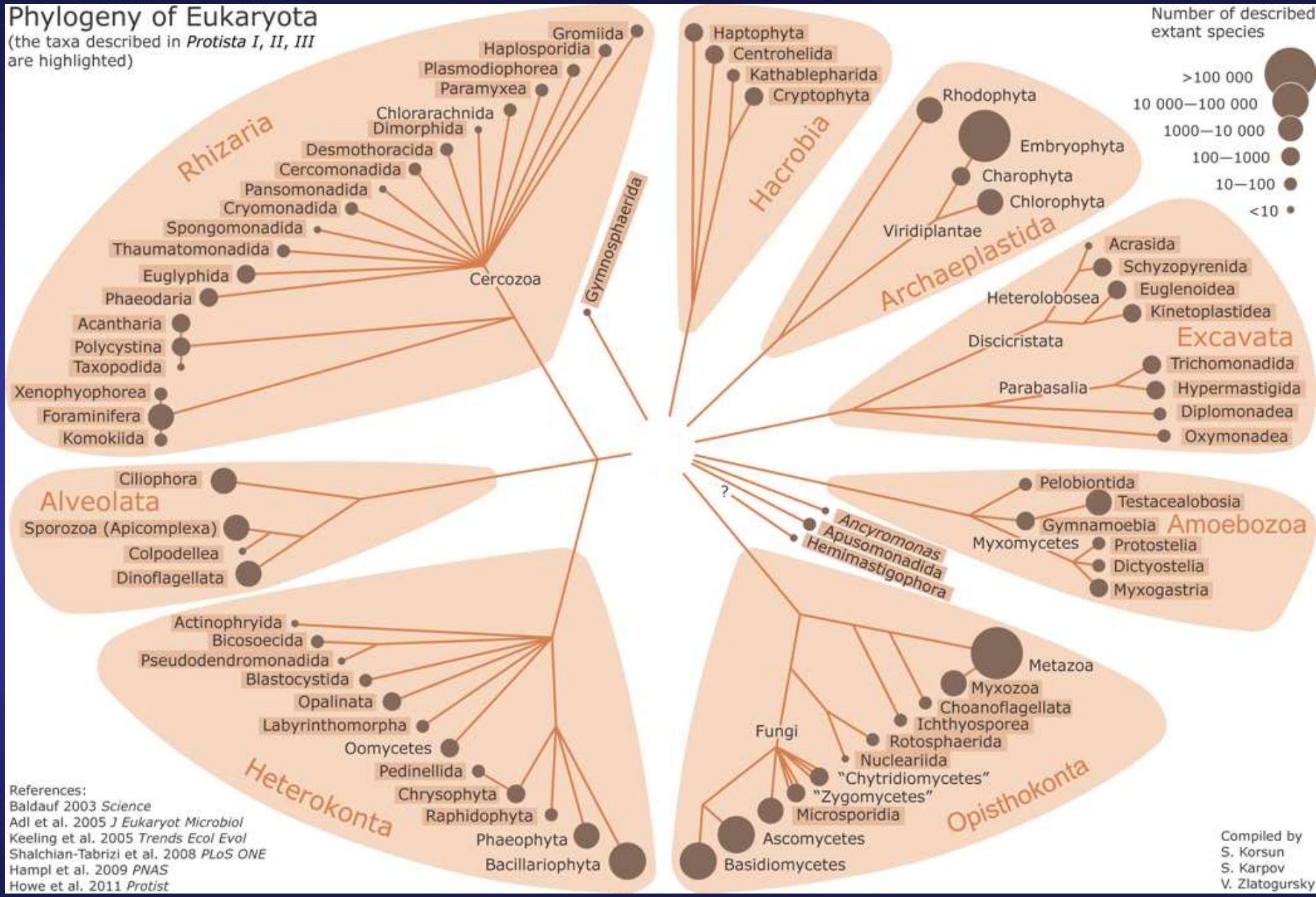

References:
Baldauf 2003 *Science*
Adl et al. 2005 *J Eukaryot Microbiol*
Keeling et al. 2005 *Trends Ecol Evol*
Shalchian-Tabrizi et al. 2008 *PLoS ONE*
Hampl et al. 2009 *PNAS*
Howe et al. 2011 *Protist*

Compiled by
S. Korsun
S. Karpov
V. Zlatogursky

Vampyrellidae
Rhizaria, Cercozoa

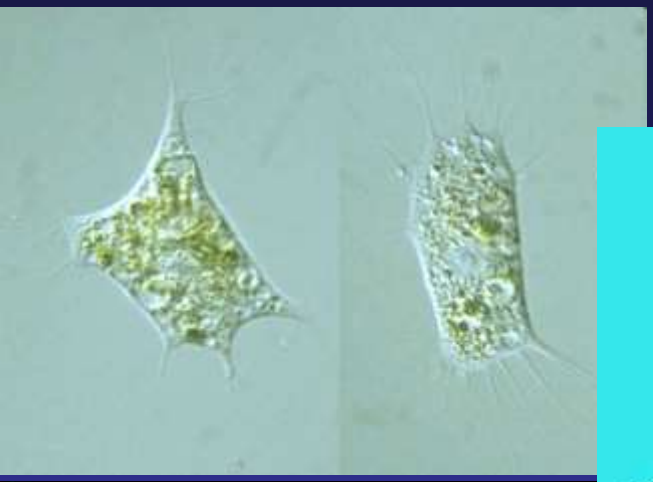

Nuclearia

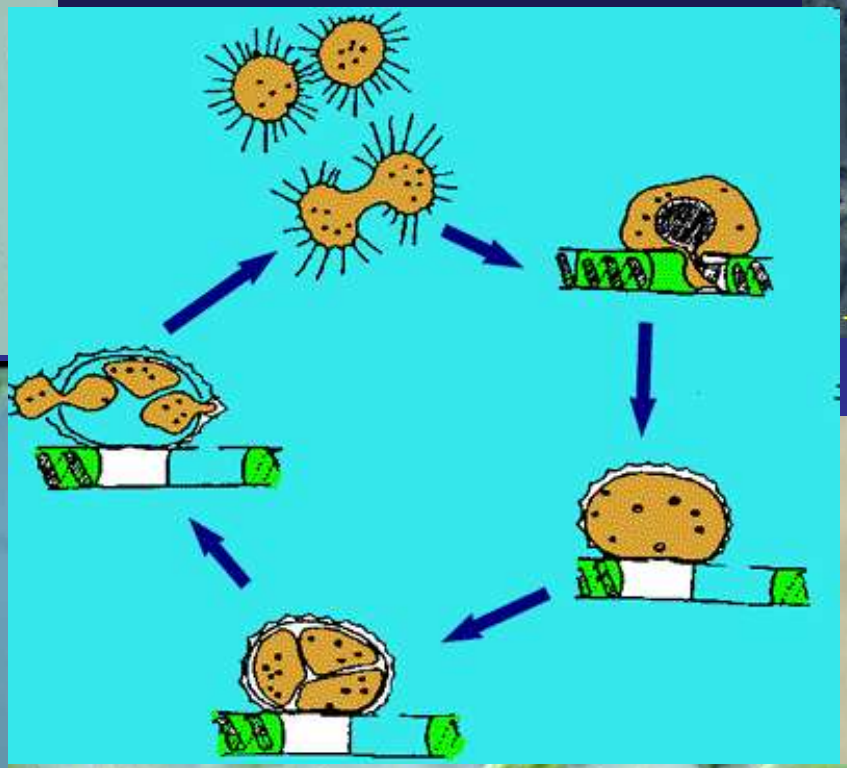

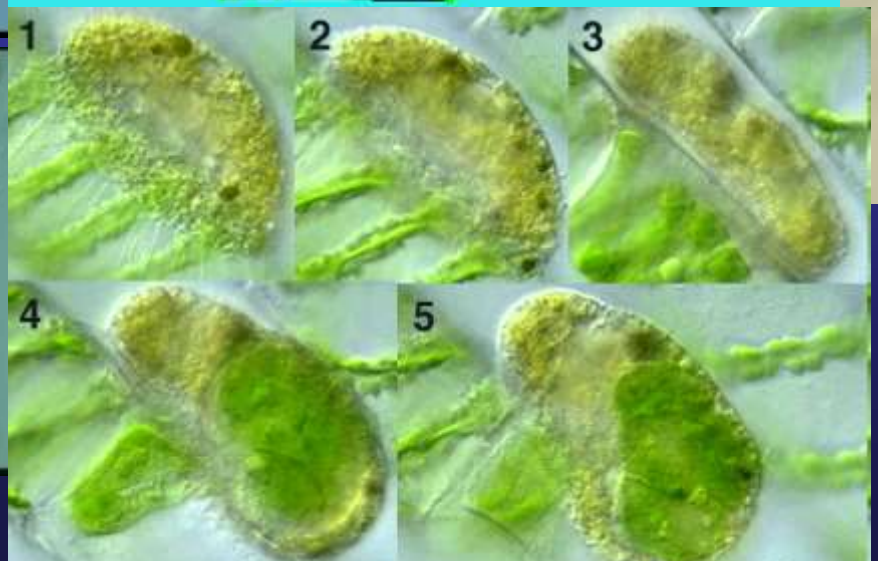

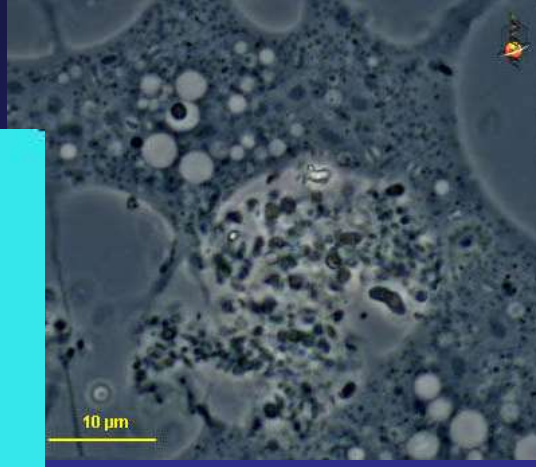

Arachnula

Vampyrella lateritia

http://ameba.i.hosei.ac.jp/BIDP/amoeba/QuickEate/

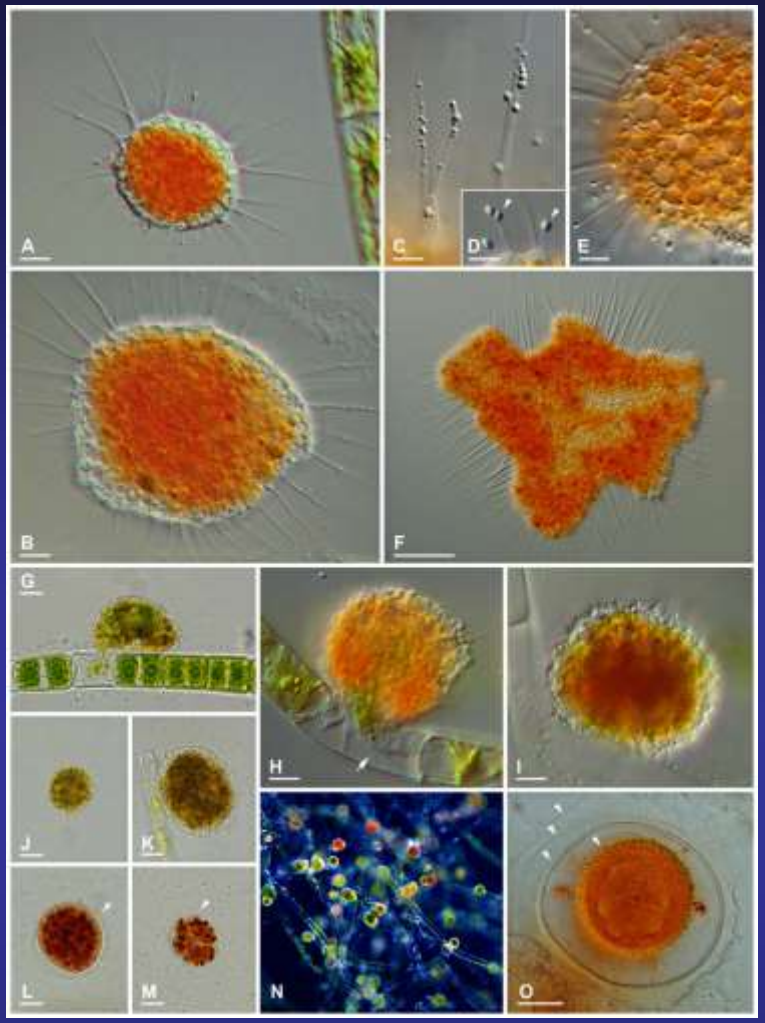

Vampyrella lateritia

Life history stages and morphological traits of *Vampyrella lateritia*. **A**. Advancing trophozoite. DIC. **B**. Large trophozoite likely a result from cell fusions. DIC. **C**. Membranosomes moving along the pseudopodia. DIC. **D**. 'pin-like' pseudopodia, arrowheads: membranosomes. DIC. **E**. Numerous vacuoles in the cell periphery. **F**. Large, bulky plasmodium. DIC. **G**. Attached *Vampyrella* cell ingesting algal cell content. Brightfield. **H**. Ingestion pseudopodium (arrow) emptying an algal cell. DIC. **I**. Immobile *Vampyrella* cell with retracted pseudopodia and spiny surface turning into digestive cyst. DIC. **J**. Green motile cell after food uptake. Brightfield. **K**. Early digestive cyst stage with greenish contents. Brightfield. **L**. Mature digestive cyst with delicate outer cyst envelope (arrowhead). Brightfield. **M**. Digestive cyst with progeny after cell divisions in characteristic arrangement, arrowhead: outer cyst envelope. Brightfield. **N**. Digestive cysts at various stages in different colours. Dark field. **O**. Resting cyst with four envelopes (arrowheads). DIC. Scale bars: A, B, H, I, O= 10 mm; C–E = 5 mm; F = 50 mm; G, J–M = 20 mm (Hess et al., 2012).

Vampyrella pendula

Trophozoites and digestive cysts of *Vampyrella pendula*. **A** & **B**. Advancing trophozoites. Brightfield. **C**. Trophozoite and digestive cyst on a filament of *Oedogonium*. Brightfield. **D**. Trophozoite with clear pseudopodia lacking membranosomes. DIC. **E** & **F**. Trophozoite producing claviform pseudopodia (arrows). DIC. **G**. Early digestive cyst stage. DIC. **H**. Mature digestive cyst. DIC. **I.** Remaining digestive cyst envelopes with food remnant. DIC. Asterisk = very faint outer sheath, hollow arrows = outer cyst envelope, hollow arrowheads = delicate strands between outer and intermediate cyst envelope, arrowheads = central stand running from innermost cyst envelope through stalk. Scale bars: 10 mm (Hess et al., 2012).

Hyalotheca dissilens is attacked by *Hyalodiscus rubicundus.*

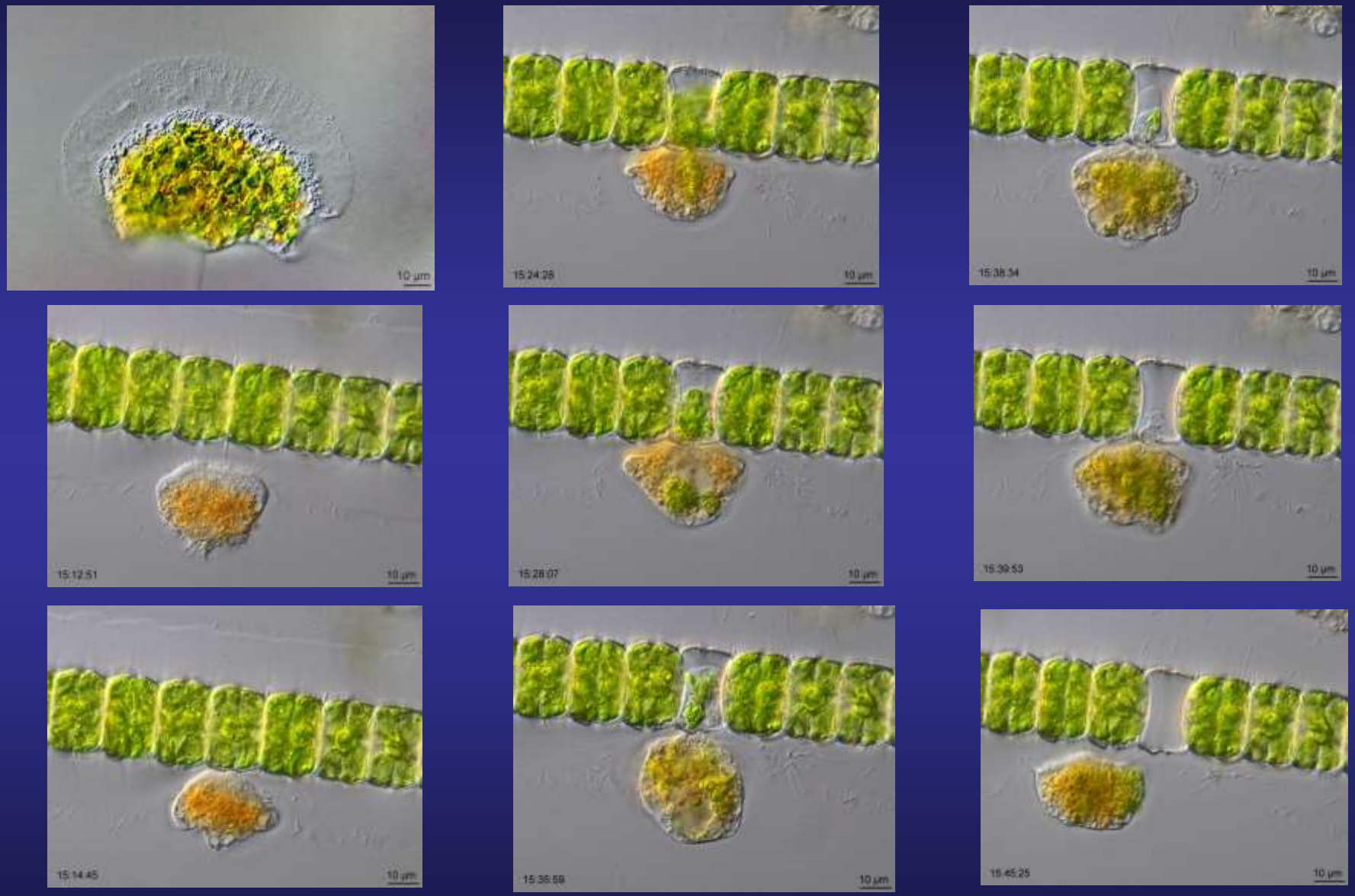

Siemensma, F. J., *Microworld, world of amoeboid organisms*. World-wide electronic publication, Kortenhoef, the Netherlands. https://www.arcella.nl.

This very instructive and beautiful video was made by Norbert Hülsmann and shows the development and mode of nutrition in *Vampyrella lateritia,* with following comment: "There are three strains of *Vampyrella lateritia* which are known to feed on green algae. One attacks *Spirogyra*, a second *Closterium* and the third *Mougeotia*. *V. lateritia* bores a hole through the algal cell wall and surrounds the protoplast with an ingestion pseudopodium. *Vampyrella* encysts after phagocytosis has been completed. Vegetative swarmers are subsequently released from the cyst.“ (**Siemensma, F. J., *Microworld, world of amoeboid organisms*. World-wide electronic publication, Kortenhoef, the Netherlands. https://www.arcella.nl.**)

Vampyrellidae: *Lateromyxa gallica*

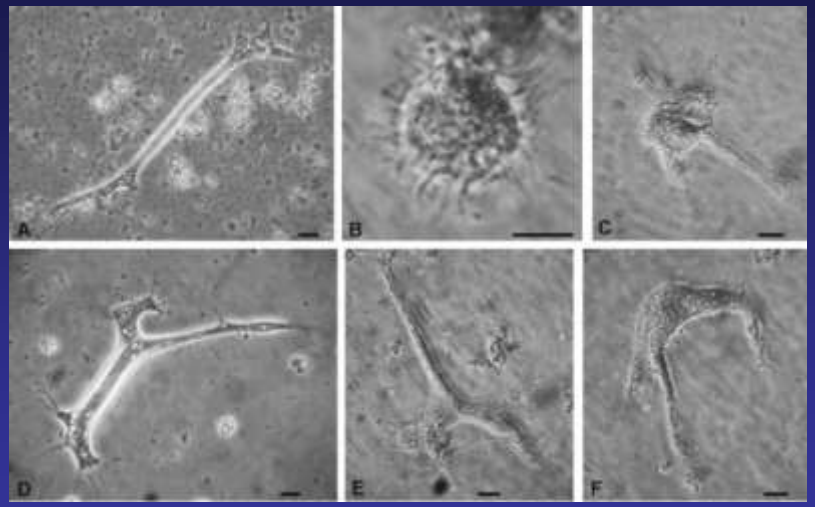

Lateromyxa gallica has been isolated several times from two lakes in central France between September 1973 and August 1989 and cultivated for several months or years under laboratory conditions. No essential variations of feeding behaviour were found over the time; all isolated strains invade the trichomes of the green alga *Oedogonium* and move, divide and encyst inside the vanished plant cells. Penetration is performed by attacking the cross walls and only primary attacks are directed against the lateral cell walls of the algae. These findings contrast with the behaviour, life cycles and fine structure of all known species of the genera *Vampyrella*, *Hyalodiscus*, *Arachnula* and *Gobiella* (Hülsmann, 2007).

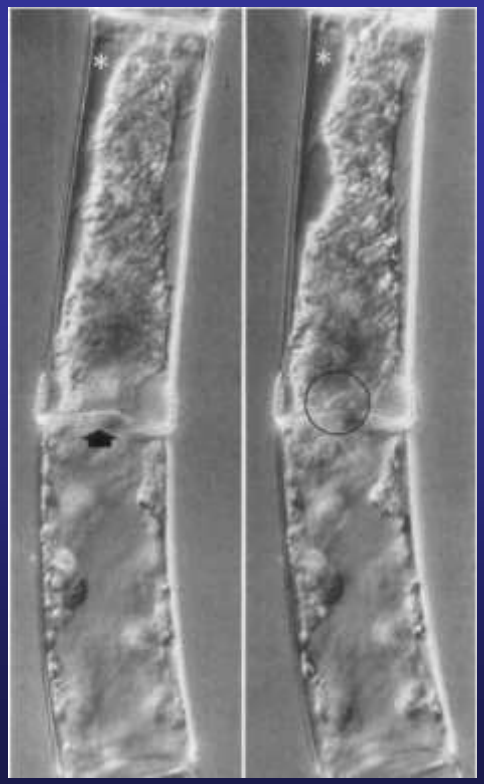

Attack of an invaded trophozoite of ***Leptomyxa gallica*** against the cross wall of an *Oedogonium* cell. **x** 800. Bar 9 mkm. The invader fills the lumen (*) of the upper (vanished) *Oedogonium* cell and exhibits again small and short filopodia. ***Left***. The front is in intimate contact with the cross wall (arrow). ***Right.*** An approx. 6 mkm operculum of the cell wall (seen in optical cross section) opens into the cytoplasm (circle) (Hülsmann, 2007).

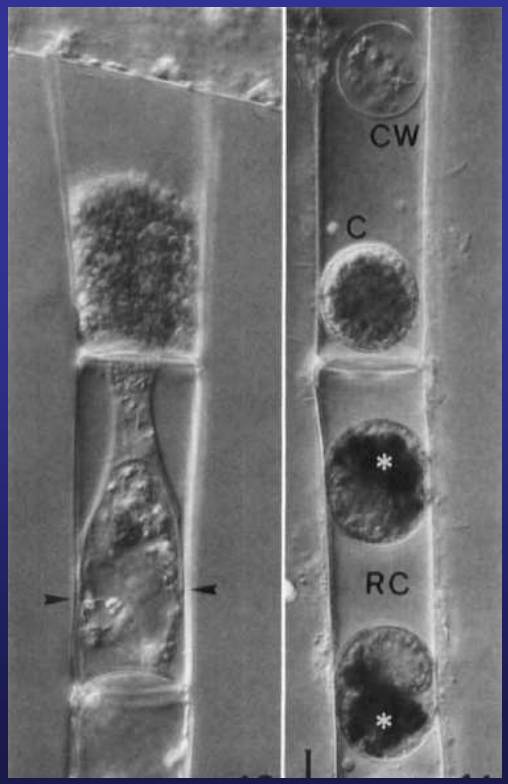

Leptomyxa gallica. Late stage of food uptake and the morphological aspects of cysts inside *Oedogonium* cells. ***Left***. The plant cytoplasm is engulfed by a protruded bell-shaped ingestion pseudopodium. The leading edge of the pseudopodium (optically longitudinally sectioned) is marked by arrowheads. ***Right.*** Empty digestive cyst (CW), digestive cyst (C) and two ovoid resting cysts each inside digestive cysts (RC). Egesta remaining outside resting cysts are marked by asterisks. Bar = 10 mkm (Hülsmann, 2007).

Vampyrellidae: *Lateromyxa gallica*

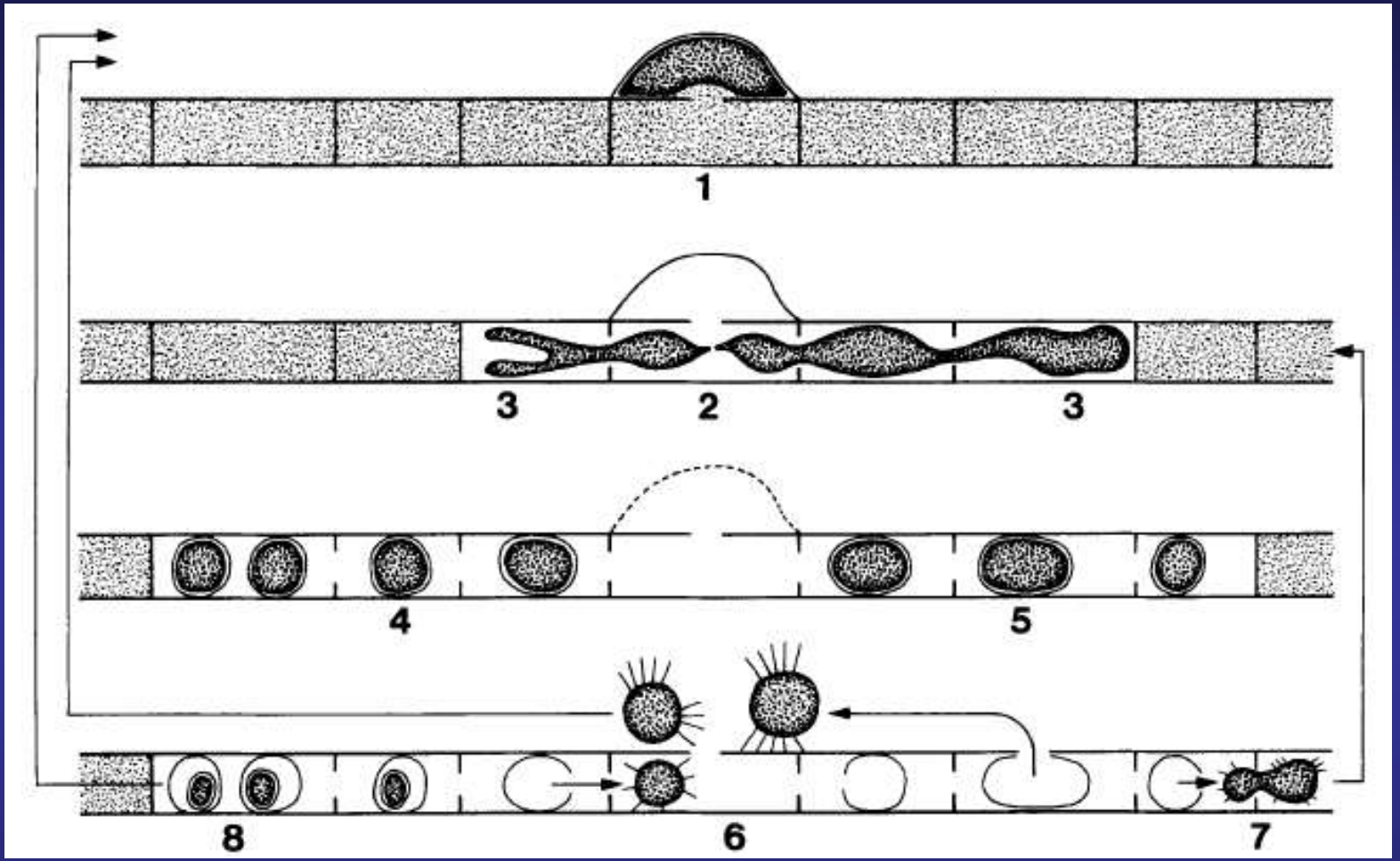

Schematic presentation of the life cycle of *Leptomyxa gallica*. (1) Beginning of a lateral attach against intact *Oedogonium* cells. The attach is preceded by secretion of a cyst-like envelope. After invasion, larger syncytia divide into smaller ones (2) which undergo further divisions during migration (3) through the algal trichome leading to the terminal and obligatory formation of digestive cysts (4) or digestive-multiplicative cysts (5). Excystation is combined with leaving the trichome (6) and starting again at (1) or by attacking the cross walls of adjacent Oedogonium cells (7 and 3). Formation of resting cysts (8) sets out from digestive or muliplicative cysts (4, 5) and coincides with the excretion of debris and with the secretion of an additional internal cystic wall (Hulsmann, 2007).

Vampyrellidae
Theratromyxa weberi

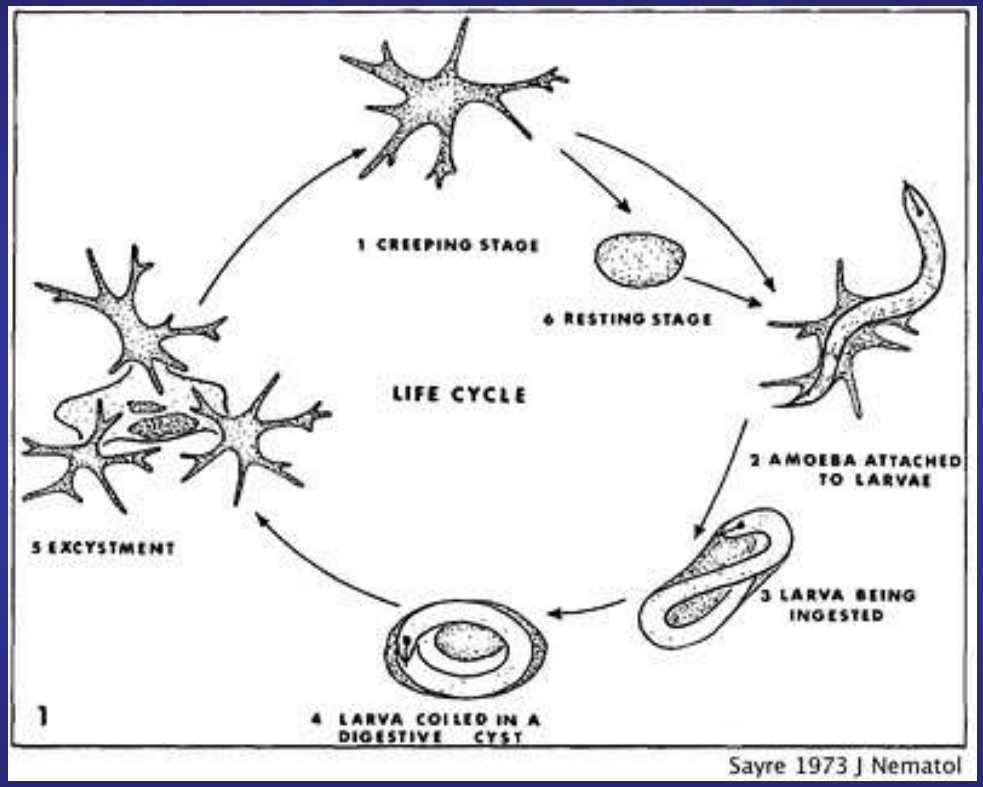

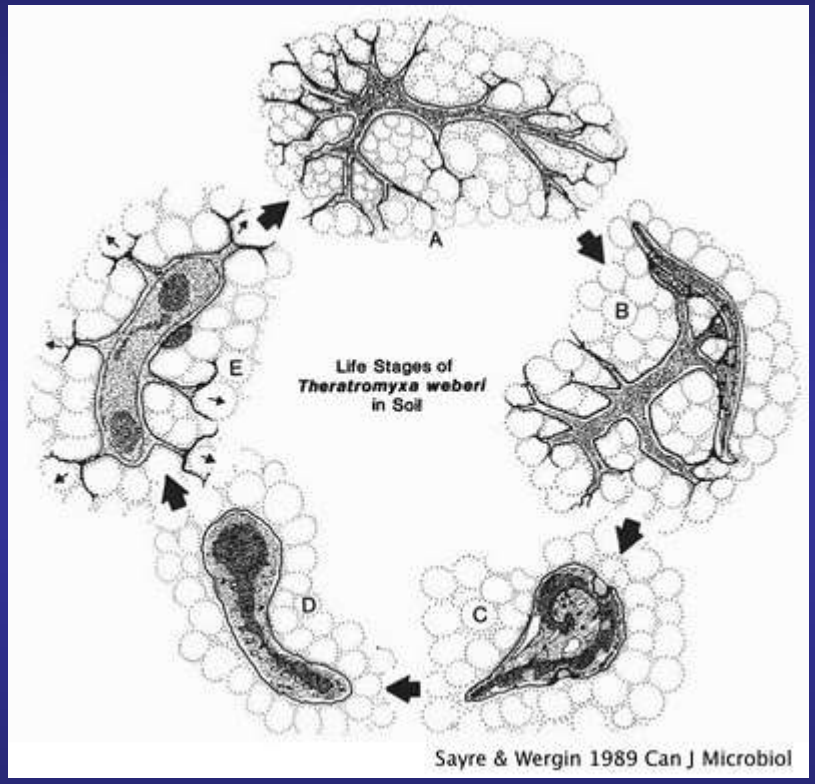

Life cycle of *Theratromyxa*, involving predation on food a little too large for its size followed by long-term digestion and slumber in cysts. Not a bad lifestyle (Sayre, 1973).

Vampyrellidae
Theratromyxa weberi

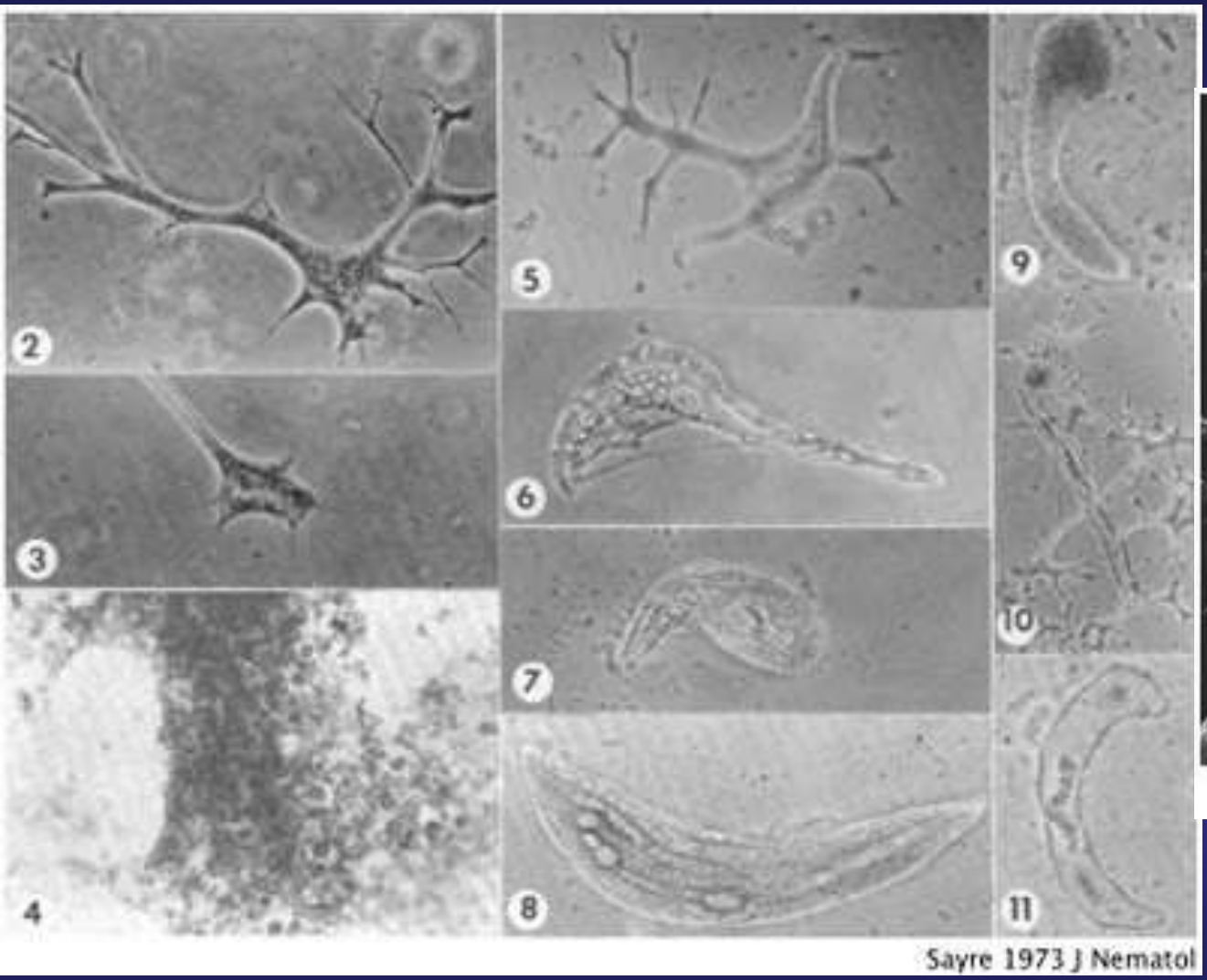

Sayre 1973 J Nematol

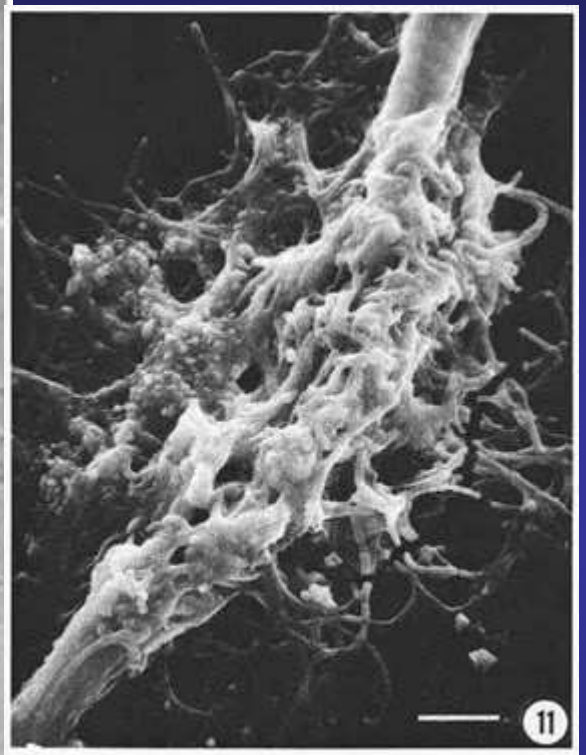

Sayre & Wergin 1989 Can J Microbiol

Theratromyxa: **capturing a nematode. Image 6 shows quite nicely how *Theratromyxa* captures the nematode. This looks rather similar in principle to the feedin veil of dinoflagellate *Ptotoperidium*. Sometimes the amoeba can capture several nematodes at once. SEM shows amoeba enveloping a nematode (Sayer, 1973; Sayer, Wergin, 1989).**

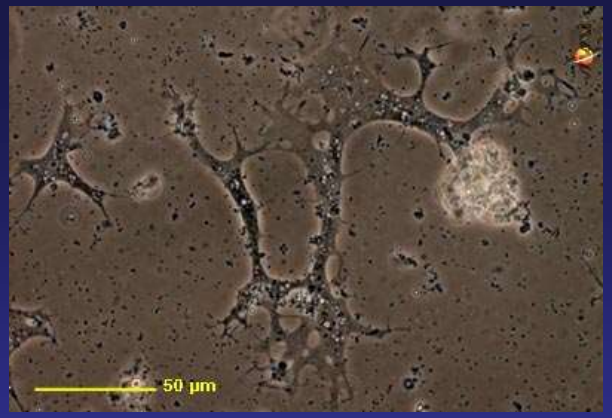

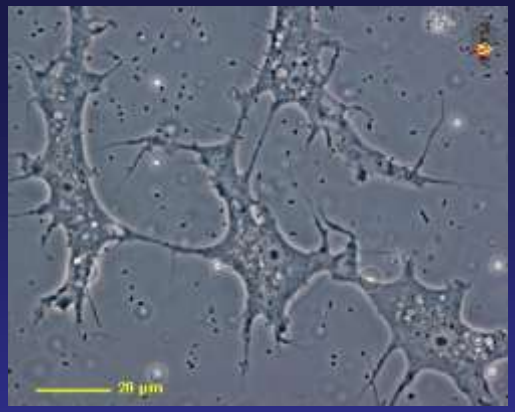

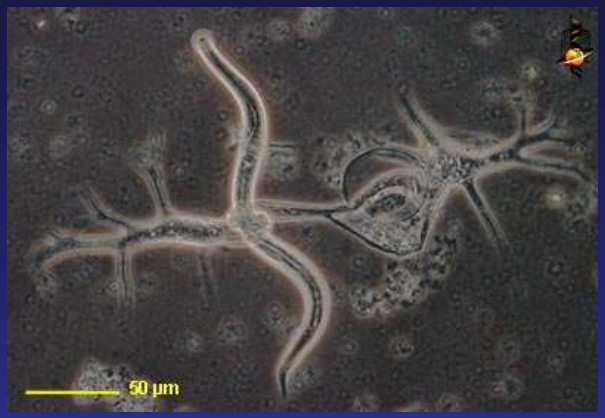

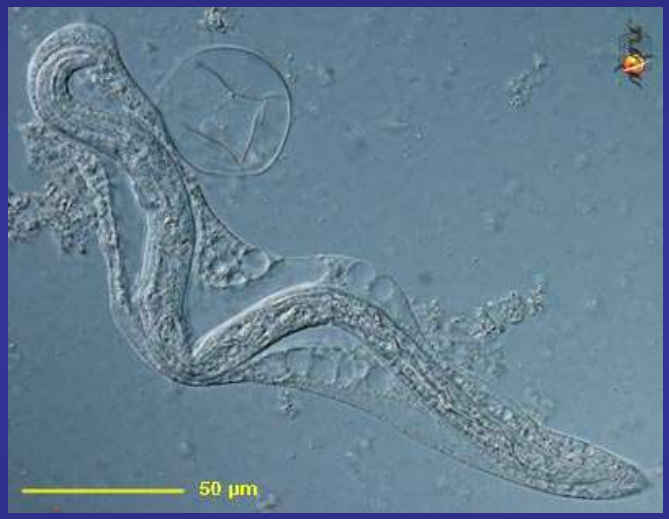

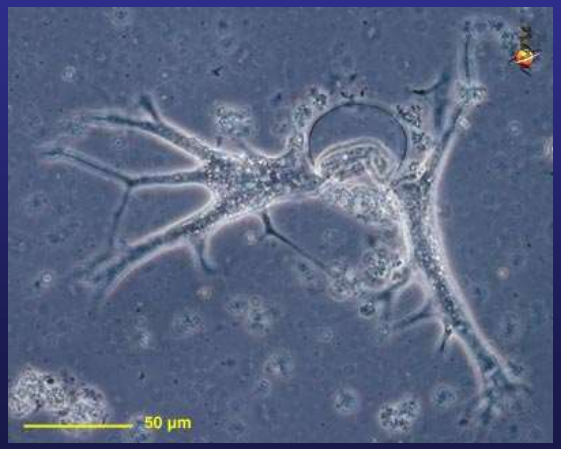

Theratromyxa weberi

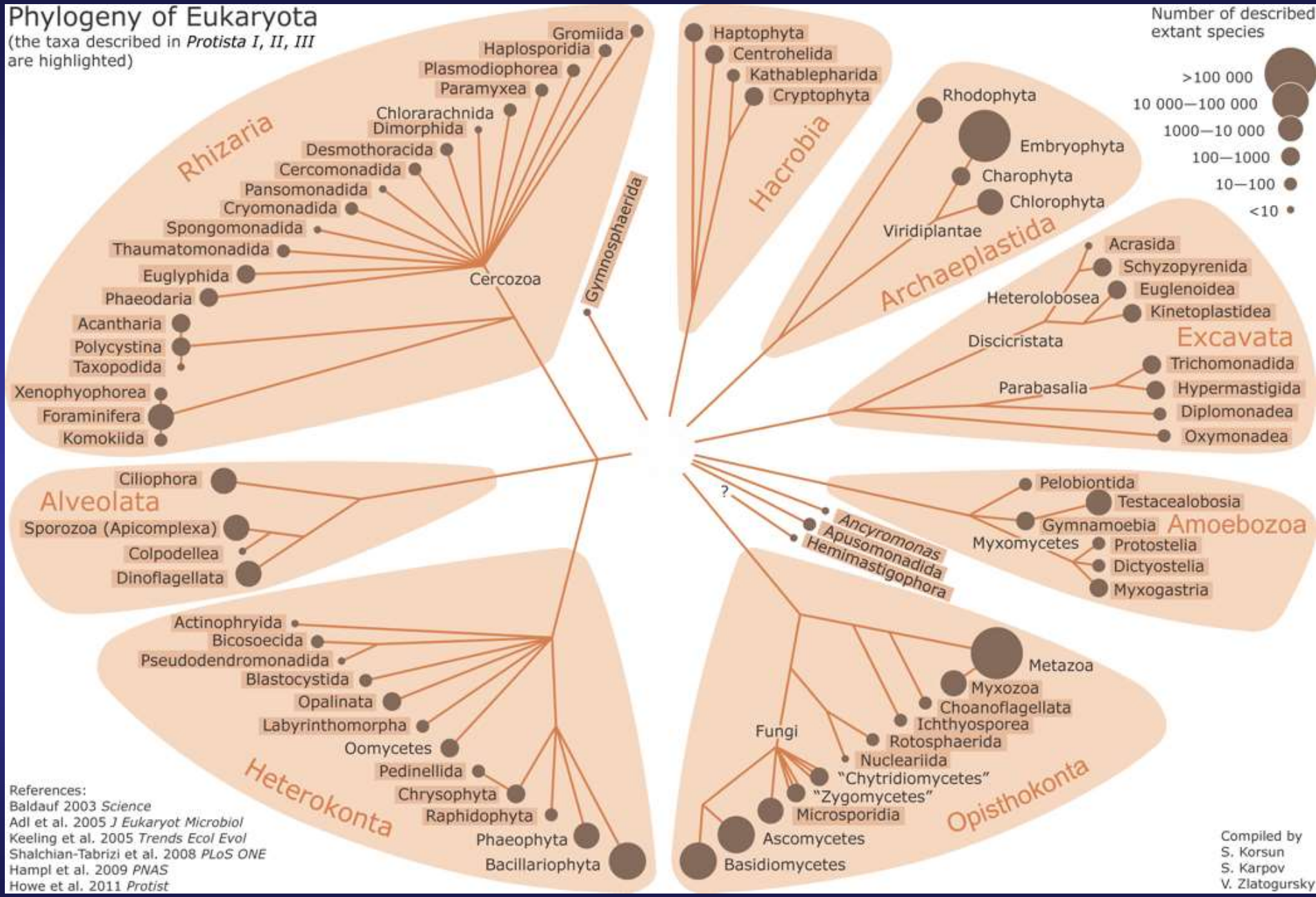

References:
Baldauf 2003 *Science*
Adl et al. 2005 *J Eukaryot Microbiol*
Keeling et al. 2005 *Trends Ecol Evol*
Shalchian-Tabrizi et al. 2008 *PLoS ONE*
Hampl et al. 2009 *PNAS*
Howe et al. 2011 *Protist*

Compiled by
S. Korsun
S. Karpov
V. Zlatogursky

Эндоцитоз: фагоцитоз и пиноцитоз

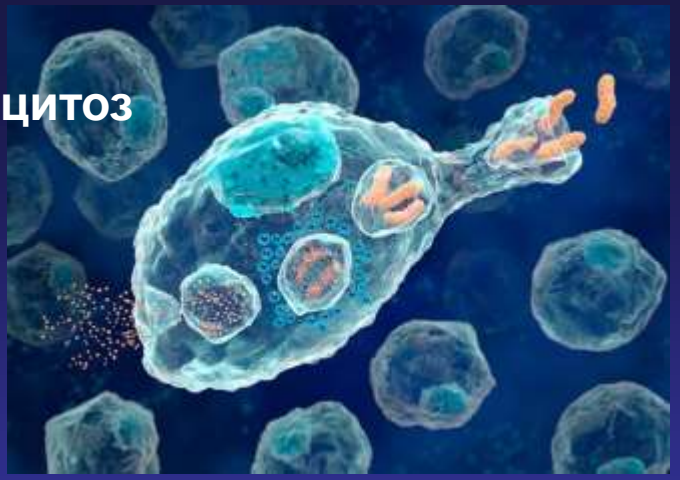

Фагоцитарные возможности нейтрофила зависят от его способности распознавать бактерию по наличию комплемента и/или антитела, прикрепленного к микроорганизму. Обозначения: H_2O_2 - перекись водорода, HOCl - хлорноватистая кислота, MPO - миэлопероксидаза, O_2^- - анион пероксида, PLA2 - фосфолипаза-А2. Нейтрофилы взаимодействуют с хемотаксическими агентами и мигрируют к местам внедрения бактерий. Для этого они проникают в посткапиллярные венулы микрогемациркуляторного русла в области проникновения бактерий. Там они объединяются с молекулами селектинов, секретируемых эндотелиоцитами венул. Взаимодействие белков-рецепторов нейтрофилов с селектинами эндотелиоцитов запускает процесс перемещения нейтрофилов к эндотелию и способствуют их медленному прокатыванию по внутренней поверхности слоя эндотелиоцитов. В результате прокатывания обеспечивается тесный контакт поверхности лейкоцитов с поверхностями эндотелиоцитов. Лейкоциты синтезируют и выводят интерлейкины и кахектины, которые запускают выведение эндотелиоцитами хемокинов. Хемокины активируют плотное прилипание лейкоцитов к поверхности эндотелия. Эндотелиоциты секретируют и выводят интегрины, которые способствуют выходу лейкоцитов из просвета кровеносного капилляра в экстрацеллюлярную жидкость соединительной ткани к месту проникновения микроорганизмов. Здесь нейтрофилы выводят лейкотриены, запускающие воспалительный процесс и начинают фагоцитоз. Вначале образуется фагосома, содержащая микроорганизм. Гидролитические ферменты фагосомы катализируют реакции расщепления веществ, составляющих структуру микроорганизмов. Кроме того, в фагосоме нейтрофилов с участием ряда ферментов образуются реактивные соединения кислорода. Гидролитические ферменты и перекисные соединения нарушают структурно-функциональную целостность микроорганизмов. После выполнения своего предназначения нейтрофилы погибают. Вещества, образовавшиеся от разрушения микроорганизмов, от погибших нейтрофилов вместе с экстрацеллюлярной жидкостью образуют в месте воспаления гной.

(Gartner L.P, Hiatt J.M. Color Textbook of Histology [изменено Трифоновым Е.В.])

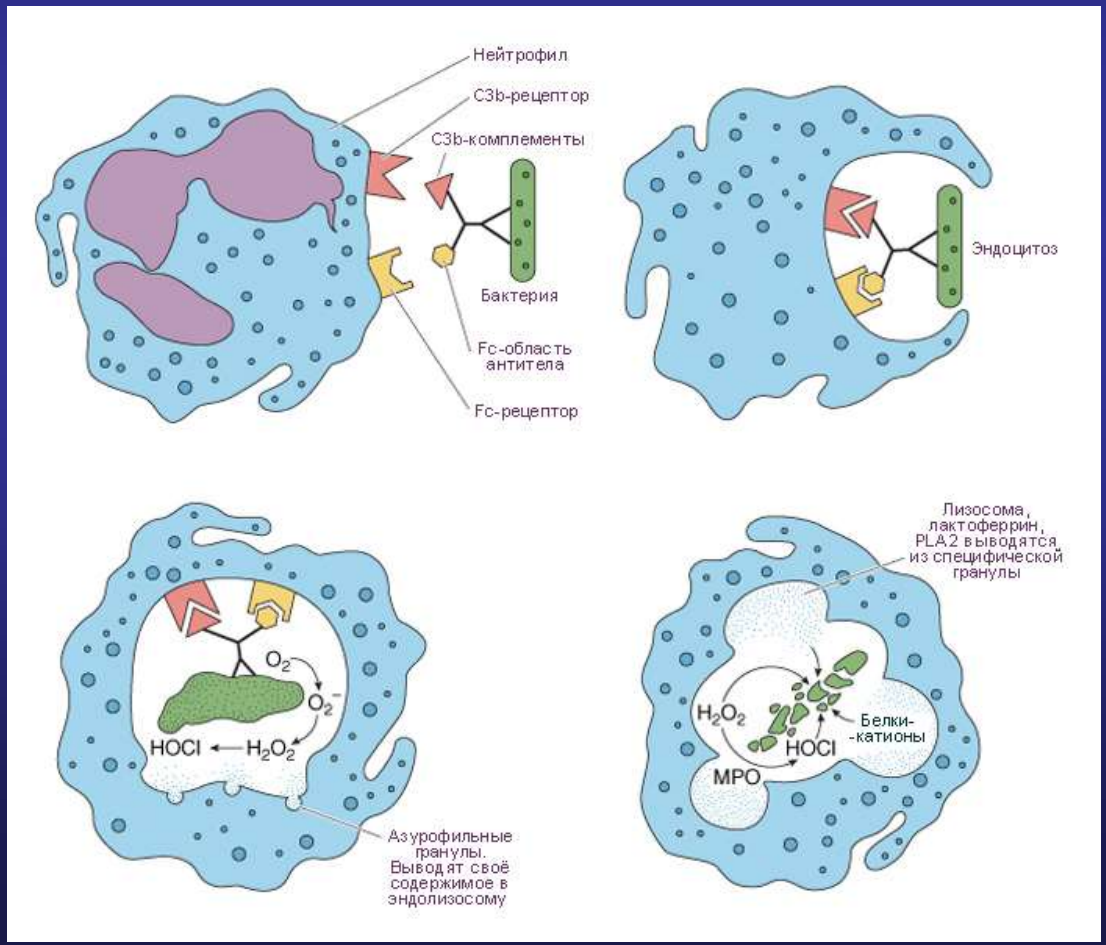

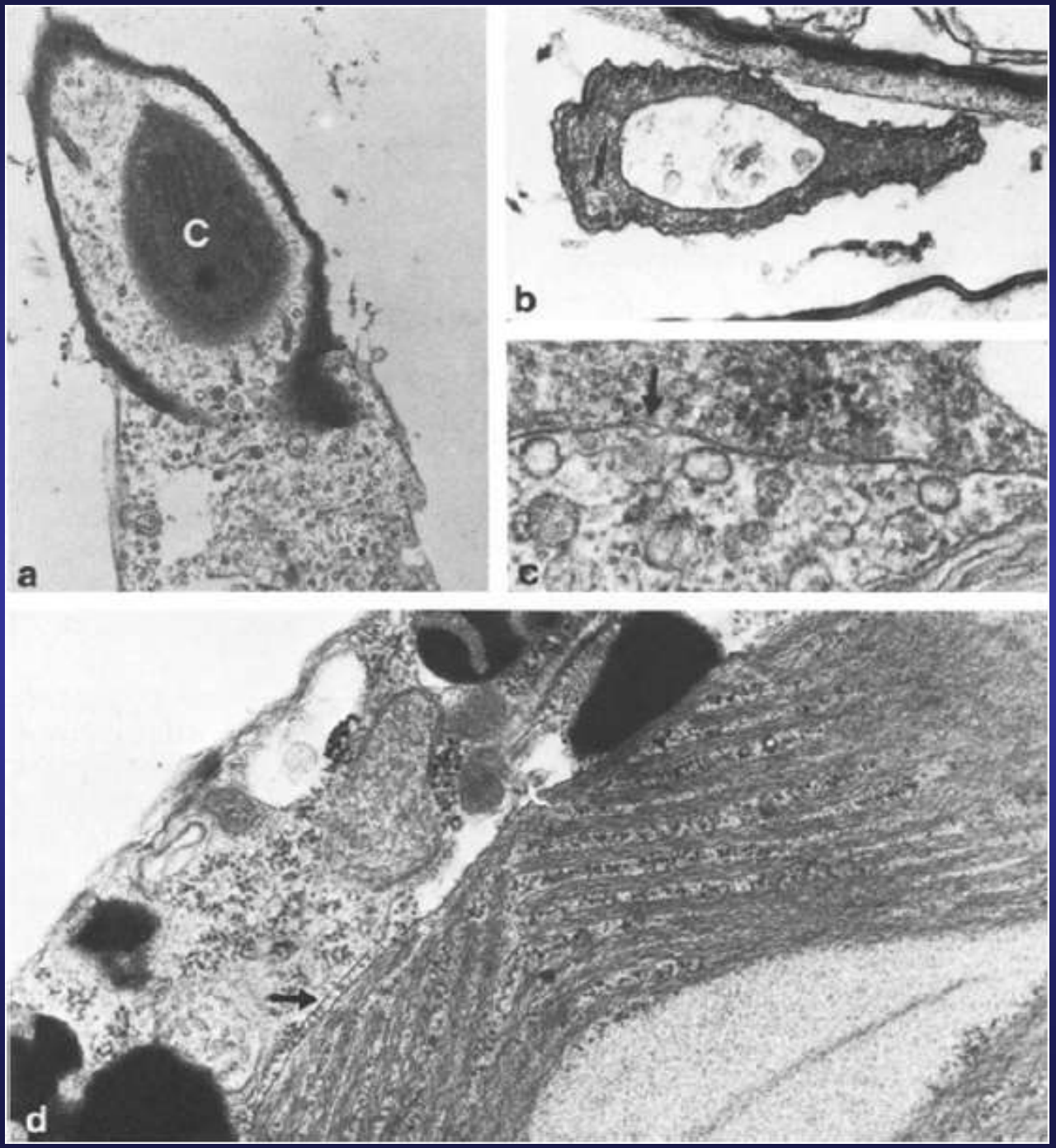

"Myzocytosis", a Kind of Endocytosis with Implications to Compartmentation in Endosymbiosis

Paulsenella (Dinoflagellata) feeding on *Streptotheca* (Bacillariophyta). a) Distal opening of the feeding tube (above) within the host cytoplasm (below) in oblique section, containing a host chloroplast C cut tangentially. 15000:1. b) Feeding tube between epicingulum (above) and hypocingulum (below) of the diatom frustule. It contains rows of microtubules in cross section and the food channel bounded only by the parasite membrane. 43000: I. c) Food vacuole (below) bounded only by one, namely the parasite membrane. The impression of a second membrane (arrow) results from an association with the membrane of a vesicle within the vacuole. 65000:1. d) Host chloroplast (right, note the good preservation) within a food vacuole (arrow: membrane of the food vacuole). 35 000 : 1 (Schnepf & Deichgraber, 1983)

Schematic drawing of a generalized motile dinoflagellate cell with theca showing ultrastructural characteristics.

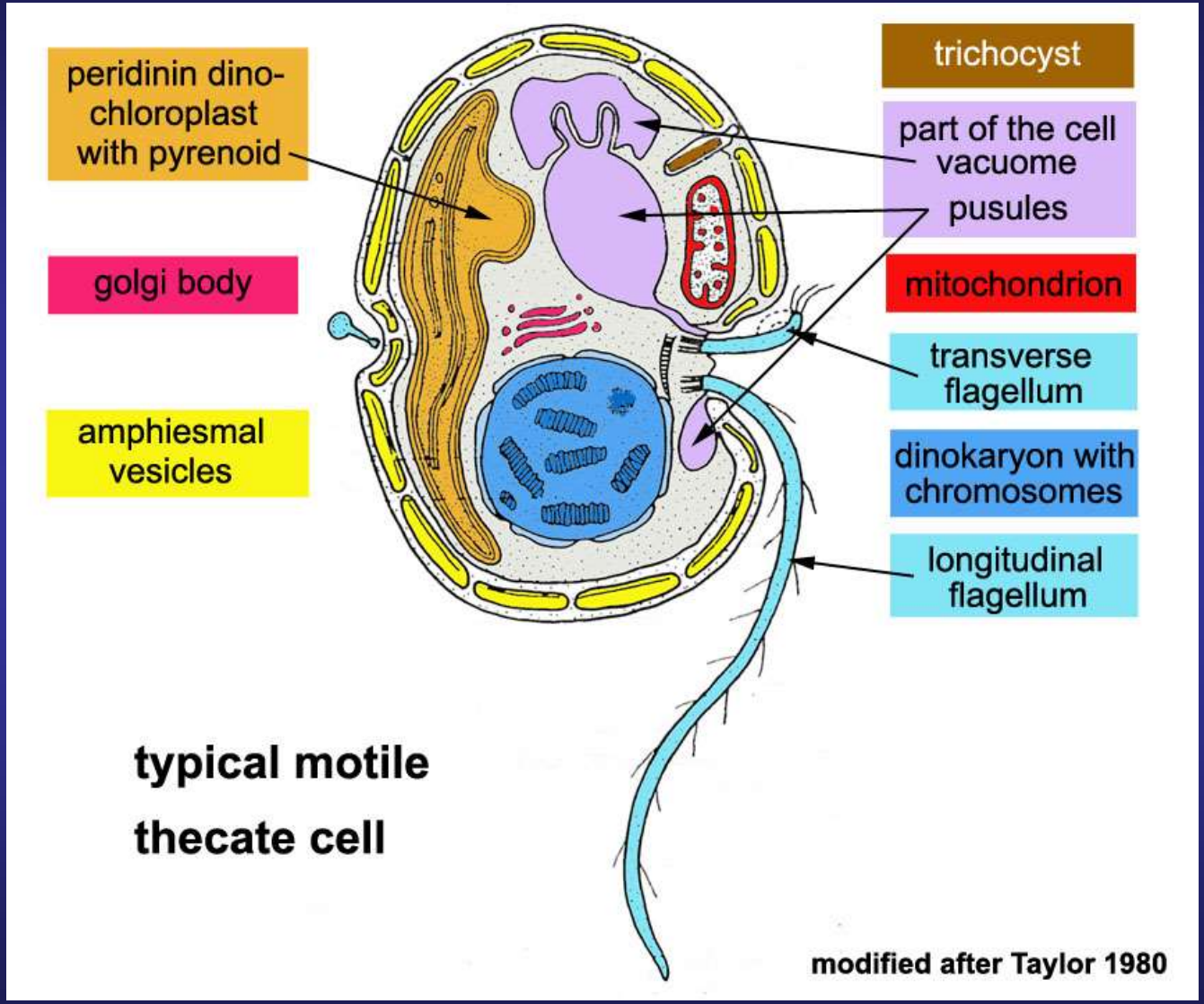

M.Hoppenrath, J.F.Saldarriaga

Food Uptake and the Fine Structure of the Dinophyte *Paulsenella sp.*, an Ectoparasite of Marine Diatoms

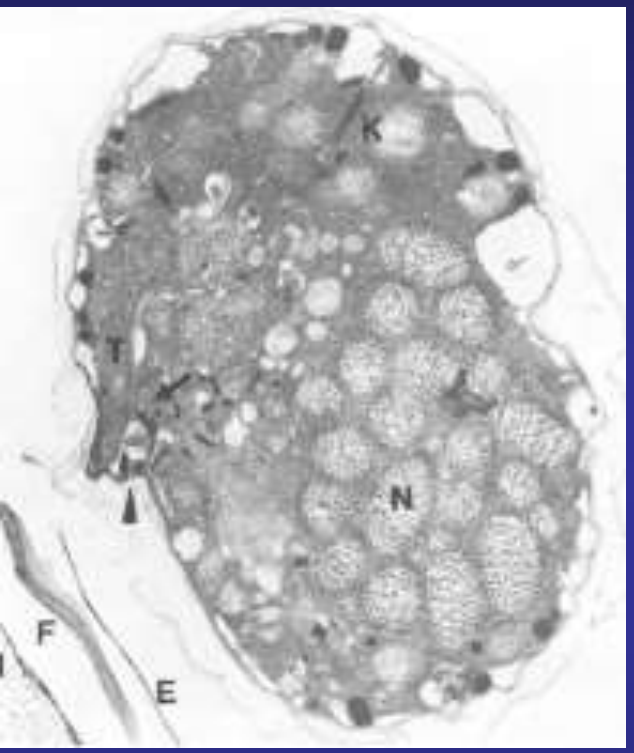

Cell K, about median-longitudinal. Feeding tube (T) and flagella (F) detached. Longitudinal flagellum abnormally situated between epi-(E) and hypocingulum (H). Arrowhead: sphincter of the longitudinal flagellum; arrow: basal body of the ring flagellum, x 9,000.

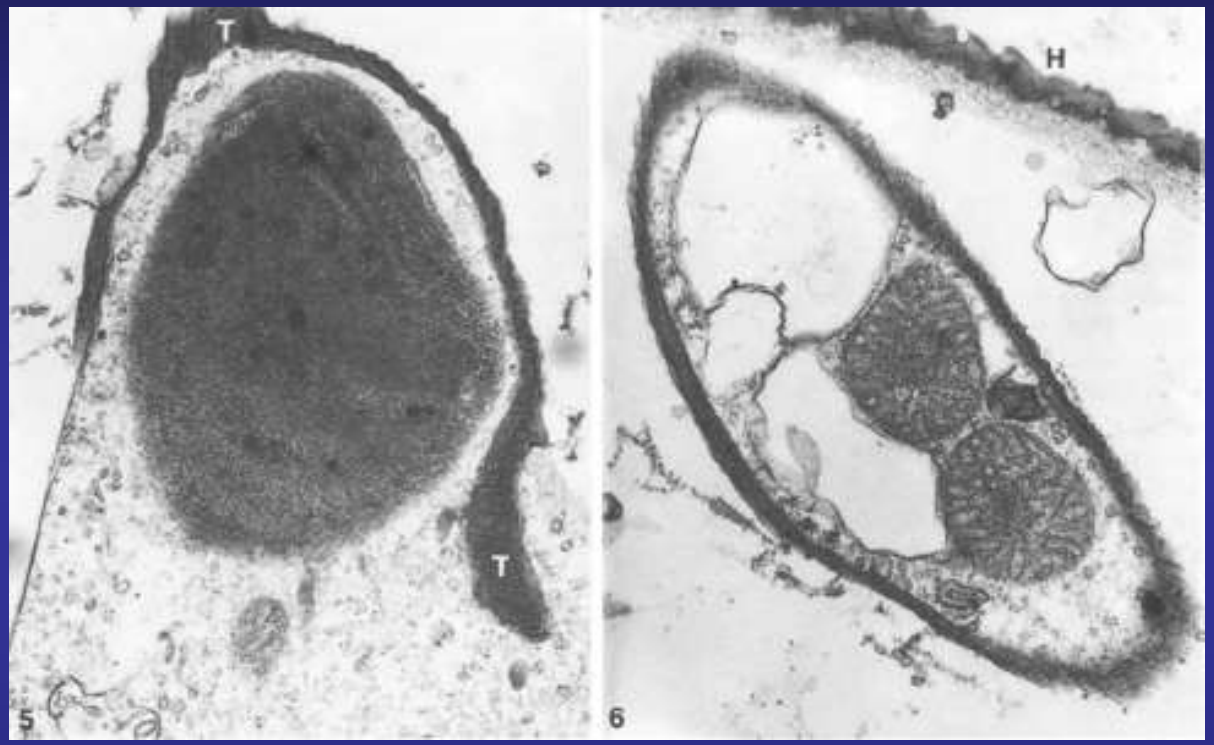

Fig. 5. Cell F, distal opening of the feeding tube (T) within the host cytoplasm, oblique-longitudinal, containing a host chloroplast cut tangentially. MTs in the feeding tube cytoplasm, x 34,000.

Fig. 6. Cell F, feeding tube with host mitochondria, oblique section. MTs in the feeding tube cytoplasm, x 31,000

(Schnepf & Deichgraber, 1985)

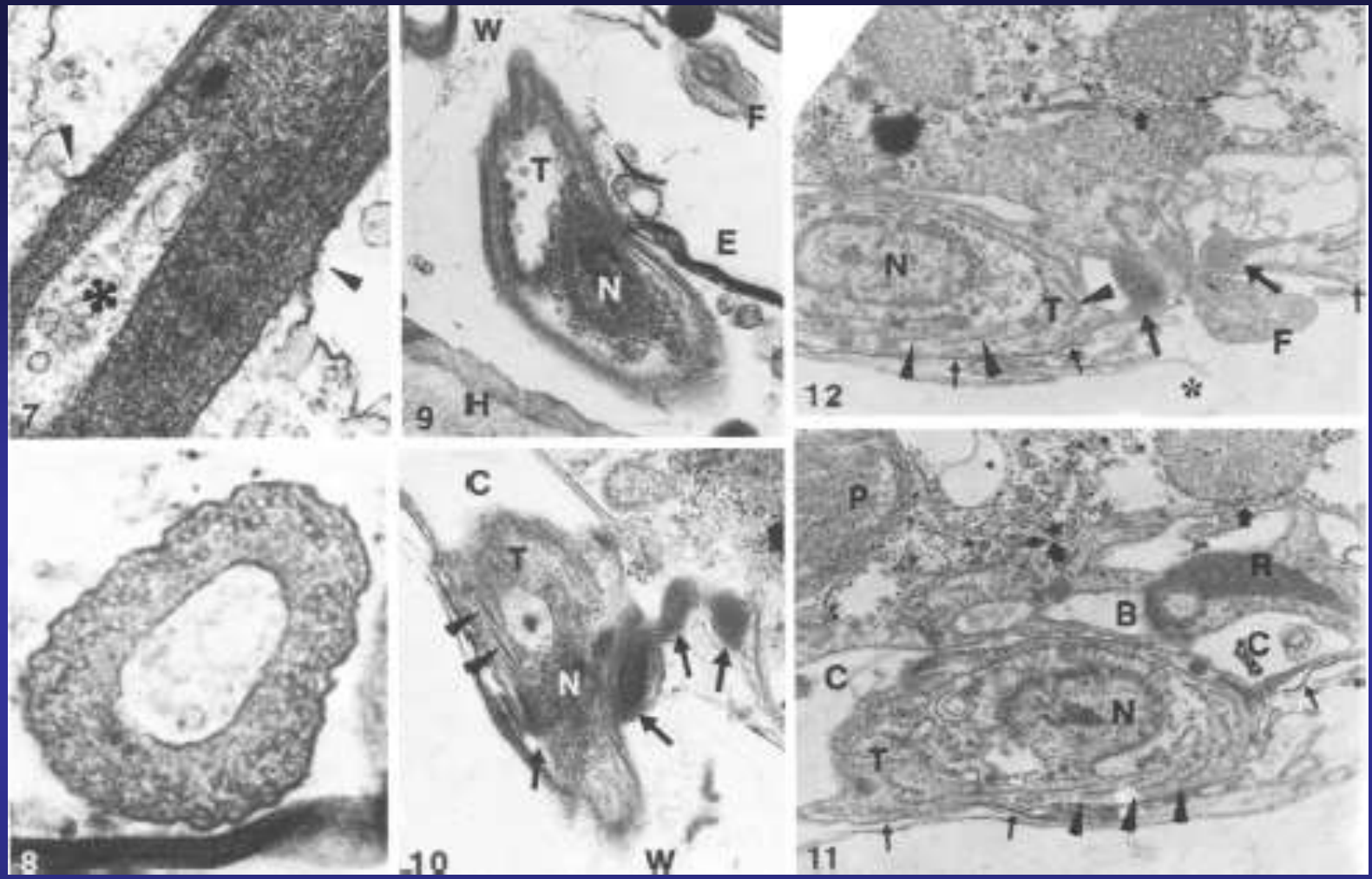

Fig. 7. Cell E, feeding tube, piercing the host plasmalemma and penetrating into the host cytoplasm (lower left corner). Arrowheads: attachment of the host plasmalemma at the feeding tube plasmalemma. Asterisk: Furrow of the feeding tube filled with host cytoplasm. x44,000. Fig. 8. Cell F, the same feeding tube as in Fig. 6, cross-section. Note the narrow internal diameter and the microtubular plates. • 87,000. Figs. 9-12. Cell L Series of sections through the feeding tube, containing the highly deformed host nucleus, numbered from distal to proximal. Fig. 9, at the outer opening of the slit between epi- and hypocingulum; Fig. I0, at the region of the sphincters of the feeding tube (arrows, left) and of the longitudinal flagellum (arrows, right); Fig. I 1, at the basis of the ring flagellum; Fig. 12, at the sphincter of the ring flagellum (F). Big arrows: sphincter; small arrows: pellicle; arrowheads: microtubular plates; asterisk: end of the former outer part of the amphiesma; short thick arrows: membrane of the food vacuole; P chloroplast within the food vacuole, x 26,000.

(Schnepf & Deichgraber, 1985)

Food Uptake and the Fine Structure of the Dinophyte *Paulsenella sp.*, an Ectoparasite of Marine Diatoms

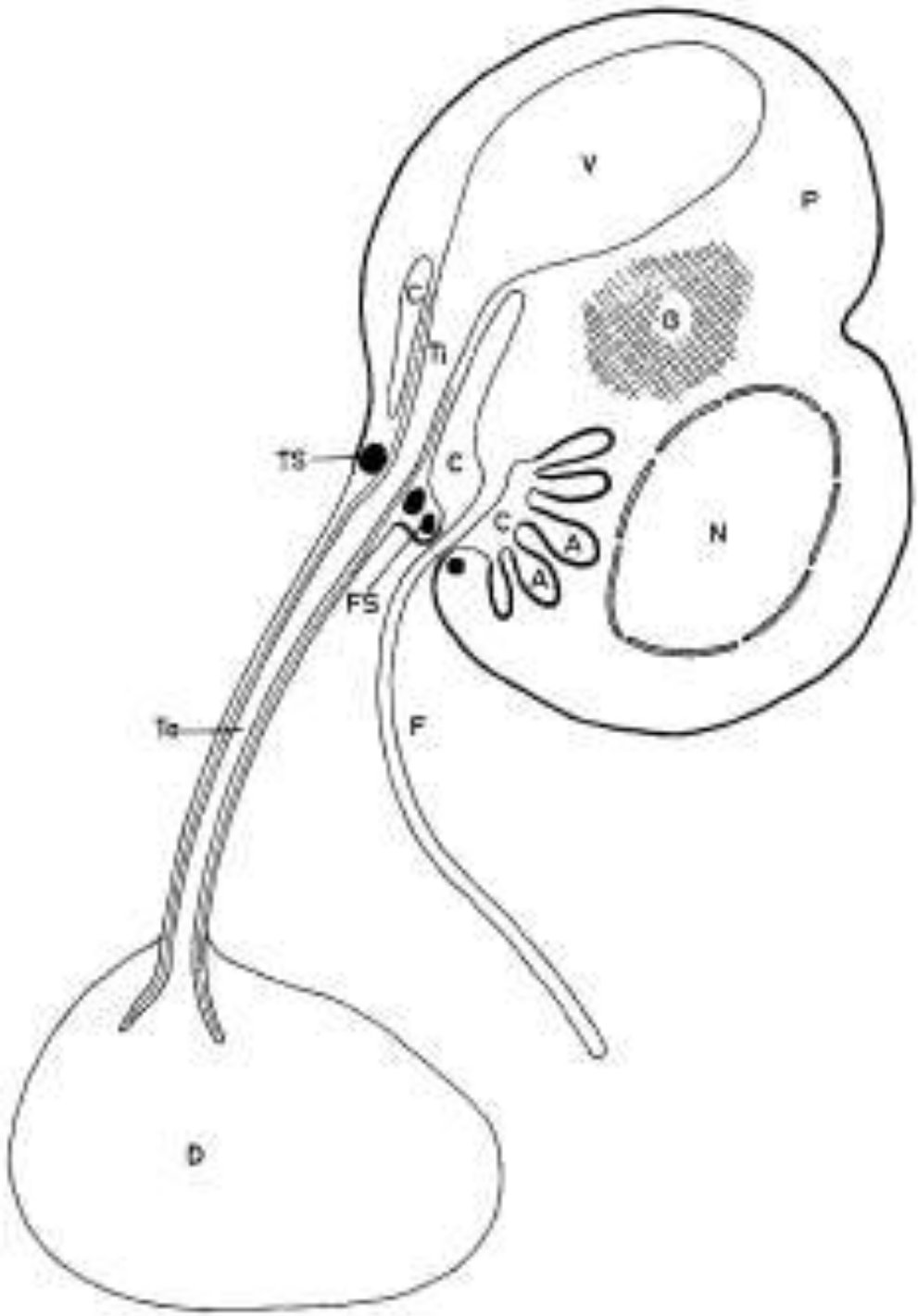

Feeding *Paulsenella* cell, schematically. A, ampullae of the pusule open towards the common cavity (C) around the flagellar bases [only the longitudinal flagellum (F) is drawn] and the internal part *(Ti)* of the feeding tube, its exits are surrounded by the flagellar sphincters (FS). The outer part of the feeding tube *(To)* merges into the cytoplasm of the diatom cell (D) (frustule not drawn); at its entry into the cell body the feeding tube sphincter (TS). G Golgi apparatus, N nucleus, P cytoplasm and V food vacuole of the *Paulsenella* cell. Cell covering with amphiesmal structure: thick line; single membranes: thinner line; microtubules of the microtubular basket: very thin line.

(Schnepf & Deichgraber, 1985)

Pfiesteria shumwayae kills fish by micropredation not exotoxin secretion (Vogelbein et al., 2002. Nature, Vol.418, p.967-970)

Pfiesteria piscicida **and** ***P. shumwayae*** reportedly secrete potent exotoxins thought to cause fish lesion events, acute fish kills and human disease in mid-Atlantic USA estuaries. However, *Pfiesteria* toxins have never been isolated or characterized.

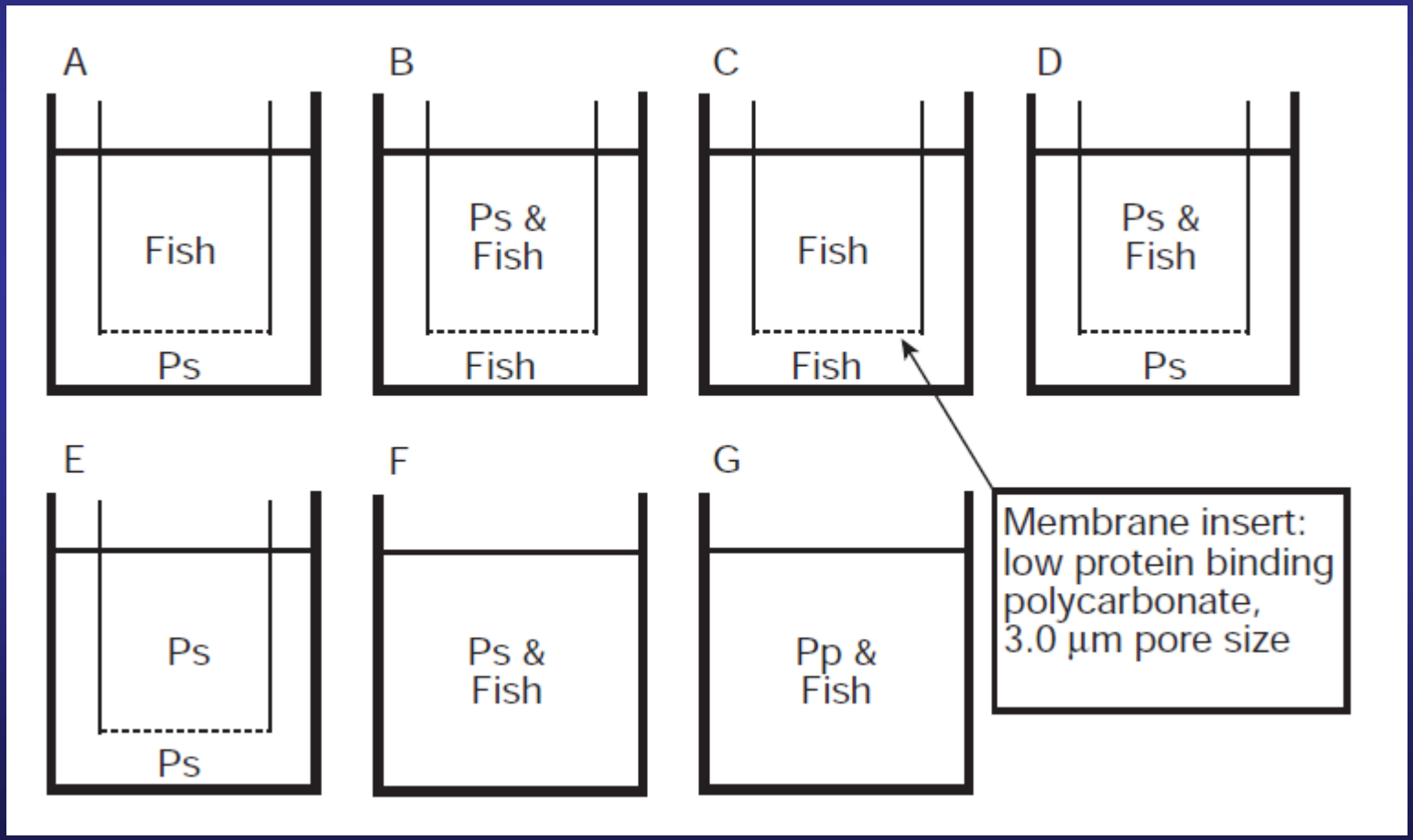

Experimental design for the membrane insert study using larval *Cyprinodon variegatus* exposed *to Pfiesteria shumwayae* (Ps) and *P. piscicida* (Pp).

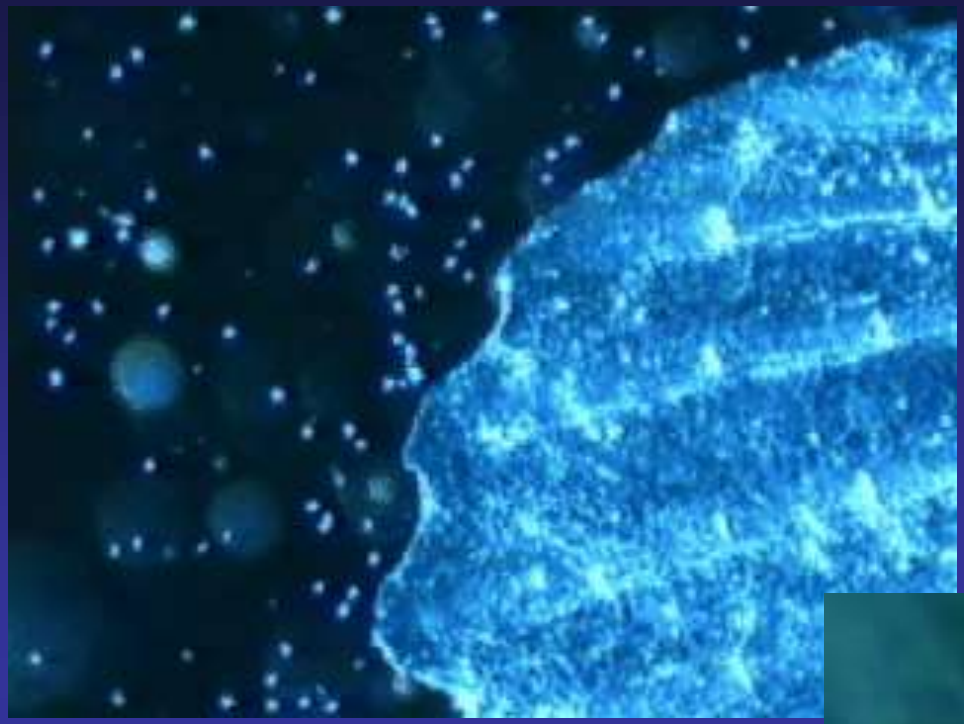

Nonpathogenic *Pfiesteria piscicida* and pathogenic *P. shumwayae* (Vogelbein et al., 2002. Nature, Vol.418, p.967-970)

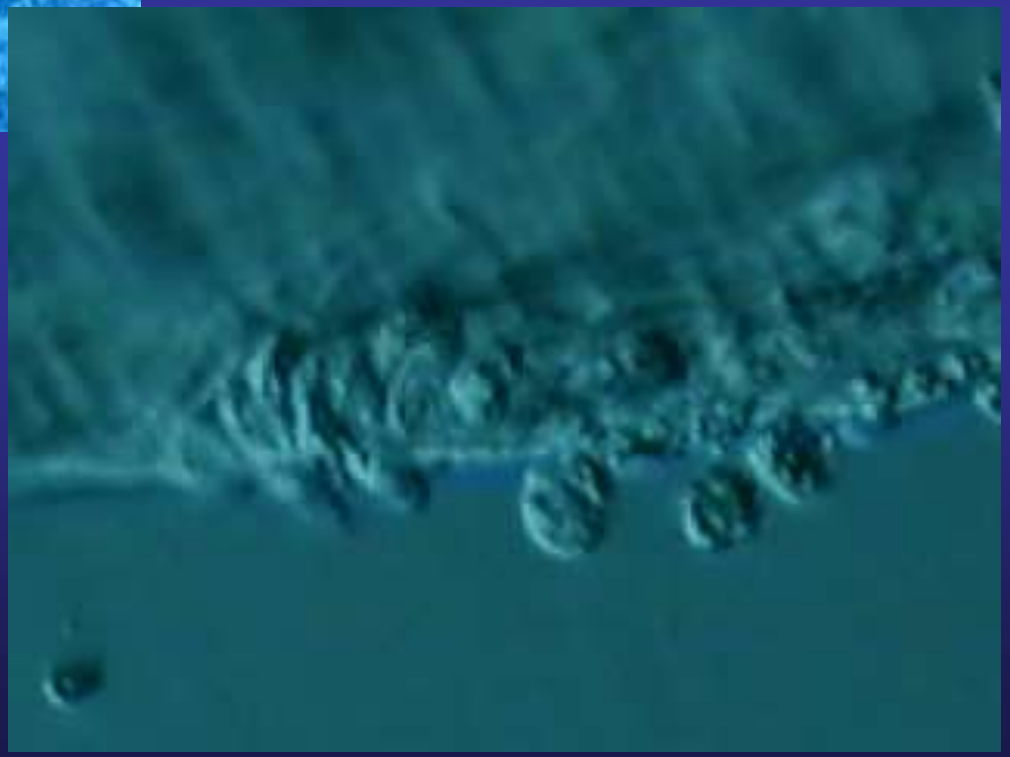

Pfiesteria shumwayae feeding by myzocytosis (Vogelbein et al., 2002. Nature, Vol.418, p.967-970)

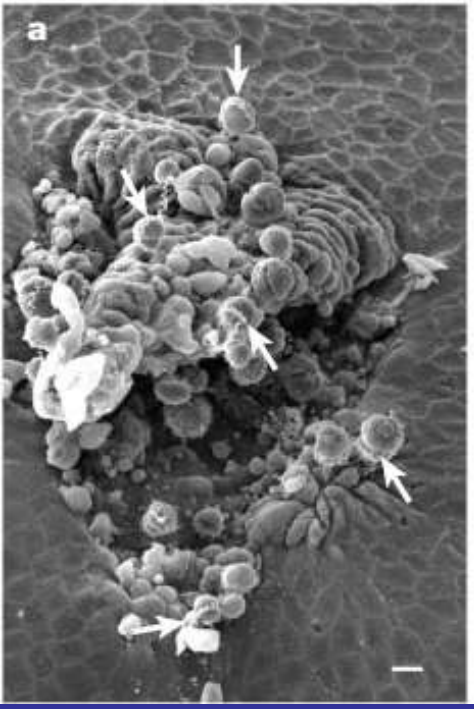

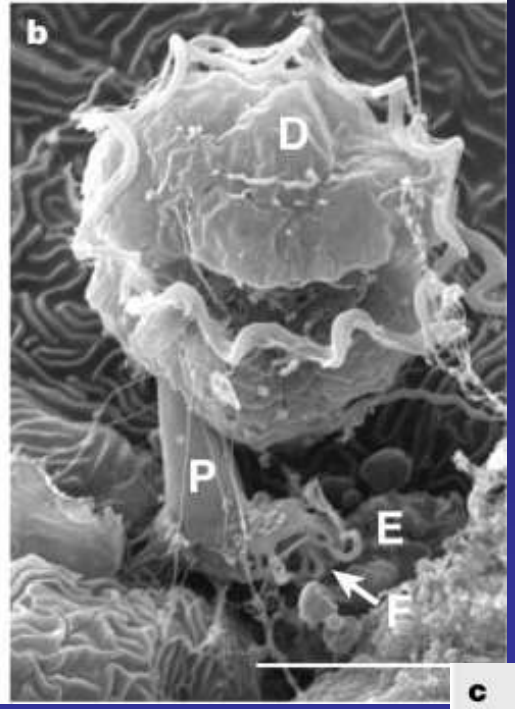

Pfiesteria shumwayae kills fish by micropredation not exotoxin secretion

Myzocytosis by *Pfiesteria shumwayae* on the epidermis of larval *Cyprinodon variegatus*. a, Scanning electron micrograph (SEM) of early epidermal erosion (0,5 min) with numerous attached dinospores (arrows). b, SEM of single dinospore (D) attached to and feeding on damaged epidermal cell (E). Note the distal end of peduncle (P) exhibiting filopodial projections (F). c, Transmission electron micrograph (TEM) of dinospore (D) attachment (arrow) and feeding on epidermal cells. Note the epidermal cytoplasm and organelles within the dinospore peduncle (P), and the cytoplasmic rarefaction and nuclear degeneration of affected cells (arrowheads). Inset, TEM of distal portion of an unattached peduncle showing filopodial extensions and rod-shaped electron-dense granules (G). Scale bars: a, c, 10 mm; b, 5 mm; inset, 1 mm.

(Voglbein et al., 2002)

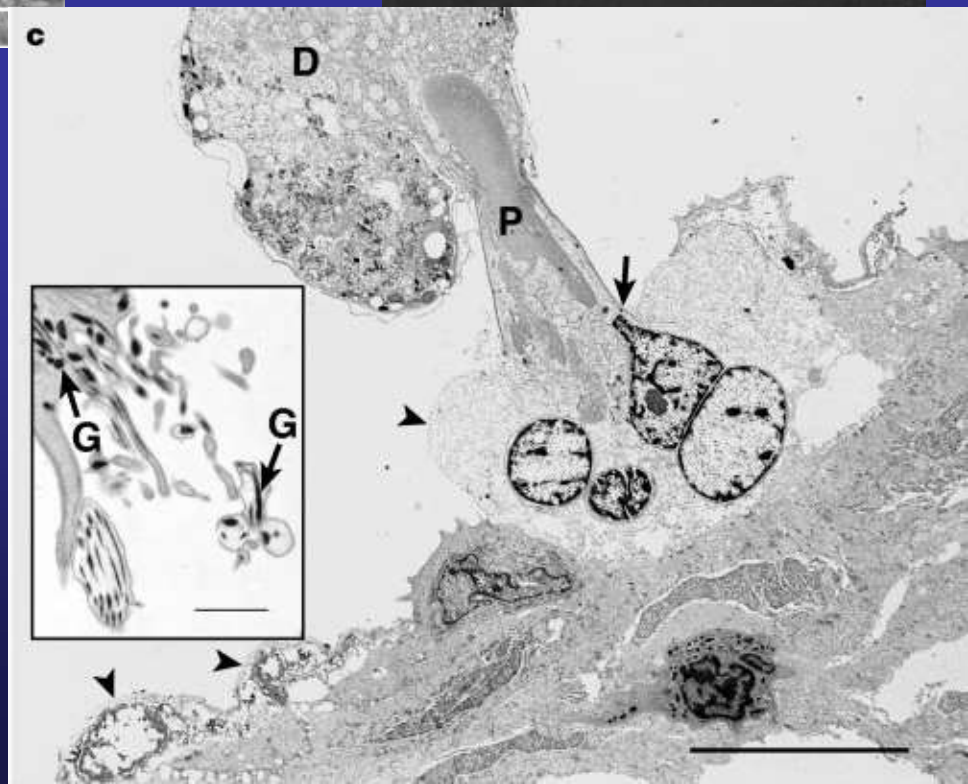

Do Suctoria really feed by suction?

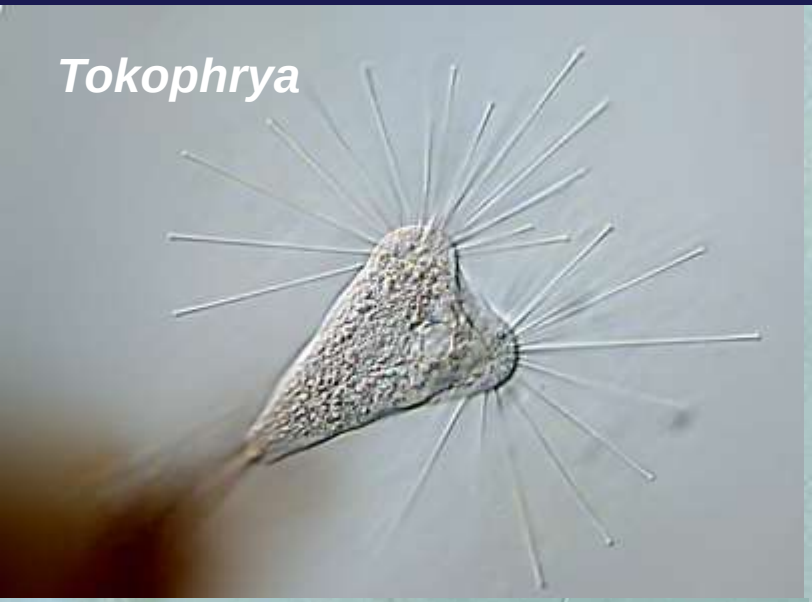

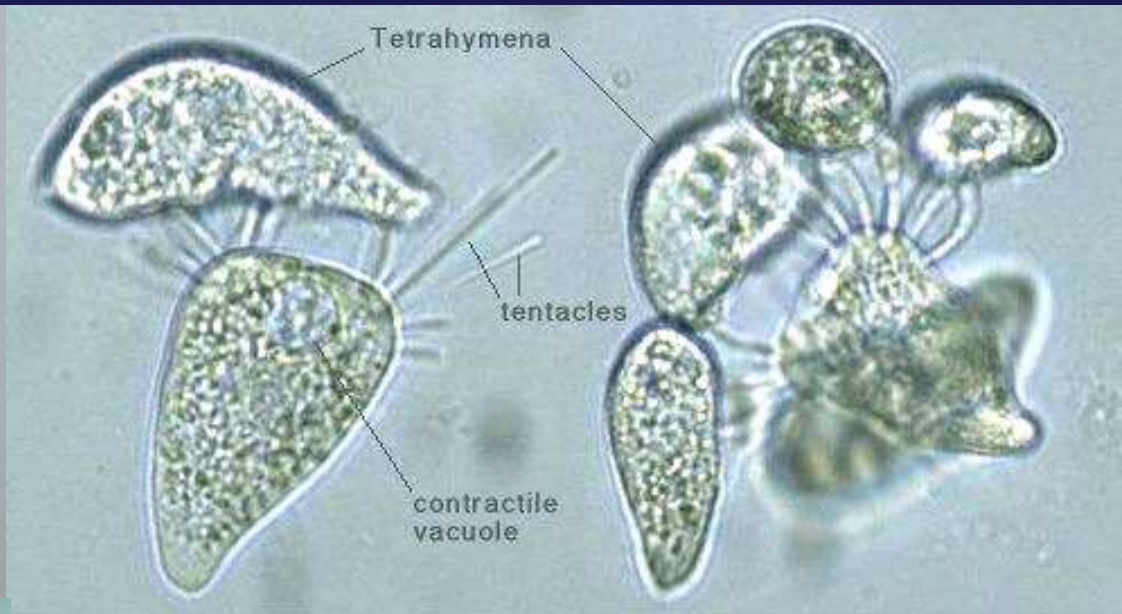

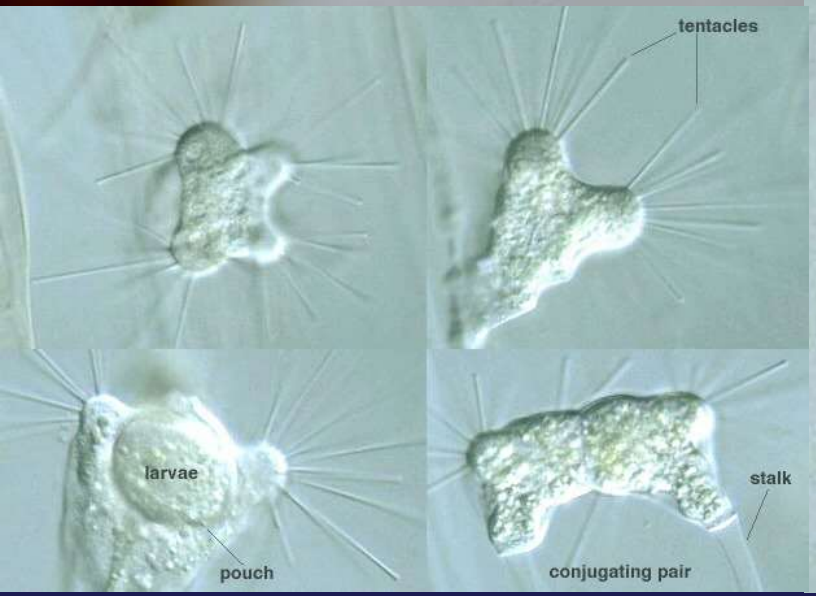

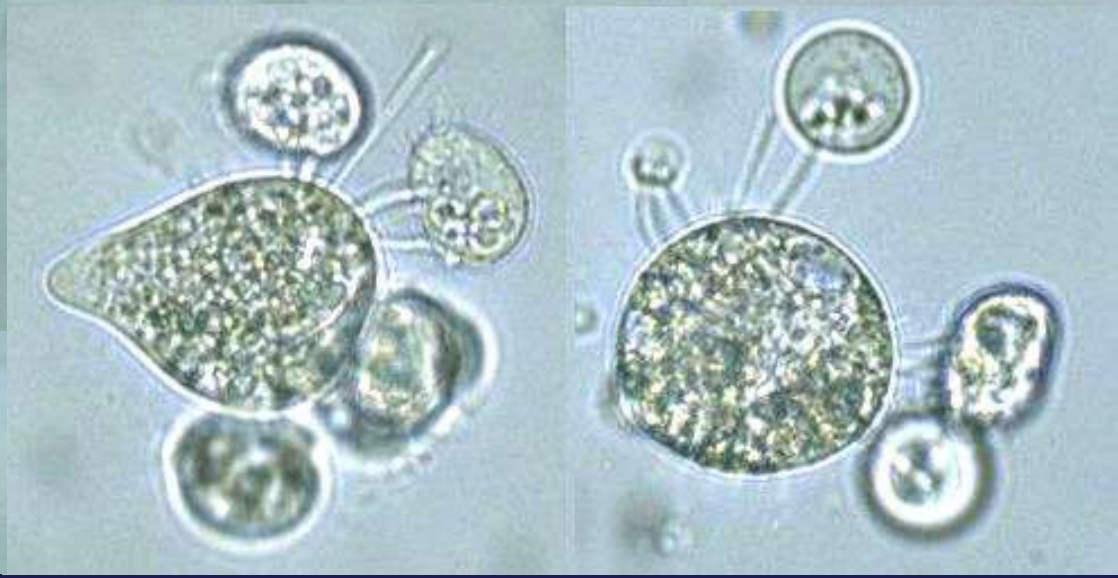

(different Internet sources; Rudzinska, 1970)

The Mechanism of Food Intake in *Tokophrya infusionum* and Ultrastructural Changes in Food Vacuoles during Digestion.

1. Longitudinal section thru internal (it) and external (e) parts of tentacle in *Tokophrya infusionum*. The former extends deep into the cytoplasm and consists only of the inner tube (i) while the external part of the tentacle (e) has an outer tube (o) also and is covered by the plasma membrane and pellicle which are continuous with the membranes covering the body (arrow). X19,000. 2. Section thru the scalloped knob of the tentacle. The missile-like bodies (mb) are located at the periphery of the knob in the evaginations of the membrane covering the knob (at arrow). X46,000. 3. Lateral section thru distal part of tentacle with knob (k). The shaft of the tentacle is covered by the pellicle (p) and plasma membrane (pm), the knob by a single membrane only (arrows). Most of the missile-like bodies (mb) are seen in cross-sections. X46,000. 4. Knob (K) of feeding tentacle embedded in cytoplasm of *Tetrahymena* (T). In the lumen of the tentacle is a mitochondrion (mi) from *Tetrahymena*. Note that the pellicle of the tentacle (p) is continuous with the pellicle of *Tetrahymena* (pi). X38,000.

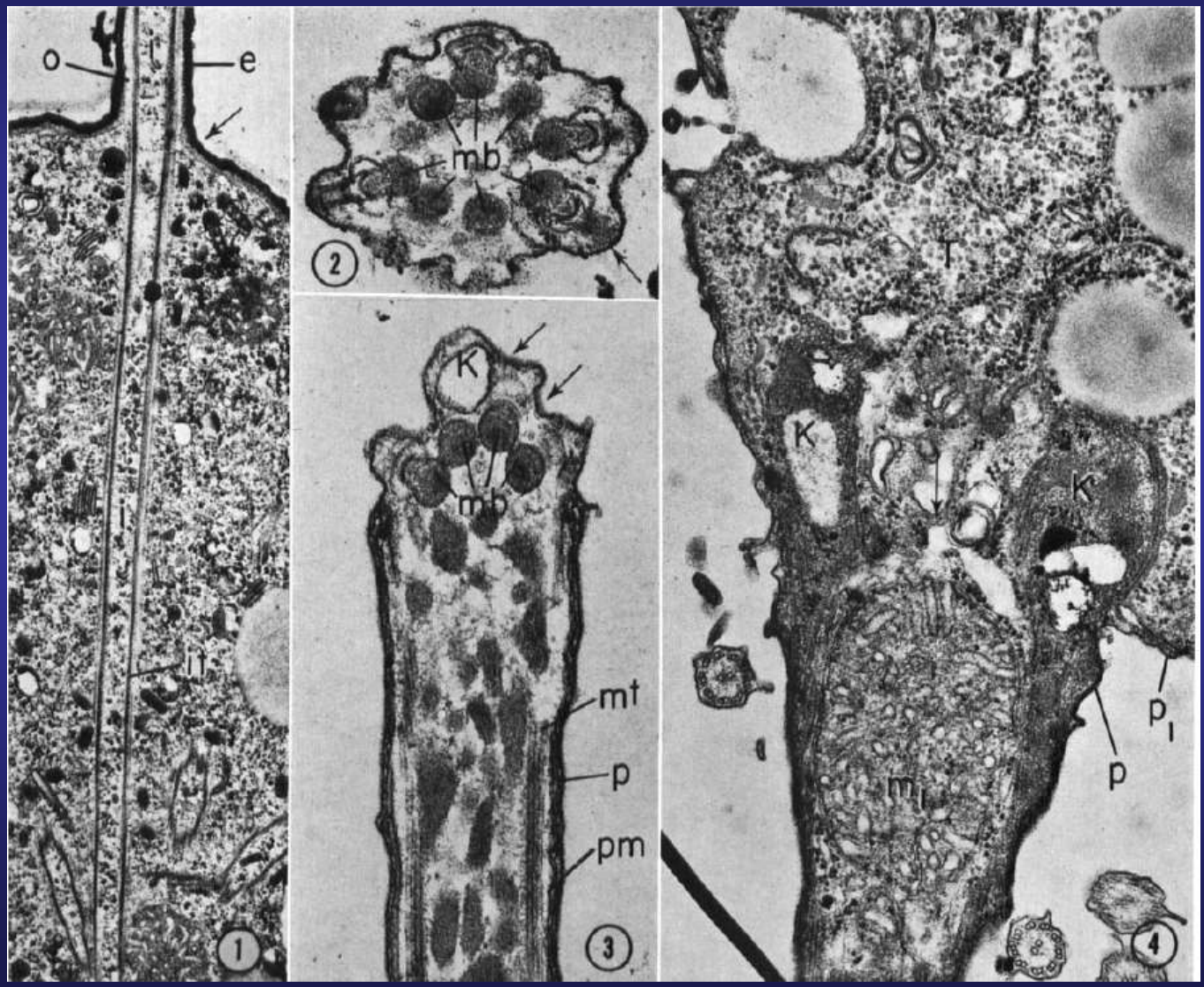

(Rudzinska, 1970)

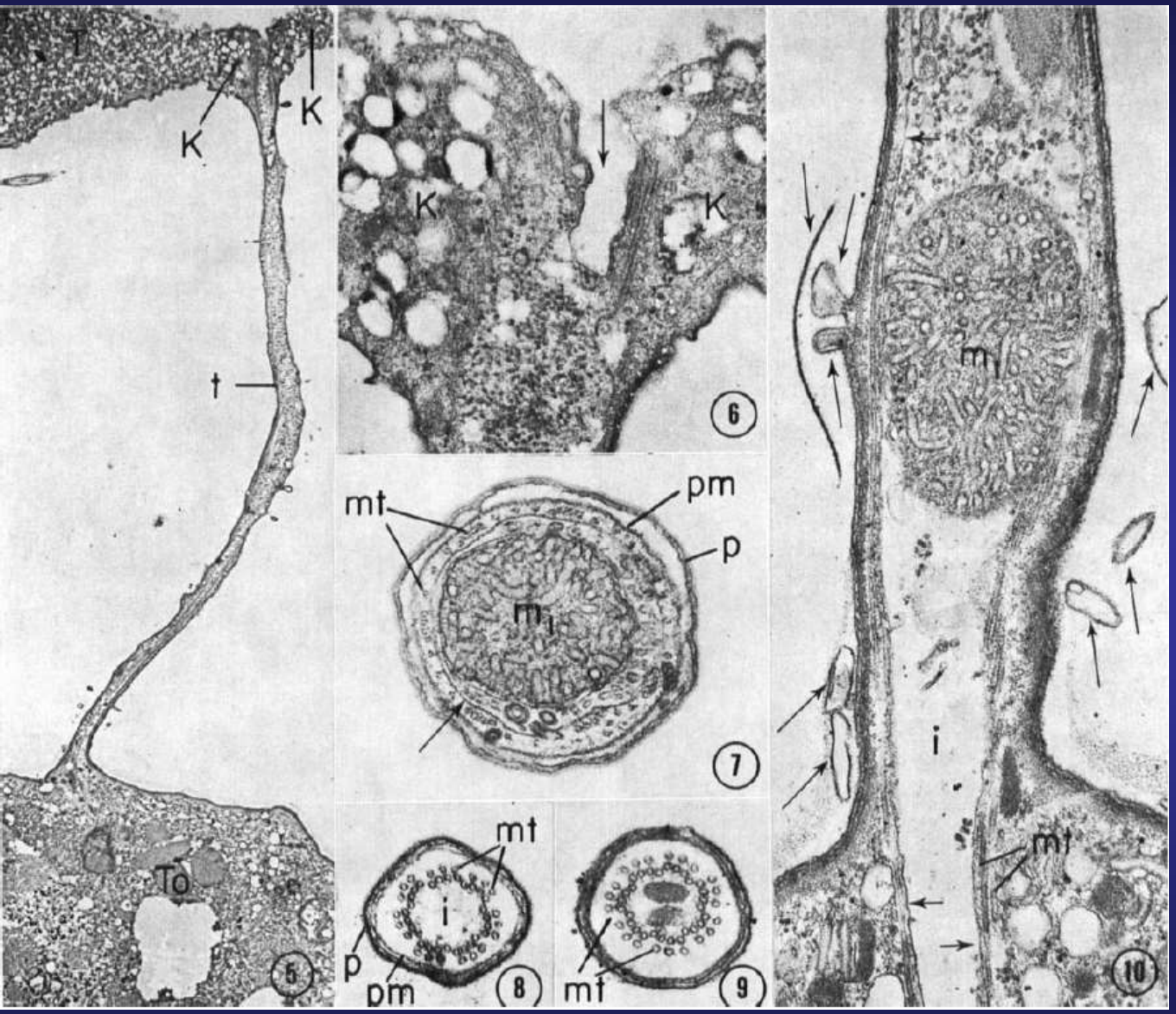

(Rudzinska, 1970)

5. *Tokophrya* (To) and *Tetrahymena* (T) connected by tentacle (t). The knob (K) of the tentacle is embedded in the cytoplasma of *Tetrahymena* (T). X9,000. 6. Serial section of knob (K) to show at higher magnification the beginning of the invagination (at arrow) of the membrane covering the knob. X37,000. 7. Cross-section of feeding tentacle. The tentacle is covered by the pellicle (p) and plasma membrane (pm). Below the plasma membrane are microtubules (mt) arranged in one row in groups of 3 and 4, and below them is a membrane (at arrow). This membrane lines the inner tube of the tentacle and is present only in feeding tentacles. In the inner tube is a mitochondrion (m1) and some other structures from *Tetrahymena*. X46,000. 8, 9. Cross-sections thru non-feeding tentacles. The inner tube (i) of the tentacle in both sections is not lined by a membrane as in 7. The wall of the inner tube is composed only of microtubules (mt), which are arranged in 2 rows. The magnification of these tentacles is the same as in 7. x46,000. 10. Longitudinal section thru a feeding tentacle. The inner tube (i) of the tentacle is lined by a membrane (short arrows). Outside the membrane are the microtubules (mt). A mithochondrion (m1) and granular material from *Tetrahymena* are in the inner tube (i) of the tentacle. The pellicle of the tentacle is folded in the form of loops (long arrows). X45,000.

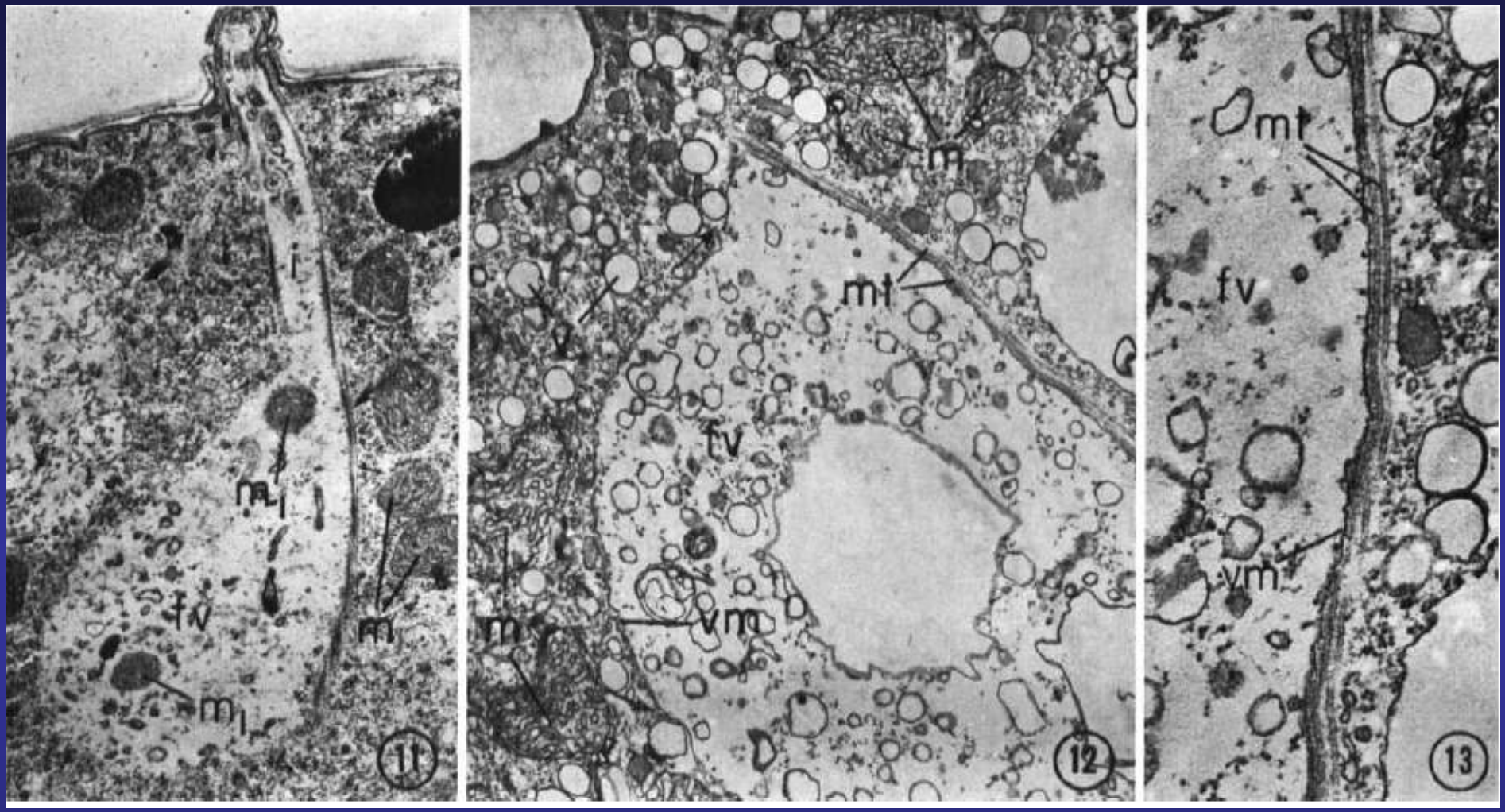

Fig. 11. Section thru food vacuole (fv) in the stage of its formation still connected with the inner tube of the tentacle (i) . In the forming food vacuole 2 mitochondria (ml) from *Tetrahymena* and some pieces of membranes are present; similar material is in the inner tube (i) of the tentacle. The fibrils (at arrow) on the right side of the food vacuole are continuous with the microtubules of the tentacle; they are in fact microtubules as seen in Fig.**13** (mt). Several mitochondria (m) of *Tokophrya* are present in the cytoplasm. x 12,200. Fig. 12. Section thru a food vacuole (fv) most probably still connected with the inner tube of the tentacle. The content is composed of membranous material, an indication that this is one of the first food vacuoles. The food vacuolar membrane (vm) is clearly seen as well as the microtubules (mt) on the right side of the food vacuole. In the cytoplasm of *Tokophrya* are several mitochondria (m) and round vesicles (v) some of which are in the close vicinity of the food vacuole (arrows). x 12,700. Fig. 13. Higher magnification of right side of food vacuole in Fig. 12 to show the microtubules (mt) and their location outside the food vacuolar membrane (vm). X 47,600.

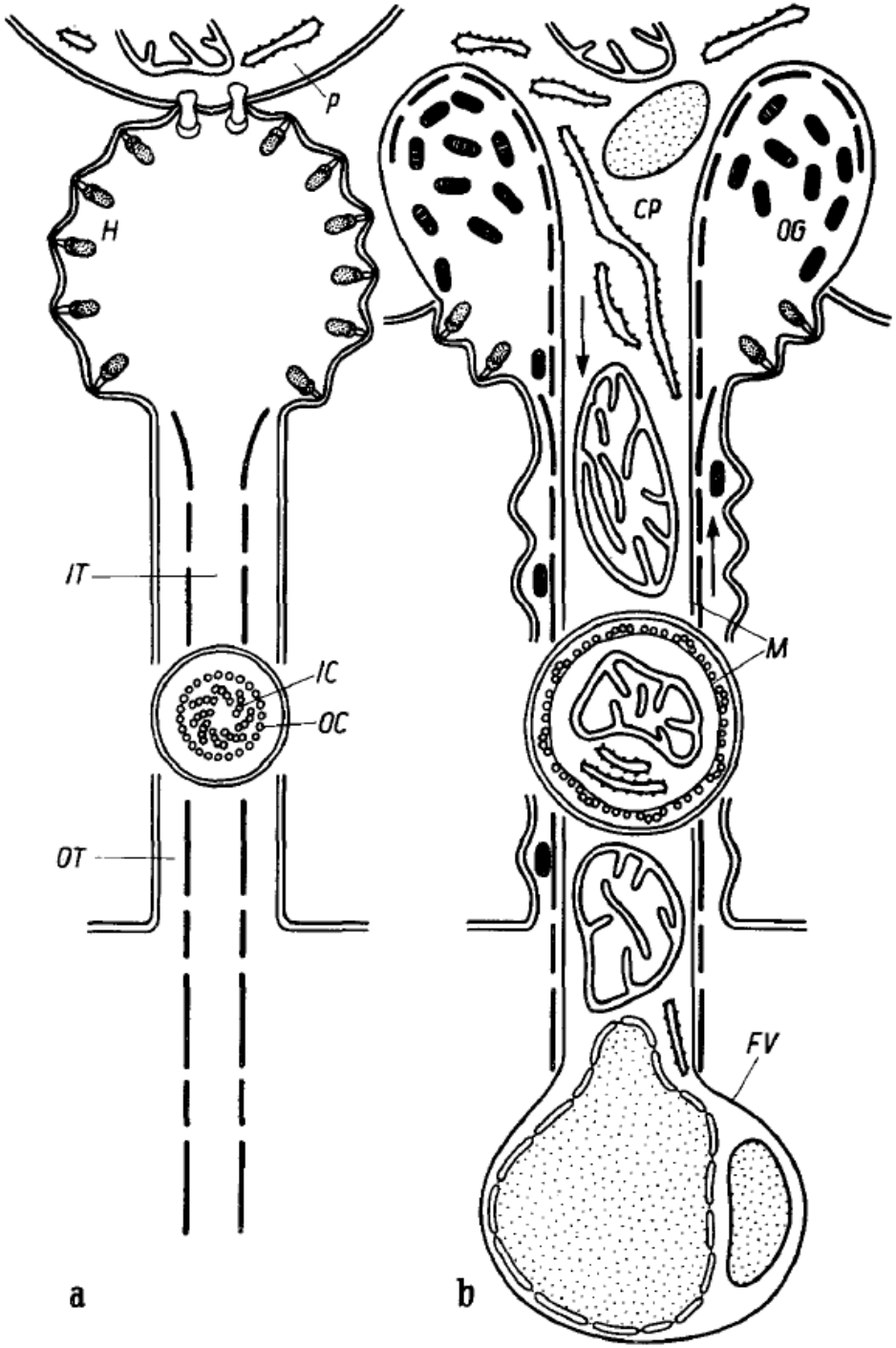

A Microtubule Model for Ingestion and Transport in the Suctorian Tentacle

Suctorian tentacle in non-feeding (a) and feeding (b) state.

a, The tentacle shaft is composed of an outer tube (OT) confined by the pellicle and an inner tube (IT), the "wall" of which consists of an outer cylinder (OC) of single microtubules and an inner cylinder *(IC)* of microtubule ribbons. Two of the haptocysts (H) have just made contact to the prey (P).

b, During feeding the microtubule ribbons protrude into the knob, where they are, at times, arranged in a funnel-like array. The membrane of the knob (M), with the prey's cytoplasm *(CP)* adhering, is pulled in and transported downward through the lumen of the microtubular tube; a food vacuole (FV) is pinched off at its proximal end. At the same time osmiophilie granules *(OG)* move upward in the outer tube.

(Bardele, 1971, 1972)

A Microtubule Model for Ingestion and Transport in the Suctorian Tentacle

In the mechanism proposed, ingestion and transportation of the prey's cytoplasm (dotted) are suggested to result from a repeated sliding back and forth of the inner microtubule ribbons, coupled with a cyclic bridging- and release mechanism of small projection between the microtubule ribbons and the "growing" membrane of the knob.

(Bardele, 1971, 1972)

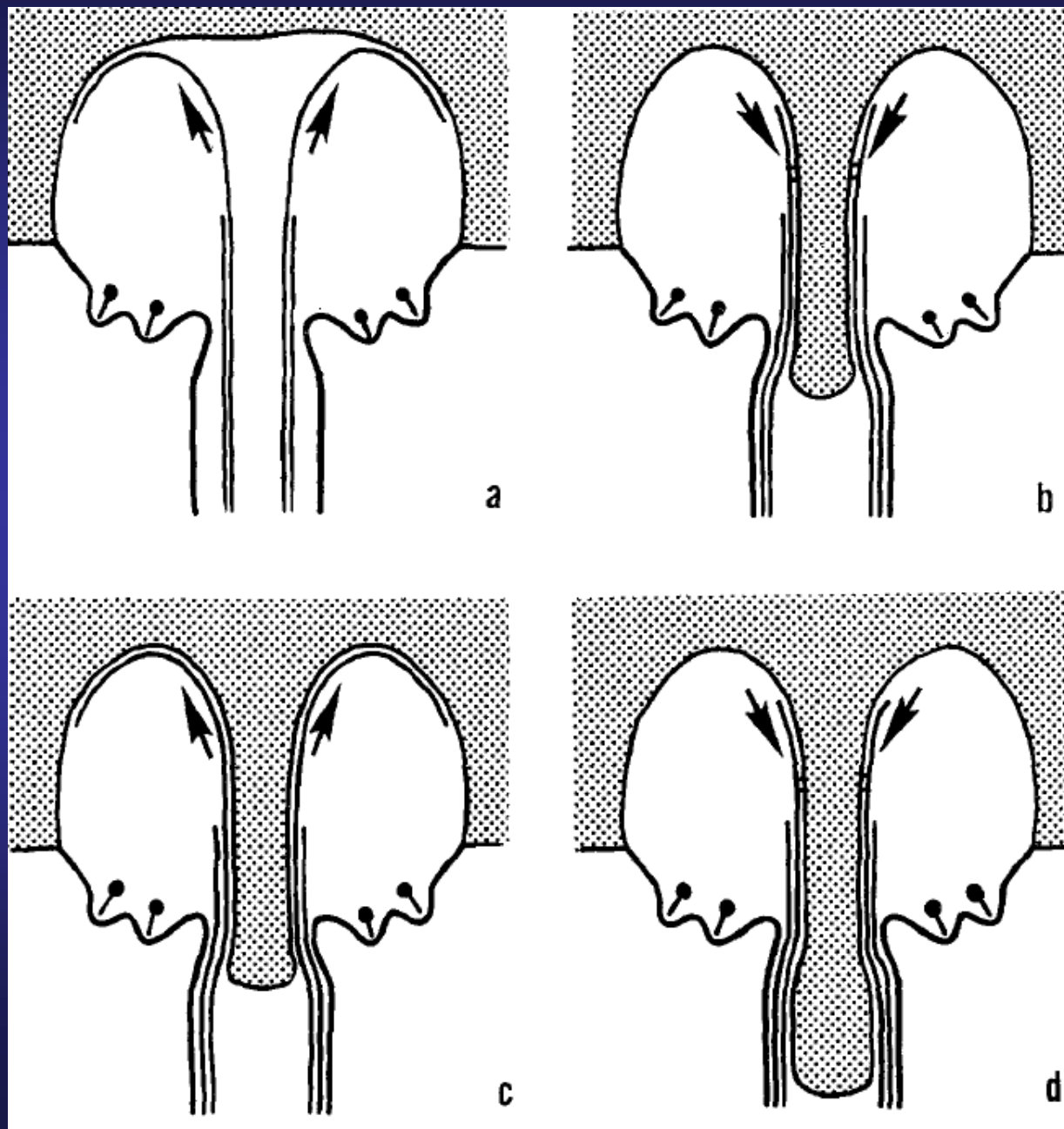

Tokophrya lemnarum, sucking ciliate

https://www.youtube.com/watch?v=QLTS_zkHcd8

DIVERSITY AND EVOLUTIONARY HISTORY OF PLASTIDS AND THEIR HOSTS

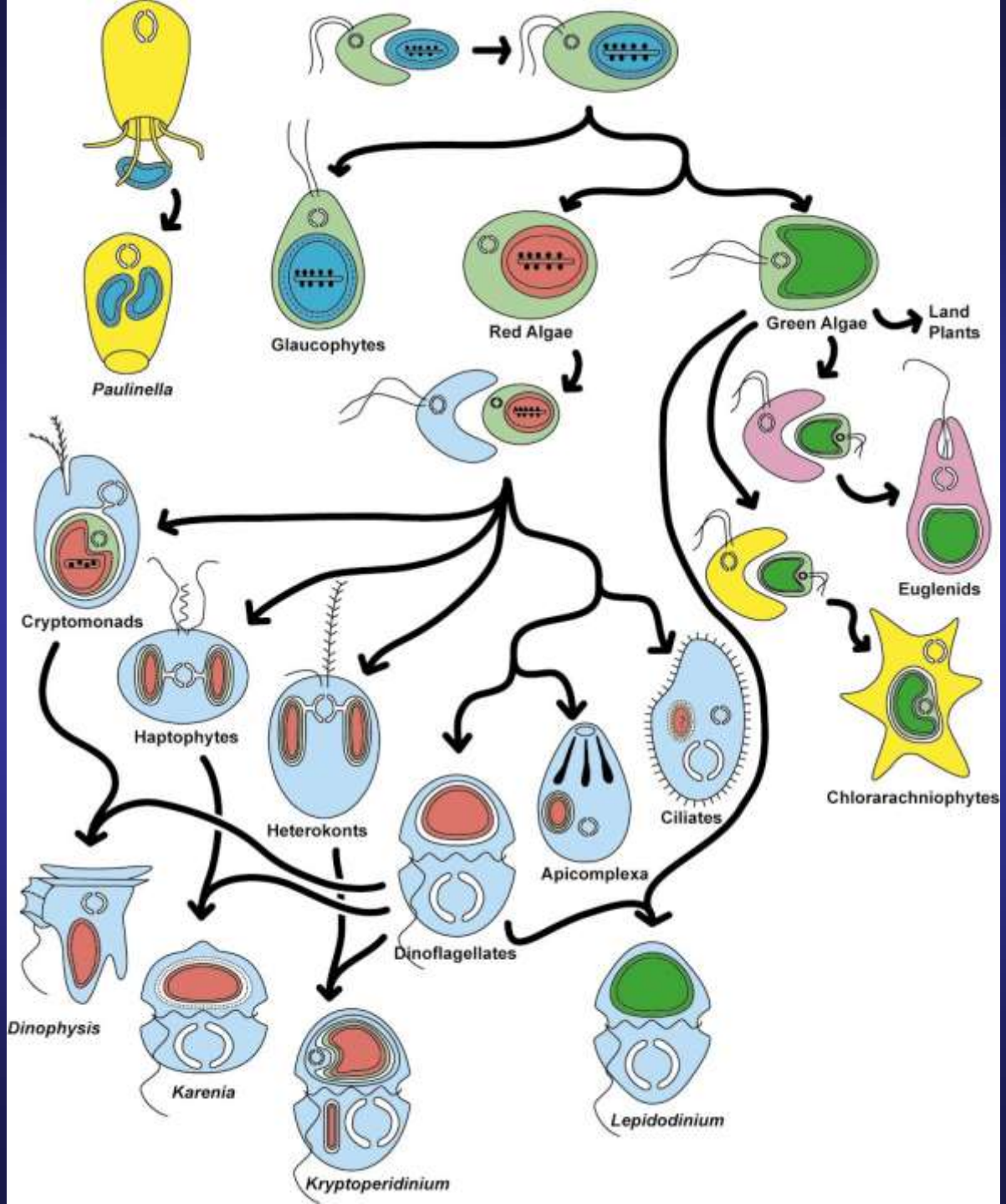

(Keeling, 2004)

DIVERSITY AND EVOLUTIONARY HISTORY OF PLASTIDS AND THEIR HOSTS

Endosymbiosis in the history of plastid evolution. All primary (top), secondary (middle), serial secondary and tertiary (bottom) endosymbiotic associations are represented here. Cells are color-coded so that the cytoplasmic color matches the color of the supergroup to which that eukaryote belongs (Cercozoa are yellow, plants are green, excavates are purple, and chromalveolates are blue). Plastids are color-coded to distinguish the three primary plastid lineages (cyanobacteria and glaucophyte plastids are both blue-green, red algal plastids are red, and green algal plastids are dark green). Primary endosymbiosis: At the top left, the cercozoan euglyphid amoeba *Paulinella* takes up a *Synechococcus*-like cyanobacterium and retains two apparently permanent endosymbionts, losing its feeding pseudopods. This may represent an independent primary endosymbiosis. At the top center, a cyanobacterium of unknown type is taken up by an ancestor of the plant supergroup, the direct descendent of which are the three primary algal lineages, glaucophytes, red algae, and green algae. Glaucophytes and red algae retain phycobilisomes, and glaucophytes retain the peptidoglycan wall. Plants are derived from green algae. Secondary endosymbiosis: At the center right, two green algae are independently taken up by two eukaryotes, one cercozoan (yellow) and one excavate (purple) giving rise to the chlorarachniophytes and euglenids, respectively. Euglenids have three-membrane plastids, and chlorarachniophytes retain a nucleomorph. At the center, a red alga is taken up by an ancestor of the chromalveolates (light blue), giving rise to cryptomonads, haptophytes, heterokonts, and alveolates (dinoflagellates, apicomplexa, and ciliates). In cryptomonads, haptophytes, and heterokonts, the outer membrane of the plastid is continuous with the rough ER and nuclear envelope, and cryptomonads also retain a nucleomorph and phycobilisomes (which are inside the thylakoid lumen rather than on the outer surface). The presence of a plastid in ciliates is purely conjectural at present, and there is no direct evidence for this organelle. Dinoflagellates have a three-membrane plastid (the peridinin-containing plastid) that has been replaced on several occasions by serial secondary and tertiary endosymbiosis: At bottom right, a green alga is taken up by a dinoflagellate in a serial secondary endosymbiosis giving rise to *Lepidodinium* and close relatives. At bottom left, three different dinoflagellates take up a cryptomonad, a haptophyte, and a diatom, giving rise to *Dinophysis*, *Karenia*, and *Kryptoperidinium*, respectively. Each of these plastids has lost one or more membranes, and how plastid targeting works is completely unknown. *Kryproperidinium* retains the diatom nucleus and also a three-membrane eyespot, suggested to be the ancestral plastid.

(Keeling, 2004)